Date of issue: June 30, 2017

The Mextram Bipolar Transistor Model

level 504.12

G. Niu, R. van der Toorn, J.C.J. Paasschens, and W.J. Kloosterman

Mextram definition document

Authors' address data: Guofu Niu (Auburn University)
R. van der Toorn (Delft University of Technology)
J.C.J. Paasschens (NXP Semiconductors)
W.J. Kloosterman (NXP Semiconductors)

Keywords: Mextram, compact modelling, bipolar transistors, large-signal modelling, distortion modelling, circuit simulation, semiconductor technology, integrated circuits

Abstract: This document presents definition of the CMC world stardard bipolar transistor model Mextram, including parameter set, equivalent circuit and equations for currents, charges and noise sources. The physics background of Mextram and parameter extraction procedure are also described.

Preface

October 2004

The Mextram bipolar transistor model has been put in the public domain in Januari 1994. At that time level 503, version 1 of Mextram was used within Koninklijke Philips Electronics N.V. In June 1995 version 503.2 was released which contained some improvements.

Mextram level 504 contains a complete review of the Mextram model. The preliminary version has been completed in June 2000. This report documents version 504.5.

October 2004, J.P.

March 2005

In the fall of 2004, Mextram was elected as a world standard transistor model by the *Compact Model Council (CMC)*, a consortium of representatives from over 20 major semiconductor manufacturers.

This report documents version 504.6.

March 2005, RvdT.

Spring 2008

In 2007, the notion of flexible topology was introduced by the community of compact model developers and model implementation specialists. In the spring 2008 release of Mextram, this was used to extend the topology of Mextram and add the distribution of the collector resistance in a backwards compatible manner.

This report documents version 504.7.

Spring 2008, RvdT.

Q4 2008, Q1 2009

This document presents version 504.8, which adds a model for Zener tunneling currents in the Emitter base junction.

Q4 2009 – Q1 2010

This document presents version 504.9, which extends collector-substrate modelling capabilities.

Q4 2010 – Q1 2011

This document presents version 504.10, which extends parasitic main current modelling capabilities.

Q3 2015

504.12 documentation. Major revisions include new sections on physical basis, epi-layer physics, emitter charge NQS effect, improved high frequency correlated noise and avalanche noise implementations.

Guofu Niu, 7/28/2015.

History of model and documentation

June 2000 : Release of Mextram level 504 (preliminary version)
Complete review of the model compared to Mextram level 503

April 2001 : Release of Mextram 504, version 0 (504.0)
Small fixes:
– Parameters $\mathsf{R_{th}}$ and $\mathsf{C_{th}}$ added to MULT-scaling
– Expression for α in Eq. (4.227) fixed
Changes w.r.t. June 2000 version:
– Addition of overlap capacitances $\mathsf{C_{BEO}}$ and $\mathsf{C_{BCO}}$
– Change in temperature scaling of diffusion voltages
– Change in neutral base recombination current (4.179)
– Addition of numerical examples with self-heating

September 2001 : Release of Mextram 504, version 1 (504.1)
Lower bound on $\mathsf{R_{th}}$ is now $0°\mathrm{C/W}$
Small changes in F_{ex} (4.166a) and $Q_{B_1B_2}$ (4.173) for robustness

March 2002 : Release of Mextram 504, version 2 (504.2)
Numerical stability improvement of x_i/W_{epi} at small $\mathcal{V}_{\mathrm{C_1C_2}}$, p. 58
Numerical stability improvement of p_0^*, Eq. (4.209)

December 2002 : Minor changes in documentation, not in model

October 2003 : Release of Mextram 504, version 3 (504.3)
MULT has been moved in list of parameters
Lower clipping value of $\mathsf{T_{ref}}$ changed to $-273°\mathrm{C}$
Added I_C, I_B and β_{dc} to operating point information

April 2004 : Release of Mextram 504, version 4 (504.4)
Noise of collector epilayer has been removed

October 2004 : Release of Mextram 504, version 5 (504.5)

Addition of temperature dependence of thermal resistance
Addition of noise due to avalanche current

March 2005 : Release of Mextram 504, version 6 (504.6)
Added parameter $\mathsf{dA_{ls}}$ for fine tuning of temp. dep. of $\mathsf{I_{sT}}$; eqn. (4.37)
"$G_{\rm EM} = 0$" added to equation (4.68)
Upper clipping value 1.0 of $\mathsf{K_{avl}}$ introduced

March 2008 : Release of Mextram 504, version 7 (504.7)
Added resistances of buried layer $\mathsf{R_{Cblx}}$and $\mathsf{R_{Cbli}}$, and their temperature scaling parameter $\mathsf{A_{Cbl}}$.
Lower clipping value of resistances $\mathsf{R_E}$, $\mathsf{R_{BC}}$, $\mathsf{R_{BV}}$, $\mathsf{R_{Cc}}$, $\mathsf{R_{Cv}}$, $\mathsf{SCR_{Cv}}$ increased to $1\mathrm{m}\Omega$
Bug fix high temperature limit B_{nT} .

June 2009 : Release of Mextram 504, version 8 (504.8),
Zener tunneling current in emitter-base junction:
– Sections: 2.1.4, 3, 4.7.5, 4.15
– Parameters: $\mathsf{I_{zEB}}$, $\mathsf{N_{zEB}}$
– Material constants, implemented as parameters: $\mathsf{V_{gzEB}}$, $\mathsf{A_{VgEB}}$, T_{VgEB}
– Equations: (4.51b) to (4.51e), (4.117a), (4.184), (4.199)
– OP-info: $g_{\pi,x}$, $I_{\rm ztEB}$

Q2, 2010 : Release of Mextram 504, version 9 (504.9):

Small Fix w.r.t. 504.8:
– added lower clip value to parameter T_{VgEB} (§4.3)
Added to operating point information:
– external terminal voltages V_{BE}, V_{BC}, V_{CE}, V_{SE}, V_{BS}, V_{SC}
– external terminal currents I_E, I_S
Collector-substrate model:

– Parameters: $\mathsf{I_{CSs}}$, $\mathsf{A_{sub}}$
– physics based temperature scaling ideal collector-substrate current
– See: § 2.3.5, § 2.6.1, § 4.5, Eqns. (4.44), (4.64)

Q1, 2011 : Release of Mextram 504, version 10 (504.10):

Parasitic BCS transistor model:
– See: § 2.7.3, 2.3.5
– Parameter: EXSUB,
– See: Eqns. (2.35), (2.39), (4.62a), (4.62b), (4.65), (4.67)

– See: Eqns. (4.160), (4.162), (4.163a), (4.163b)

Revised documentation of $G_{\rm min}$:
– $G_{\rm min}$ is an industrial standard convergence aid and is as such

not a part of the physics-based Mextram model definition:
– Revised Sec. 4.4: $G_{\min}$ is *not* a model constant.
– See: revised doc. of Eqns. (4.60) and (4.61)
– See Sec. 4.14.1: Eqns. (4.200) and (4.201)

Q1, 2012 : Release of Mextram 504.10.1.
– Bugfix: OP-info f_T: Eqn. (4.233)
– Bugfix: Equilibrium state parasitic BCS transistor:
• Eqn's. (4.65), (4.66), (4.67)
• Eqn's. (4.160), (4.161), (4.162)

Q4, 2012 : Release of Mextram 504.11.0,
– Added for operating point information of I_{qs} :
$I_{qs} = 0$ when $I_{C_1C_2} \leq 0$; (See: note at end of section 4.17).
– Extend range of EXMOD (see table of parameter ranges, page 32):
• If $\mathsf{EXMOD} = 2$, $XI_{\rm ex}$ and $XQ_{\rm ex}$ will not have Ohmic asymptote.
• Modified Eqn's. (4.166a): condition $\mathsf{EXMOD} = 1$ added
• New Eqn. (4.166b)

Q3, 2015 : Release of Mextram 504.12.0.

Excess phase shift model parameters:
– Section: 2.1.8, 4.10
– New parameters: $\mathsf{X_{Q_B}}$, $\mathsf{K_E}$
– Equations: (2.14), (2.15), (4.175), (4.176), (4.177)
– Operating point info (4.17): $C_{be,x}$: included factor $(1 - \mathsf{K_E} * \mathsf{EXPHI})$

Improved high frequency correlation noise implementation:
– Section: 4.12.2
– New parameters: $\mathsf{K_C}$, $\mathsf{F_{taun}}$
– Equations: (4.186), (4.187)

Improved avalanche noise implementation:
– Section: 4.12.2
– Equation: (4.191)

Q2, 2016 : Release of Mextram 504.12.1.

Emitter charge formulation to fix reverse V_{BE} noise:
– Q_E, Equation: (4.145)
– Corresponding capacitance, (4.173), or lateral excess phase.

Contents

1 Introduction

Mextram is an advanced compact model for bipolar transistors that contains many features that the widely-used Gummel-Poon model lacks. Mextram stands for Most EXquisite TRAnsistor Model. Mextram has proven excellent for Si and SiGe processes, including analog, mixed-signal, high speed RF as well as high voltage high power technologies. It accounts for high injection effects with a dedicated epi-layer model, self heating, avalanche, low-frequency and high frequency noises in physical manners, and is formulated with minimal interactions between DC and AC characteristics that simplifies parameter extraction. Mextram can be used for uncommon situations like lateral NPN-transistors in LDMOS technology as well.

1.1 History

Mextram originated from NXP Semiconductors [1]. It was initially developed by De Graaff and Kloosterman in 1985 for internal use. In 1994, Mextram 503 was released to the public. Mextram 504 was developed in the late nineties for several reasons, the main ones being the need for even better description of transistor characteristics and the need for an easier parameter extraction. In fall 2004, Mextram was elected as a world standard transistor model by the *Compact Model Coalition (CMC)*, a consortium of representatives from over 20 major semiconductor companies. In 2006, development moved to Delft University of Technology, where versions 504.6 to 504.12 beta were developed until mid 2014. Silvaco then provided intermediate development and support until April of 2015. Since then, Mextram has been developed and supported by the SiGe group at Alabama Micro/Nano Electronics Science and Technology Center, Electrical and Computer Engineering Department, Auburn University. Historically, the first digit 5 in the level or version number means it is a 5th generation bipolar transistor model, as compared to prior generation EM1, EM2, EM3 and the Gummel-Poon (GP) models.

The improved description of transistor characteristics of Mextram 504 compared to Mextram 503 were achieved by changing some of the formulations of the model. For instance Mextram 504 contains the Early voltages as separate parameters, whereas in Mextram 503 they were calculated from other parameters. This is needed for the description of SiGe processes and improves the parameter extraction (and hence the description) in the case of normal transistors. An even more important improvement is the description of the epilayer. Although the physical description has not changed, the order in which some of the equations are used to get compact model formulations has been modified. The result is a much smoother behavior of the model characteristics, i.e. the model formulations are now such that the first and higher-order derivatives are better. This is important for the output-characteristics and cut-off frequency, but also for (low-frequency) third order harmonic distortion. For the same reason of smoothness some other formulations, like that of the depletion capacitances, have been changed.

In Mextram almost all of the parameters have a physical meaning. This has been used in Mextram 503 to relate different parts of the model to each other by using the same

parameters. Although this is the most physical way to go, it makes it difficult to do parameter extraction, since some parameters have an influence on more than one physical effect. Therefore we tried in Mextram 504 to remove as much of this interdependence as possible, without losing the physical basis of the model. To do this we added some extra parameters. At the same time we removed some parameters of Mextram 503 that were introduced long ago but which had a limited influence on the characteristics, and were therefore difficult to extract.

1.2 Survey of modelled effects

Mextram contains descriptions for the following effects:

- Bias-dependent Early effect
- Low-level non-ideal base currents
- High-injection effects
- Ohmic resistance of the epilayer
- Velocity saturation effects on the resistance of the epilayer
- Hard and quasi-saturation (including Kirk effect)
- Weak avalanche in the collector-base junction (optionally including snap-back behaviour)
- Zener-tunneling current in the emitter-base junction
- Charge storage effects
- Split base-collector and base-emitter depletion capacitance
- Substrate effects and parasitic PNP
- Explicit modelling of inactive regions
- Current crowding and conductivity modulation of the base resistance
- First order approximation of distributed high frequency effects in the intrinsic base (high-frequency current crowding and excess phase-shift)
- Recombination in the base (meant for SiGe transistors)
- Early effect in the case of a graded bandgap (meant for SiGe transistors)
- Temperature scaling
- Self-heating
- Thermal noise, shot noise and $1/f$-noise

Mextram does not contain extensive geometrical or process scaling rules. A multiplication factor is provided to model perfectly ideal parallel connection of multiple transistors. The model is well scalable, however, especially since it contains descriptions for the various intrinsic and extrinsic regions of the transistor.

Some advanced features can be switched on or off by setting flags, including:

- Extended modeling of reverse behaviour.
- Distributed high-frequency effects.
- The increase of the avalanche current when the current density in the epilayer exceeds the doping level.
- The increase of intrinsic base current noise with frequency and its correlation with intrinsic collector current noise.
- Additional noises from impact ionization as well as avalanche multiplication.

The same code works for both NPN and PNP with proper sign changes in a few places. Unless specified, we assume NPN for all discussions.

Four variants of the model are provided:

- Three terminal discrete device without self heating.
- Three terminal discrete device with self heating.
- Four terminal integrated device, with a substrate connection, without self heating.
- Four terminal integrated device, with a substrate connection, with self heating.

1.3 Document Organization

Below we give the model definition of Mextram 504, including equivalent circuit topology, equations for currents, charges, resistances, noise sources, and parameter sets.

Sec. 2 describes physical basis of the model as well as model parameters in relevant subsections. Sec. 3 gives a brief introduction to parameter extraction. Most parameters can be extracted from capacitance, DC and S-parameter measurements and are process and transistor layout (geometry) dependent. Initial/predictive parameter sets can be computed from process and layout data.

Sec. 4 describes model equations as implemented in Verilog-a code and serves as an implementation guide. All model equations are *explicit* functions of internal branch voltages and therefore no internal quantities have to be solved iteratively.

Sec. 5 describes translation of Mextram 503 parameters to Mextram 504 parameters. As a help for the implementation, numerical examples are given in Sec. 6.

More in-depth discussions of the physics behind the model and parameter extraction are available in [2] and [3], respectively. An introduction into model usage can be found in Ref. [4].

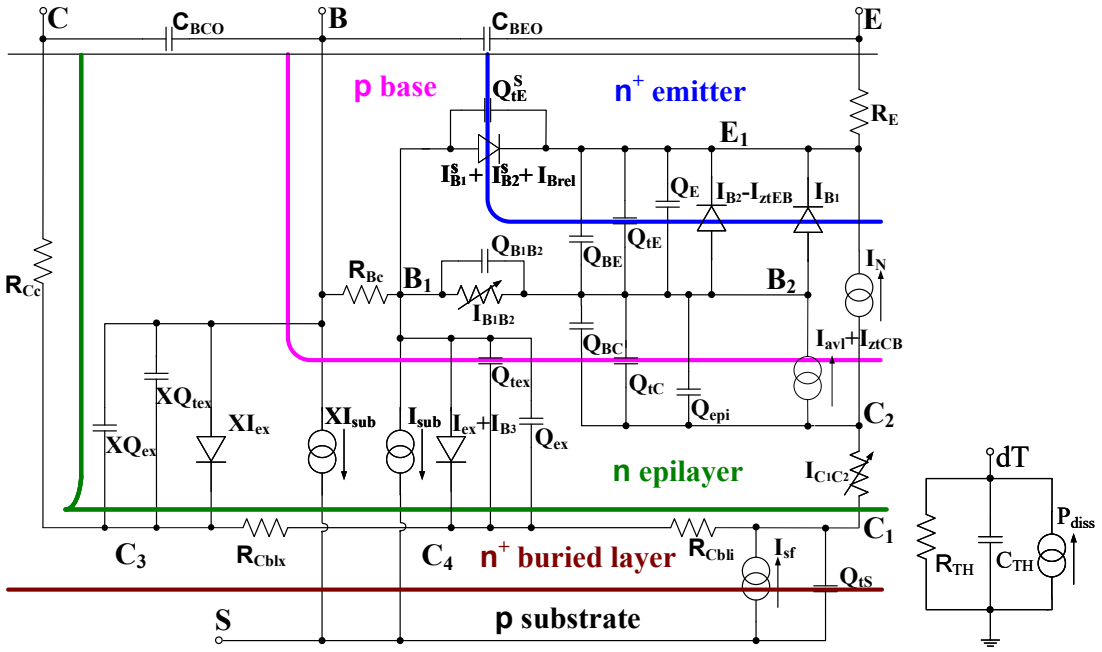

Figure 1: *The full Mextram equivalent circuit for the vertical NPN transistor. Schematically the different regions of the physical transistor are shown. The current $I_{B_1B_2}$ describes the variable base resistance and is therefore sometimes called R_{Bv}. The current $I_{C_1C_2}$ describes the variable collector resistance (or epilayer resistance) and is therefore sometimes called R_{Cv}. The extra circuit for self-heating is discussed below in Sec. 4.13.*

2 Physics of the model

We now introduce the physics behind Mextram. Reference to classic Gummel-Poon model [5] is made where appropriate to help understanding. For extensive details of the physics and derivation of Mextram, refer to Ref. [2].

Mextram, as any other bipolar compact model, describes transistor electrical characteristics using an equivalent circuit. Fig. 1 shows the equivalent circuit used in current release, with currents and charges placed on a drawing of NPN transistor 2D cross section to show their physical origins.

Fig. 2 shows another version with standard counterclockwise placement of the collector (C), base (B), emitter (E) and substrate (S) terminals, as found in transistor symbols used by typical process design kit (PDK). B_2, C_2 and E_1 are intrinsic NPN terminals. B_1 is an internal node for base resistance related parasitic effects. C_1, C_3 and C_4 are internal nodes for collector resistance related parasitic effects, the most significant of which is the epilayer related quasi-saturation effect. C_3 and C_4 are for distributive buried layer resistance effects and turned off by default.

I_N, I_{B_1}, I_{B_2}, I_{avl}, Q_{BE}, Q_{BC}, Q_{tE}, Q_{tC}, Q_E are placed between C_2, B_2 and E_1 to model

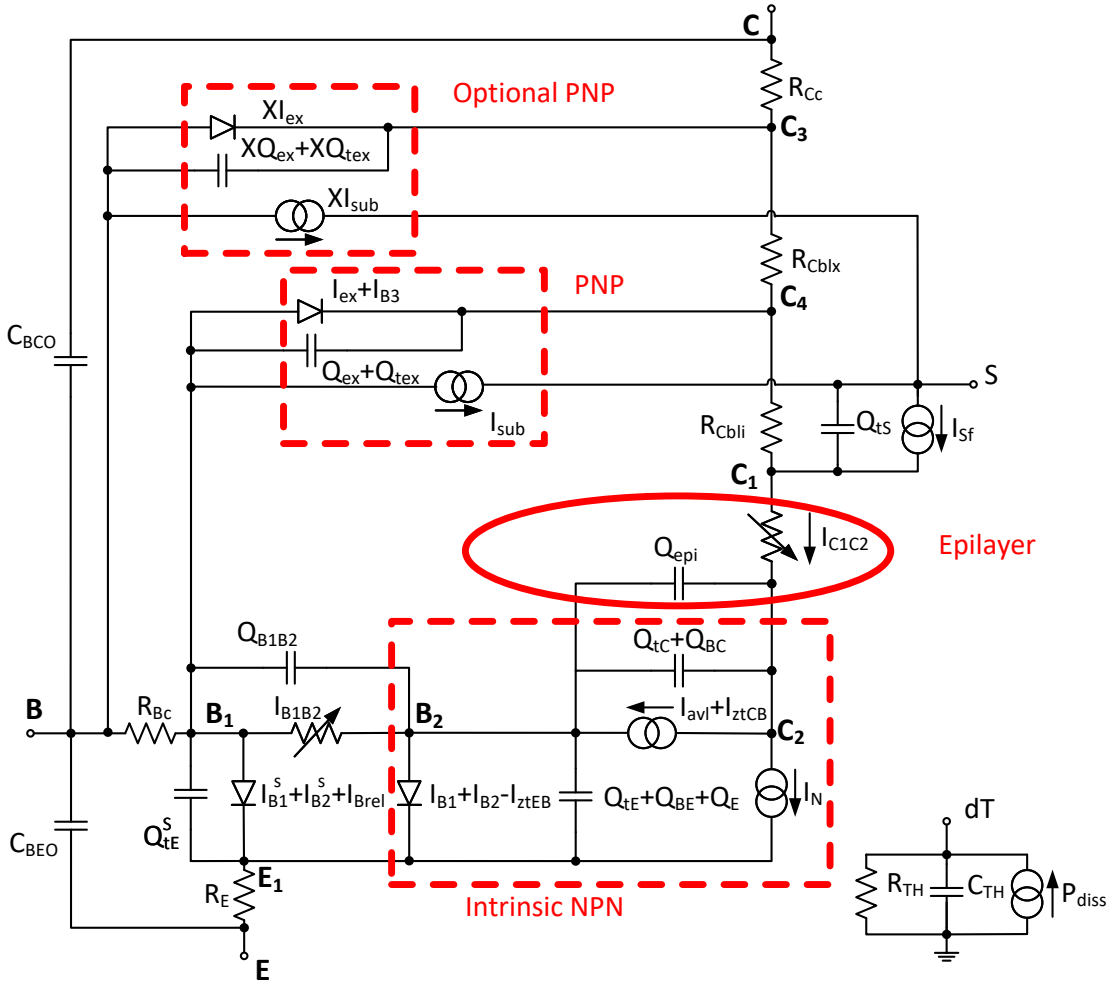

Figure 2: *Mextram equivalent circuit drawn with counterclockwise placement of the collector, base, emitter and substrate terminals as found in bipolar transistor symbols.*

the intrinsic NPN transistor. I_N is the main electron transport current, I_{B_1} and I_{B_2} are forward ideal and non-ideal base currents, $I_{\rm avl}$ is avalanche current. Q_{tE} and Q_{tC} are EB and CB junction depletion charges.

Unlike the GP model, Mextram does not have reverse base currents between B_2 and C_2 in its intrinsic transistor description. Instead, reverse base currents are modeled by the parasitic PNP base currents $I_{\rm ex}$, I_{B_3}, and PNP emitter to collector transport current $I_{\rm sub}$. The parasitic PNP transistor is formed by the extrinsic p-base of the NPN, which acts as emitter of the PNP, n-collector of the NPN, which acts as base of the PNP, and the p-substrate, which acts as the collector of the PNP. The parasitic PNP can be optionally further partitioned to account for distributive effect as shown.

Tables 1 and 2 summarize description of the currents and charges respectively. Below we describe in more details every current and charge in this equivalent circuit.

To improve clarity, we use a sans-serif font, e.g. $\mathsf{V_{d_E}}$ and $\mathsf{R_{Cv}}$ for model parameters, a list

of which is given in section 4.3. For the node-voltages as given by the circuit simulator, we use a calligrafic $\mathcal{V}$, e.g. $\mathcal{V}_{\mathrm{B_2E_1}}$ and $\mathcal{V}_{\mathrm{B_2C_2}}$. All other quantities are in normal (italic) font, like $I_{C_1C_2}$ and $V^*_{B_2C_2}$.

We will first describe the intrinsic transistor, and then the extrinsic parasitics.

2.1 Intrinsic transistor

2.1.1 Main current I_N

Like the GP model, I_N is based on the generalized Moll-Ross relation [6, 7], better known as the integral charge control relation (ICCR) [8]:

$$I_N = \mathsf{I_s}\left(e^{\mathcal{V}_{\mathrm{B_2E_1}}/V_T} - e^{V^*_{B_2C_2}/V_T}\right)\frac{1}{q_B}, \tag{2.1}$$

where $\mathsf{I_s}$ is saturation current, $\mathcal{V}_{\mathrm{B_2E_1}}$ and $V^*_{B_2C_2}$ [†] are forward biases of the intrinsic base-emitter and base-collector junctions, $V_T = kT/q$ is thermal voltage as defined in table 3, and q_B is normalized *neutral* base hole charge accounting for 1) neutral base width modulation due to depletion boundary shifts; and 2) increase of hole density to neutralize diffusion charges from minority carrier injection:

$$q_B = \frac{Q_{B0} + Q_{t_E} + Q_{t_C} + Q_{BE} + Q_{BC}}{Q_{B0}}, \tag{2.2}$$

where Q_{B0} is the equilibrium base hole charge, i.e., when both junctions are at zero biases, Q_{tE} and Q_{tC} are changes from equilibrium due to depletion boundary shift alone without accounting for minority carrier injection, which gives rise to Q_{BE} and Q_{BC}, as illustrated in Fig. 3, with a NPN transistor. Observe that the same neutral base boundaries used for Q_{tE} and Q_{tC} definition are also used in defining Q_{BE} and Q_{BC}.

While Q_{tE} and Q_{tC} are referred to as *depletion charges* which is standard in compact modeling literature for very good reason, they differ from and are easily confused with the depletion charges found in standard textbook PN junction treatment. In compact modeling, Q_{tE} refers to the increase of base majority carrier charge from its equilibrium value due to a forward EB junction bias, which physically equals the decrease of total charges on the base side of the EB junction depletion layer from its equilibrium value. Similarly, Q_{tC} refers to the increase of base majority carrier charge from its equilibrium value due to a forward CB junction bias. They are not absolute depletion charges that have a fixed sign, rather, they are *changes compared to equilibrium due to junction bias*, which are positive for forward bias and negative for reverse bias.

Q_{BE} and Q_{BC} are referred to as junction *diffusion charges* which are also subject to the same neutral base width change as represented by Q_{tE} and Q_{tC}.

[†] $V^*_{B_2C_2}$ is a calculated quantity and not the node voltage $\mathcal{V}_{\mathrm{B_2C_2}}$ due to the way Mextram implements its epi layer model. For its interpretation the difference is not very important, but for the smoothness of the model it is. See Sec. 2.2.

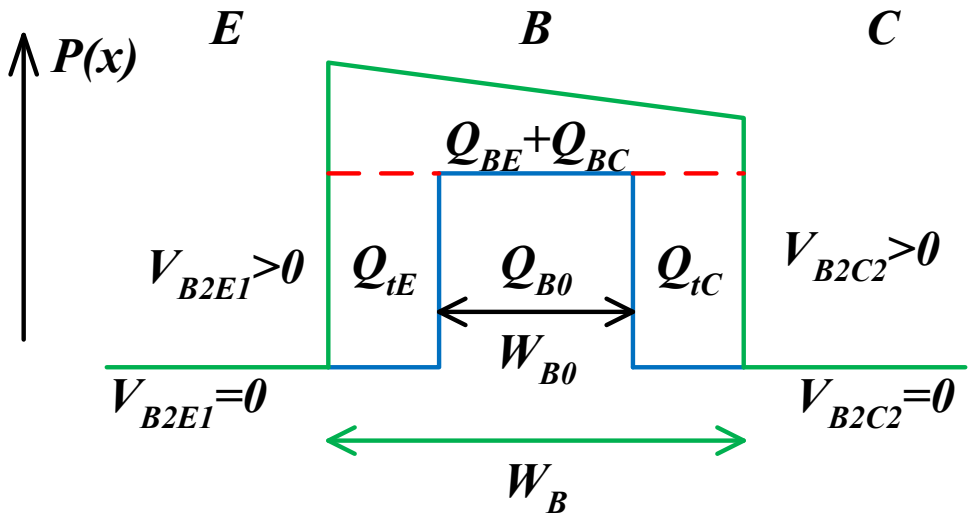

Figure 3: *Definition of depletion and diffusion charges used in Mextram.*

An inspection of Fig. 3 immediately leads to q_B as a product of two terms, a q_1 term representing neutral base width change, and another term representing minority carrier injection:

$$q_B = q_1\ (1 + \tfrac{1}{2}n_0 + \tfrac{1}{2}n_B), \tag{2.3}$$

where n_0 and n_B are the electron densities at the emitter and collector edge of the neutral base. Both are normalized to the (average) base doping and directly depend on the internal junction voltages $\mathcal{V}_{\mathrm{B_2E_1}}$ and $V_{B_2C_2}$ according to pn product junction laws at the neutral base edges. This way, high injection effect in the base is naturally included, using a single knee current $\mathsf{I_k}$ as opposed to two in the GP model.

The q_1 term represents relative neutral base width change that can be evaluated from integration of depletion capacitance-voltage curves, and parameterized in terms of voltages:

$$q_1 = \frac{Q_{B0} + Q_{t_E} + Q_{t_C}}{Q_{B0}} = 1 + \frac{W_B}{W_{B0}} = 1 + \frac{V_{t_E}(\mathcal{V}_{\mathrm{B_2E_1}})}{\mathsf{V_{er}}} + \frac{V_{t_C}(\mathcal{V}_{\mathrm{B_2C_1}}, I_{C_1C_2})}{\mathsf{V_{ef}}}, \tag{2.4}$$

where $\mathsf{V_{ef}}$ and $\mathsf{V_{er}}$ are forward and reverse Early voltages to signal their relation to Early effects, and V_{t_E} and V_{t_C} are evaluated from C-V integration. For smoothness, the base-collector junction bias used for V_{t_C} is not the same as $V^*_{B_2C_2}$ but relates to it in implementation, and will be denoted as V_{junc}.

V_{t_E} and V_{t_C} represent *relative* neutral base width changes, and hence relate to capacitance model parameters that describe relative changes of C-V or Q-V curves, i.e., curvatures instead of magnitude.

In model implementation, V_{t_E} and V_{t_C} are calculated first and then used to calculate Q_{tE} and Q_{tC} as: $Q_{t_E} = (1 - \mathsf{XC_{jE}}) \cdot \mathsf{C_{jE}} \cdot V_{t_E}$ and $Q_{t_C} = \mathsf{XC_{jC}} \cdot \mathsf{C_{jC}} \cdot V_{t_C}$. The zero bias depletion capacitances, $\mathsf{C_{jE}}$ and $\mathsf{C_{jC}}$ as well as $\mathsf{XC_{jE}}$, $\mathsf{XC_{jC}}$, the partition factors, thus do not affect the main current. More details are given below in 2.1.5 and 2.1.6.

Table 1: *The currents of the equivalent circuit given in Fig. 1 on page 4.*

Currents	
I_N	Main current
$I_{C_1C_2}$	Epilayer current
$I_{B_1B_2}$	Pinched-base current
$I^S_{B_1}$	Ideal side-wall base current
I_{B_1}	Ideal forward base current
I_{B_2}	Non-ideal forward base current
I_{B_3}	Non-ideal reverse base current
$I_{\rm avl}$	Avalanche current
$I_{\rm ex}$	Extrinsic reverse base current
$XI_{\rm ex}$	Extrinsic reverse base current
$I_{\rm sub}$	Substrate current
$XI_{\rm sub}$	Substrate current
$I_{\rm Sf}$	Substrate failure current

The model parameters involved are:

$\mathsf{I_s}$	The transistor main saturation current
$\mathsf{I_k}$	The knee current for high injection effects in the base
$\mathsf{V_{ef}}$ and $\mathsf{V_{er}}$	The forward and reverse Early voltages

The model parameters for the charges are discussed below in section 2.1.5 and 2.1.6.

2.1.2 Ideal forward base current

The ideal forward base current is defined in the usual way. The total base current has a bottom and a sidewall contribution. The separation is given by the factor $\mathsf{XI_{B_1}}$. This factor can be determined by analysing the maximum current gain of transistors with different geometries.

$$I_{B_1} = (1 - \mathsf{XI_{B_1}})\,\frac{\mathsf{I_s}}{\mathsf{\beta_f}}\,\left(e^{\mathcal{V}_{\rm B_2E_1}/V_T} - 1\right), \tag{2.5}$$

$$I^S_{B_1} = \mathsf{XI_{B_1}}\,\frac{\mathsf{I_s}}{\mathsf{\beta_f}}\,\left(e^{\mathcal{V}_{\rm B_1E_1}/V_T} - 1\right). \tag{2.6}$$

The parameters are:

$\mathsf{\beta_f}$	Ideal forward current gain
$\mathsf{XI_{B_1}}$	Fraction of ideal base current that belongs to the sidewall

2.1.3 Non-ideal forward base current

The non-ideal forward base current originates from the recombination in the depleted base-emitter region and from many surface effects. A general formulation with a non-

Table 2: *The charges of the equivalent circuit given in Fig. 1 on page 4.*

Charges	
Q_{BEO}	Base-emitter overlap charge
Q_{BCO}	Base-collector overlap charge
Q_E	Emitter charge or emitter neutral charge
Q_{t_E}	Base-emitter depletion charge
$Q_{t_E}^S$	Sidewall base-emitter depletion charge
Q_{BE}	Base-emitter diffusion charge
Q_{BC}	Base-collector diffusion charge
Q_{t_C}	Base-collector depletion charge
$Q_{\rm epi}$	Epilayer diffusion charge
$Q_{B_1B_2}$	AC current crowding charge
$Q_{\rm tex}$	Extrinsic base-collector depletion charge
$XQ_{\rm tex}$	Extrinsic base-collector depletion charge
$Q_{\rm ex}$	Extrinsic base-collector diffusion charge
$XQ_{\rm ex}$	Extrinsic base-collector diffusion charge
Q_{t_S}	Collector-substrate depletion charge

Table 3: *A list of some of the physical quantities used to describe the transistor.*

q	Unit charge
V_T	Thermal voltage kT/q
$L_{\rm em}$	Emitter length
$H_{\rm em}$	Emitter width
$A_{\rm em}$	Emitter surface $H_{\rm em}\,L_{\rm em}$
Q_{B0}	Base (hole) charge at zero bias
n_i	Intrinsic electron and hole density.
n_0	Normalized electron density in the base at the emitter edge
n_B	Normalized electron density in the base at the collector edge
$n_{B\rm ex}$	Normalized electron density in the extrinsic base at the collector edge
p_0	Normalized hole density in the collector epilayer at the base edge
p_W	Normalized hole density in the collector epilayer at the buried layer edge
$W_{\rm epi}$	Width the collector epilayer
$N_{\rm epi}$	Doping level of the collector epilayer
ε	Dielectric constant
$v_{\rm sat}$	Saturated drift velocity
μ	Mobility

ideality factor is used:

$$I_{B_2} = \mathsf{I_{Bf}} \left(e^{\mathcal{V}_{\mathrm{B_2E_1}}/\mathsf{m_{Lf}} V_T} - 1 \right). \tag{2.7}$$

When recombination is the main contribution we have $\mathsf{m_{Lf}} = 2$.

$\mathsf{I_{Bf}}$	Saturation current of the non-ideal forward base current
$\mathsf{m_{Lf}}$	Non-ideality factor of the non-ideal base current

2.1.4 Zener tunneling current in the emitter base junction

Mextram 504.8 adopted a model of Zener tunneling current in the emitter-base junction.

The Mextram 504.8 formulation is based on analytical formulations as documented in the semiconductor device physics literature [9], [10], [11]. which describe a Zener tunneling current as it flows in the emitter-base junction when the junction is forced in *reverse* bias ($V_{EB} > 0$).

In Mextram, in the *forward* bias regime it is assumed that the Zener tunneling current can always be negelected. This is implemented by formally setting the value of the Zener tunneling current identically equal to zero in forward bias and gives the computational advantage that Zener current does not need to be evaluated in forward bias.

It follows that all derivatives of the Zener current with respect to bias are identically equal to zero for $0 < V_{be}$ and hence in the limit $V_{be} \downarrow 0$. Smoothness of the tunneling current at zero bias then implies that *all* derivatives of the Zener current with respect to bias should vanish in the limit $V_{be} \uparrow 0$ at zero bias. This concerns the actual formulation of the Zener current in reverse bias and has been addressed as follows.

The Zener tunneling current depends on a factor commonly denoted by "D" [9], which takes degrees of occupation of conduction and valence bands into account. In the Mextram formulation of tunneling current, we adopt an advanced formulation [11] of D which furthermore takes effects of direction of electron momentum into account. It turns out that continuity at zero bias of current with respect to bias, up to and including the first derivative, is then automatically established. Subsequently, by dedicated adjustment of the description of the electric field, as applied in the D factor, continuity of *all* derivatives of current with respect to voltage has been established.

The temperature scaling of the model is fully physics based, which brings the advantage that the parameters of the temperature scaling model are material (bandgap) parameters. Values for these, for given semiconductor material, can be found in the literature. Since the Zener effect is not very sensitive to temperature in the first place, we expect that literature values for these parameters will in general suffice so that no dedicated parameter extraction will be needed in this respect.

The two remaining parameters, $\mathsf{I_{zEB}}$ and $\mathsf{N_{zEB}}$ of the Zener current model have been chosen with care so as to minimize their interdependence.

Regarding noise, we follow the JUNCAP2 [12] model and assume that the Zener tunneling current exhibits full shot noise.

2.1.5 Base-emitter depletion charge

The depletion charges are modeled in the classical way, using a grading coefficient. This classical formulation, however, contains a singularity, that is, capacitance becomes infinite when the forward bias equals the built-in voltage. In implementation, the capacitance is smoothly clipped to a constant, as illustrated in Fig.4. This maximum value is the zero-bias capacitance times a pre-defined factor α_j, which is 3.0 for the base-emitter depletion charge and 2.0 for the other depletion charges.

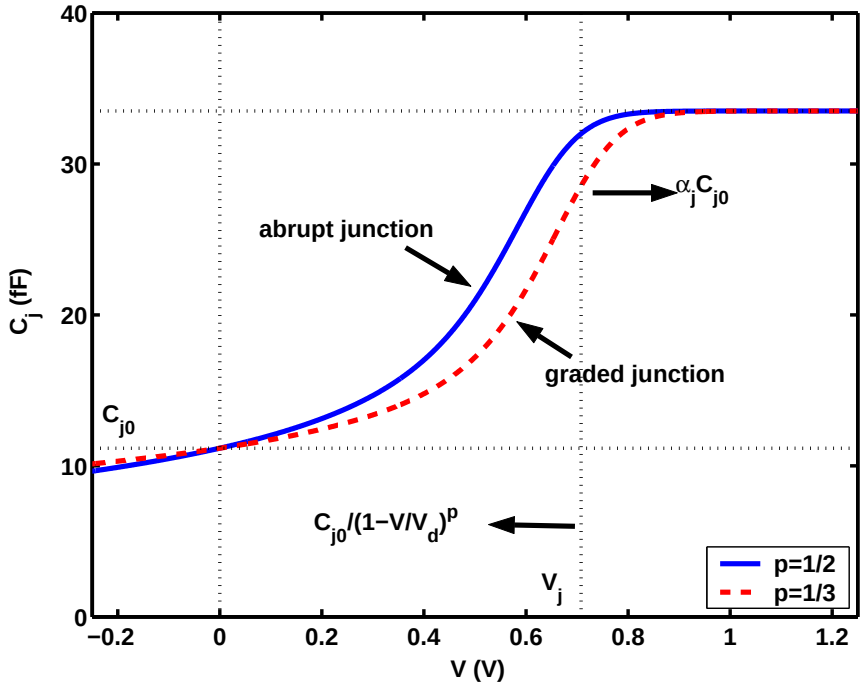

Figure 4: *An example of depletion capacitance C_j versus forward voltage V for an abrupt junction ($p = 1/2$) and a graded junction ($p = 1/3$) with clipping.*

The base-emitter depletion capacitance is partitioned into a bottom and a sidewall component by the parameter $\mathsf{XC_{jE}}$:

$$C_{t_E} = \frac{\mathrm{d}Q_{t_E}}{\mathrm{d}\mathcal{V}_{\mathrm{B_2E_1}}} = (1 - \mathsf{XC_{jE}})\,\frac{\mathsf{C_{jE}}}{(1 - \mathcal{V}_{\mathrm{B_2E_1}}/\mathsf{V_{dE}})^{\mathsf{pE}}}, \tag{2.8}$$

$$C^S_{t_E} = \frac{\mathrm{d}Q^S_{t_E}}{\mathrm{d}\mathcal{V}_{\mathrm{B_1E_1}}} = \mathsf{XC_{jE}}\,\frac{\mathsf{C_{jE}}}{(1 - \mathcal{V}_{\mathrm{B_1E_1}}/\mathsf{V_{dE}})^{\mathsf{pE}}}. \tag{2.9}$$

Smoothed versions are used to formulate V_{tE}, Q_{tE} and XQ_{tex} in implementation.

The model parameters are:

$\mathsf{C_{jE}}$	Zero bias emitter base depletion capacitance
$\mathsf{V_{dE}}$	Emitter base built-in voltage
$\mathsf{p_E}$	Emitter base grading coefficient
$\mathsf{XC_{jE}}$	The fraction of the BE depletion capacitance *not* under the emitter (sidewall fraction)

2.1.6 Base-collector depletion charge

The base-collector depletion capacitance C_{t_C} underneath the emitter takes into account the finite thickness of the epilayer and current modulation:

$$C_{t_C} = \frac{\mathrm{d}Q_{t_C}}{\mathrm{d}V_{\mathrm{junc}}} = \mathsf{XC_{jc}}\ \mathsf{C_{jc}}\ \left((1-\mathsf{X_p})\frac{f(I_{C_1C_2})}{(1-V_{\mathrm{junc}}/\mathsf{V_{dc}})^{\mathsf{pc}}} + \mathsf{X_p}\right), \tag{2.10}$$

$$f(I_{C_1C_2}) = \left(1 - \frac{I_{C_1C_2}}{I_{C_1C_2} + \mathsf{I_{hc}}}\right)^{\mathsf{m_C}}. \tag{2.11}$$

The junction voltage V_{junc} is calculated using the external base-collector bias minus the voltage drop over the epilayer, as if there were no injection and differs from $V^*_{b_2c_2}$ used for n_B in diffusion charge calculation. The current modulation (Kirk effect) has its own 'grading' coefficient $\mathsf{m_C}$ and uses the parameter $\mathsf{I_{hc}}$ from the epilayer model.

$\mathsf{C_{jc}}$	Zero bias collector-base depletion capacitance
$\mathsf{V_{dc}}$	Collector-base built-in voltage
$\mathsf{p_C}$	Collector-base grading coefficient
$\mathsf{XC_{jc}}$	The fraction of the BC depletion capacitance under the emitter.
$\mathsf{X_p}$	Ratio of depletion layer thickness at zero bias and epilayer thickness
$\mathsf{m_C}$	Collector current modulation coefficient [$\mathsf{m_C} \simeq 0.5\ (1-\mathsf{X_p})$].

2.1.7 Base diffusion charges

The base diffusion charges are obtained from integration of minority electrons in neutral base:

$$Q_{BE} = \tfrac{1}{2} q_1\ Q_{B0}\ n_0, \tag{2.12}$$

$$Q_{BC} = \tfrac{1}{2} q_1\ Q_{B0}\ n_B, \tag{2.13}$$

where q_1 models neutral base width modulation, n_0 and n_B are minority electron densities at the neutral base boundaries or minority carrier injection points, and Q_{B0} is the equilibrium base hole charge, as discussed earlier.

Q_{B0} is modeled as $Q_{B0} = \tau_{\mathsf{B}} \cdot \mathsf{I_k}$, with τ_{B} being the base transit time. In forward operation, n_0 is approximately proportional to $I_C/\mathsf{I_k}$, thus Q_{BE} is almost independent of $\mathsf{I_k}$, and so is the transit time. The same holds for reverse operation as well.

τ_{B}	The base transit time

2.1.8 Base-charge partitioning

Distributed high-frequency effects [13] are modeled, in first order approximation, both in lateral direction (high-frequency current-crowding) and in vertical direction (excess phase-shift). The distributed effects are an optional feature of the Mextram model and can be switched on and off by flag EXPHI.

Excess phase shift can only be modeled accurately when all the charges and resistances, especially in the extrinsic transistor and in the interconnect, are modeled properly. Even then the intrinsic transistor can have a (small) influence. This is modeled in Mextram using base-charge partitioning. For simplicity it is only implemented with a single partitioning factor, based on high-level injection. The previously calculated diffusion charges are changed according to:

$$Q_{BC} \rightarrow \mathsf{X_{Q_B}} \cdot (Q_{BE} + \mathsf{K_E} Q_E) + Q_{BC} \tag{2.14}$$

$$Q_{BE} \rightarrow (1 - \mathsf{X_{Q_B}}) \cdot (Q_{BE} + \mathsf{K_E} Q_E) \tag{2.15}$$

where $\mathsf{X_{Q_B}}$ represents the amount of the total charge in the base which is supplied by the collector instead of the base. The value of $\mathsf{X_{Q_B}}$ in Mextram is set to $\frac{1}{3}$ by default. The parameter $\mathsf{K_E}$ provides the option to include Q_E in the charge re-allocation; by default its value is zero.

In lateral direction (current crowding) a charge is added parallel to the intrinsic base resistance:

$$Q_{B_1B_2} = \tfrac{1}{5}\, \mathcal{V}_{\mathrm{B_1B_2}}\ (C_{t_E} + C_{BE} + C_E)\,. \tag{2.16}$$

2.2 Epilayer model

We now describe the physics of the epilayer model, perhaps the most difficult as well as most important part of Mextram. To effectively use the epilayer model, let us first develop some intuitions on how the internal charge, electric field and electron concentration distributions respond to current increase for a fixed external CB junction reverse bias, a configuration highly relevant in practice. From these intuitions, we introduce various modes of epilayer operation, namely, ohmic drift, space-charge-region drift (SCR drift), ohmic quasi-saturation (ohmic QS) and SCR quasi-saturation (SCR QS). For clarity, let us keep only the intrinsic NPN and the epilayer elements of Fig. 2.

2.2.1 Intuitions of ohmic drift, SCR drift, ohmic QS and SCR QS

Consider fixing the reverse external CB junction bias $V_{C_1B_2} > 0$ and increasing $V_{B_2E_1}$ to increase collector current.

Low CB voltage

Assume $V_{C_1B_2}$ is low, e.g. 1V, so CB junction field is low, and there is no velocity saturation, at least at low current. The base side of the epilayer is depleted, by a width dependent on internal bias $V_{C_2B_2}$=$V_{C_1B_2}$-$I_{C_1C_2}R_{epi}$, as shown in Fig. 5 (a). At low current, the rest of the epilayer simply behaves as an ohmic resistor, with a resistance dependent on the width of the charge neutral ohmic drift region. We denote this mode of epilayer operation *ohmic drift*.

At a sufficiently high current, the ohmic voltage drop is so large that $V_{C_2B_2}$ becomes sufficiently negative, corresponding to a forward internal junction bias $V_{B_2C_2}$ equal to built-in potential $\mathsf{V_{dC}}$. CB junction depletion layer disappears, and the whole epilayer becomes charge neutral, with $n = N_{epi}$, as shown in Fig. 5 (b). From ohm's law, the current at which ohmic quasi-saturation occurs can be estimated as $I_{qs,ohmic} \approx (V_{C_2B_2} + \mathsf{V_{dC}})/\mathsf{R_{Cv}}$, with $\mathsf{R_{Cv}}$ being the maximum resistance when the whole epilayer is ohmic.

With further increase of current, $V_{B_2C_2}$ essentially stays at $\mathsf{V_{dC}}$. As $V_{B_2C_1}$ is fixed, epilayer voltage drop $V_{C_1C_2}$ stays the same, a further increase of current is physically made possible by a decrease of resistance, through shrink of the ohmic drift region width. An region with significant injection of carriers forms, as shown in Fig. 5 (c). The drift region resistance is simply modified to $\mathsf{R_{Cv}}(1 - x_i/W_{epi})$. We denote this mode of epilayer operation as *ohmic quasi-saturation*. The increase of x_i decreases resistance, allowing further current increase.

At some current, current density reaches $qN_{epi}v_{sat}$, the maximum ohmic drift value possible. Ohmic drift can no longer support further increase of current. Instead, electron density becomes greater than N_{epi} to allow a further current increase. As $n > N_{epi}$, space charge region (SCR) forms near the end of the epilayer. The threshold current for this is denoted as $\mathsf{I_{hc}}$ in Mextram. This mode is denoted as *SCR quasi-saturation*, as shown in Fig. 5 (d). A numerical example of how x_i increases with current at a low V_{C1B2} is shown in Fig. 6.

High CB voltage

The evolution of epilayer operation mode with increasing current described above occurs at relatively low external CB junction voltage, in devices with relatively high $\mathsf{R_{Cv}}$, such as power devices, where the required I_{qs} is small compared to $\mathsf{I_{hc}}$. This can also be easily seen from $I_{qs,ohmic} \approx (V_{C_2B_1} + \mathsf{V_{dC}})/\mathsf{R_{Cv}}$.

At higher external CB junction voltage, or in devices with low $\mathsf{R_{Cv}}$, ohmic quasi-saturation current is higher than $\mathsf{I_{hc}}$, so that ohmic quasi-saturation never occurs. Instead, once current exceeds $\mathsf{I_{hc}}$, electron density in the CB junction depletion layer exceeds background doping density N_{epi}, net charge density reverses polarity, causing a reversal of the electric field gradient. The whole epilayer has space charge, and electrons drift across the whole space charge layer at saturation velocity, with a resistance corresponding to that for space charge limited drift, $\mathsf{SCR_{Cv}}$. We denote this epilayer operation mode *SCR drift*.

With further current increase, net charge density and hence field gradient increases. The

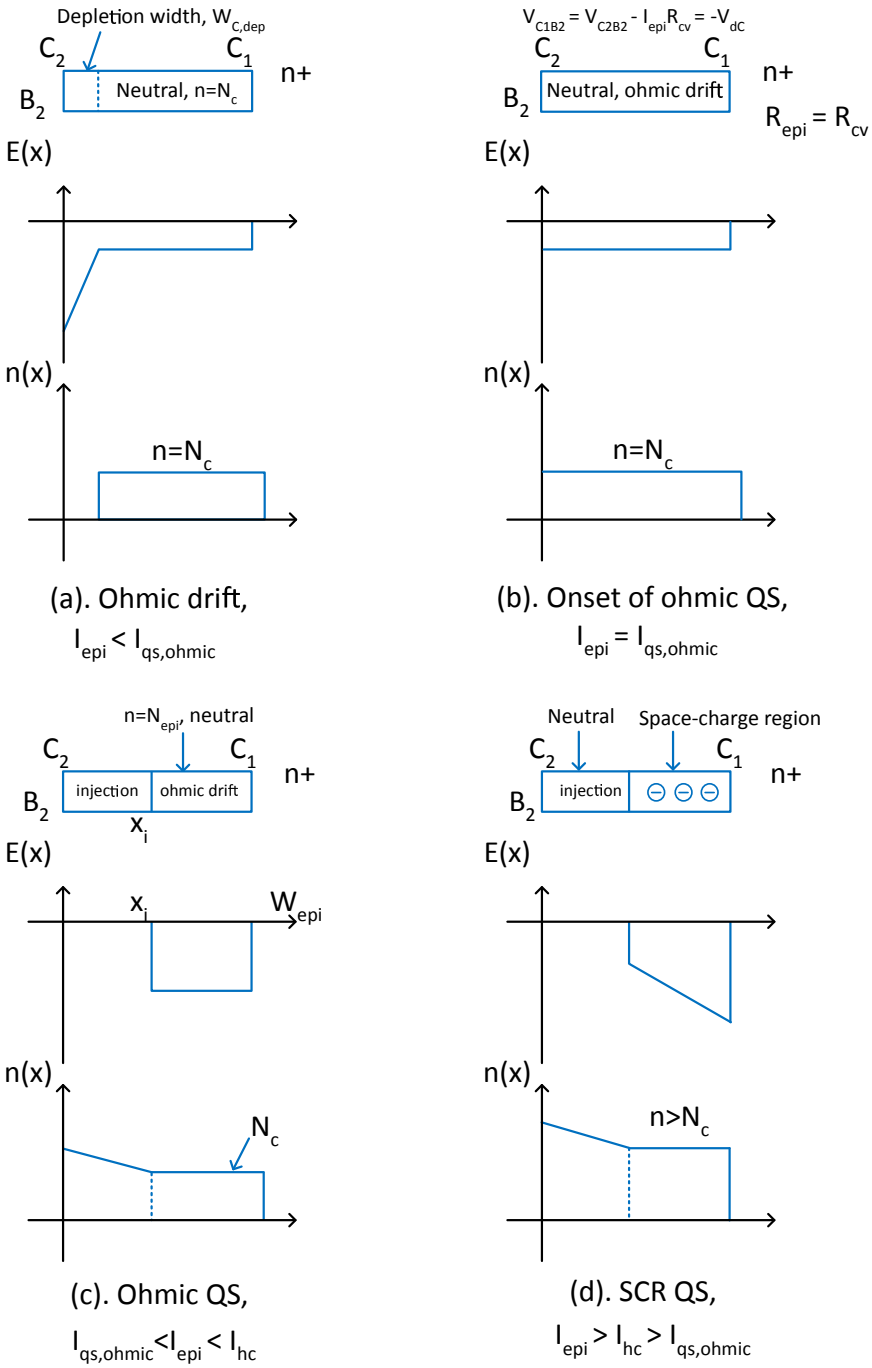

Figure 5: *Epilayer state evolution with increasing current at a low* V_{CB}.

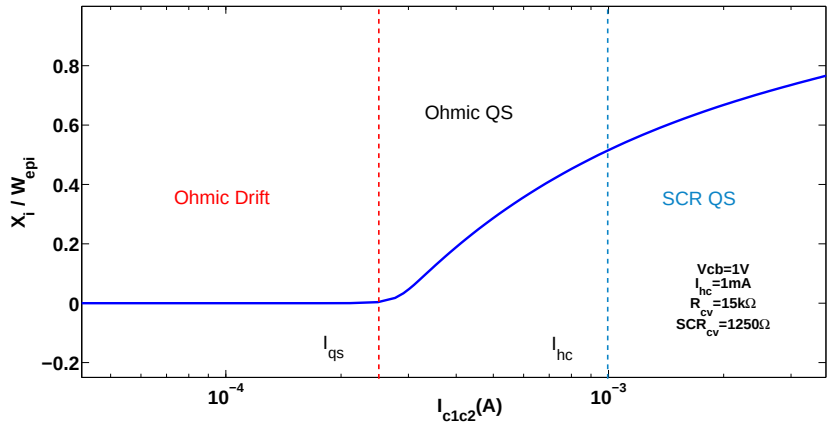

Figure 6: *A numerical example of x_i/W_{epi} as a function of $I_{C_1C_2}$ at a low V_{CB} for a device with high* $\mathsf{R_{Cv}}$

field at the base end of the epilayer decreases, while the field at the buried layer end increases, to maintain the same total voltage drop. At some point, the field at base/epilayer junction decreases to a low enough value, 0 in classic treatment, the critical field required for velocity saturation in Mextram, injection of holes and electrons occur again, often referred to as "base push-out." A quasi neutral injection region forms near the base/epilayer junction, followed by a space charge region. We denote this as *SCR quasi-saturation*, which is better known as Kirk effect outside the Mextram world. An illustration of the operation mode evolution described above is given in Fig. 7. A numerical example of how x_i increases with current at a high V_{C1B2} is shown in Fig. 8.

f_T implications

x_i is at the heart of the epilayer model, with expressions smoothly interpolating between physics based results obtained for the various ohmic and SCR drift and quasi-saturation modes described above, and closely relate to $\mathsf{R_{Cv}}$, $\mathsf{SCR_{Cv}}$, $\mathsf{I_{hc}}$, and of course, $I_{C_1C_2}$ and $V_{C_1B_2}$.

The most important consequence of quasi-saturation at high current is a degradation of f_T, primarily due to increased Q_{BC} from forward biasing of the internal CB junction, and the extra epilayer injection region charge $Q_{\rm epi}$. The increase of total transit time due to $Q_{\rm epi}$ relates to the epilayer transit time $\mathsf{t_{epi}}$ by $(x_i/W_{epi})^2$, as expected from basic minority carrier diffusion physics.

Fig. 9 illustrates the various modes of epilayer operation overlaid on $f_T - I_C$ curves for different V_{CB}, which can also be used to help with f_T fitting during parameter extraction. The peak f_T currents are the quasi-saturation onset currents, and can be used to extract $\mathsf{I_{hc}}$, $\mathsf{SCR_{Cv}}$, and $\mathsf{R_{Cv}}$.

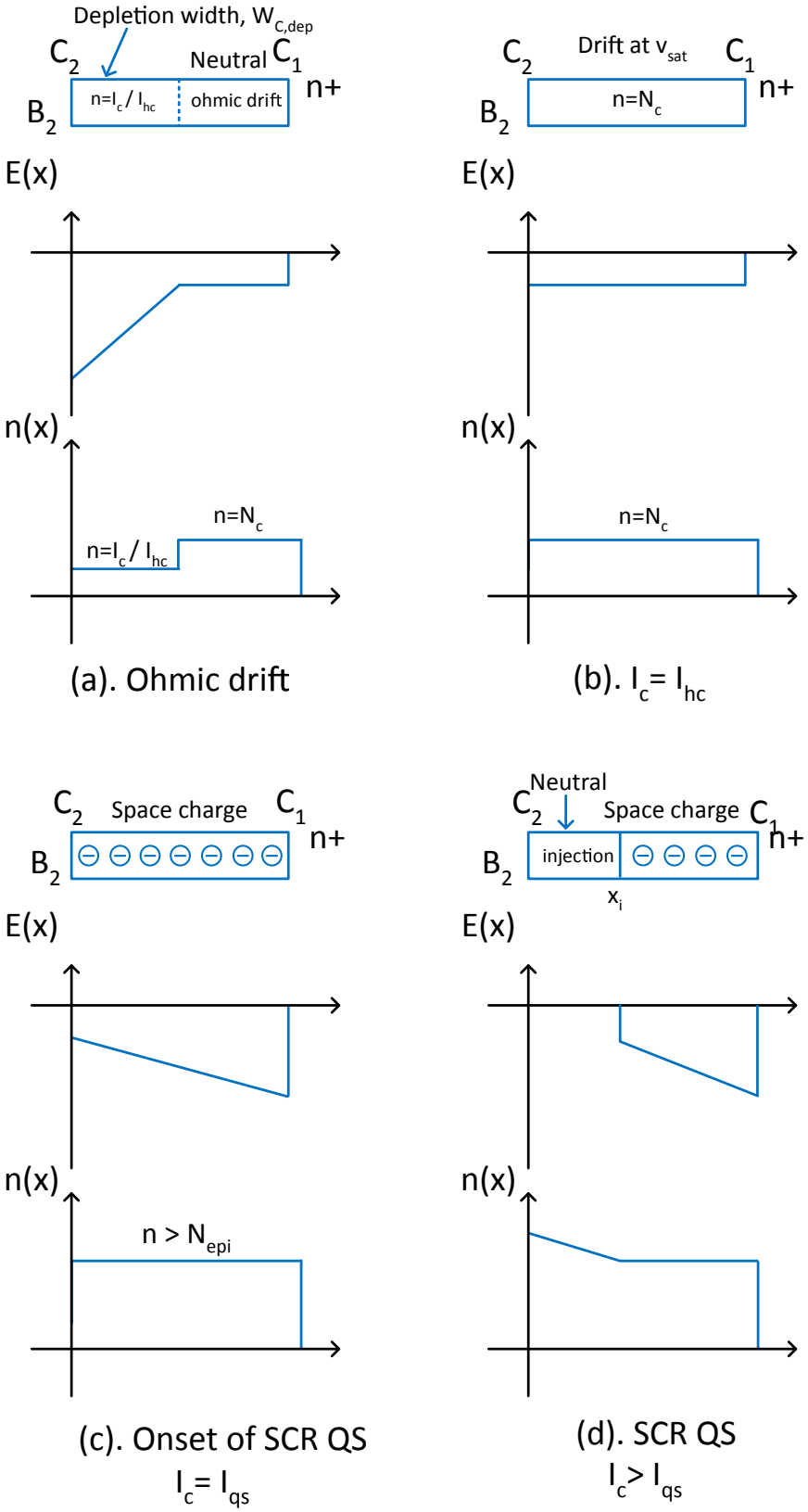

Figure 7: *Epilayer state evolution with increasing current at a high* V_{CB}.

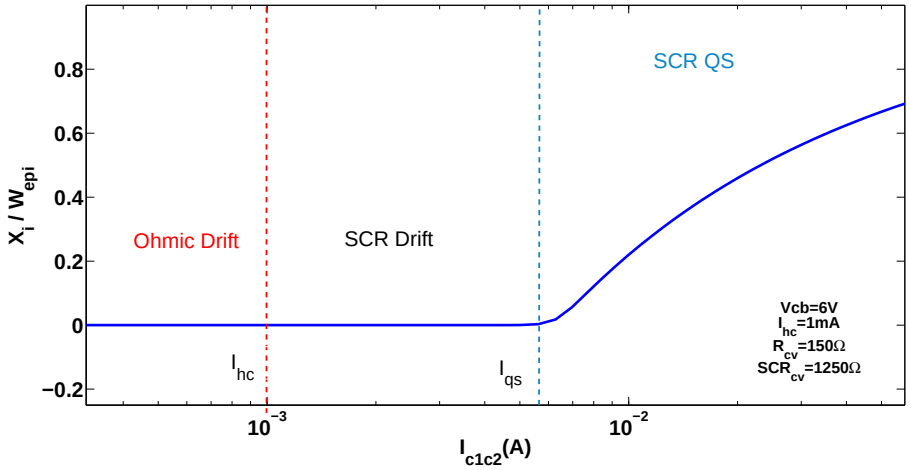

Figure 8: *A numerical example of x_i/W_{epi} as a function of $I_{C_1C_2}$ at a high V_{CB}.*

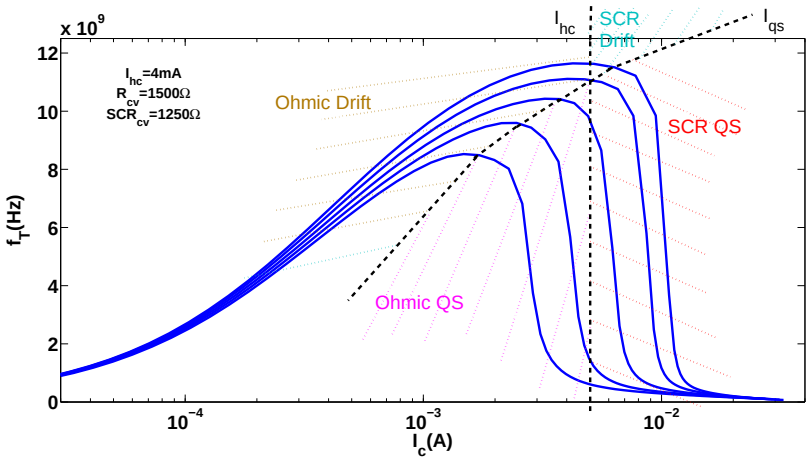

Figure 9: *Epilayer ohmic drift, SCR drift, ohmic quasi-saturation and SCR quasi-saturation operation regions overlaied on f_T versus I_C for different V_{CB}.*

2.2.2 Epilayer resistance - general consideration

This resistance is modeled as a current source $I_{C_1C_2}$, but it is also sometimes loosely denoted as $\mathsf{R_{Cv}}$, the variable part of the collector resistance. The resistance depends on the supplied collector voltage and the collector current, imposed primarily by the base-emitter voltage. In general, the effective resistance of the epilayer is strongly voltage- and current-dependent for the following reasons:

- In the forward mode of operation the internal base-collector junction voltage $\mathcal{V}_{\mathrm{B_2C_2}}$ may become forward-biased at high collector-currents (quasi-saturation). A region in the collector near the base will then be injected by carriers from the base. This injection region with thickness x_i has a low resistance.

- In the reverse mode of operation, both the external and internal base-collector junctions are forward biased. The whole epitaxial layer is then flooded with carriers and, consequently, has a low resistance.

- The current flow in the highly resistive region is Ohmic if the carrier density n is low ($n \ll N_{\mathrm{epi}}$) and space-charge limited if the carrier density exceeds the doping level N_{epi}. In the latter case the carriers move with the saturated drift velocity v_{sat} (hot-carrier current-flow).

- Current spreading in the epilayer reduces the resistance and is of special importance if the carrier density exceeds N_{epi}.

A compact model formulation of quasi-saturation is given by Kull et al. [14]. The model of Kull is only valid if the collector current is below the critical current for hot carriers:

$$\mathsf{I_{hc}} = qN_{\mathrm{epi}}v_{\mathrm{sat}}A_{\mathrm{em}}. \tag{2.17}$$

The Kull formulation has served as a basis for the epilayer model in Mextram. In the next section the model of Kull will be summarized and extended with hot carrier current flow (see also [15, 16, 17]).

2.2.3 Collector epilayer resistance model

The model of Kull is based on charge neutrality ($p + N_{\mathrm{epi}} \simeq n$) and gives the current $I_{C_1C_2}$ through the epilayer as a function of the internal and external base-collector biases. These biases are given by the solution vector of the circuit simulator. The final equations

of the Kull formulation are [14]

$$I_{C_1C_2} = \frac{E_c + \mathcal{V}_{\mathrm{C_1C_2}}}{\mathsf{R_{Cv}}}, \tag{2.18a}$$

$$E_c = V_T \left[2\,p_0 - 2\,p_W - \ln\left(\frac{p_0+1}{p_W+1}\right)\right], \tag{2.18b}$$

$$p_0 = \tfrac{1}{2}\sqrt{1 + 4\,\exp[(\mathcal{V}_{\mathrm{B_2C_2}} - \mathsf{V_{dc}})/V_T]} - \tfrac{1}{2}, \tag{2.18c}$$

$$p_W = \tfrac{1}{2}\sqrt{1 + 4\,\exp[(\mathcal{V}_{\mathrm{B_2C_1}} - \mathsf{V_{dc}})/V_T]} - \tfrac{1}{2}. \tag{2.18d}$$

The voltage source E_c takes into account the decrease in resistance due to carriers injected from the base into the collector epilayer. If both junctions are reverse biased ($\mathcal{V}_{\mathrm{B_2C_2}} < \mathsf{V_{dc}}$ and $\mathcal{V}_{\mathrm{B_2C_1}} < \mathsf{V_{dc}}$) then E_c is zero and we have a simple constant resistance $\mathsf{R_{Cv}}$. Therefore this model does not take into account the hot-carrier behavior (carriers moving with the saturated drift-velocity) in the lightly-doped collector epilayer.

The model is valid if the transistor operates in reverse mode, which means negative collector current $I_{C_1C_2}$. Normally this happens when the base-emitter junction is reverse biased and the base-collector junction is forward biased. The entire epilayer then gets filled with carriers and therefore a space-charge region will not exist.

In forward mode we have to change the formulation to include velocity saturation effects. The effective resistance for higher currents then becomes the space-charge resistance $\mathsf{SCR_{Cv}}$. Furthermore, the Kull model as described above, is not smooth enough (higher derivatives contain spikes) [16]. Mextram uses the following scheme in forward mode.

- Calculate $I_{C_1C_2}$ from the Kull model, Eq. (2.18), using the junction biases $\mathcal{V}_{\mathrm{B_2C_2}}$ and $\mathcal{V}_{\mathrm{B_2C_1}}$ given by the circuit simulator.
- Calculate the thickness x_i/W_{epi} of the injection region from the current, now including both Ohmic voltage drop and space-charge limited voltage drop

  $$I_{C_1C_2} = \frac{\mathsf{V_{dc}} - \mathcal{V}_{\mathrm{B_2C_1}}}{\mathsf{SCR_{Cv}}\,(1 - x_i/W_{\mathrm{epi}})^2} \times \frac{\mathsf{V_{dc}} - \mathcal{V}_{\mathrm{B_2C_1}} + \mathsf{SCR_{Cv}}\,\mathsf{I_{hc}}(1 - x_i/W_{\mathrm{epi}})}{\mathsf{V_{dc}} - \mathcal{V}_{\mathrm{B_2C_1}} + \mathsf{R_{Cv}}\,\mathsf{I_{hc}}}. \tag{2.19}$$

  The resulting thickness x_i will be different from that of the Kull model alone. In the implemented formulation we made sure that the equation does not lead to negative x_i/W_{epi}, by using a smoothing function with parameter $\mathsf{a_{x_i}}$.
- The Kull model is perfectly valid in the injection region. For this region we have the following equation

  $$\frac{x_i}{W_{\mathrm{epi}}}\, I_{C_1C_2}\, \mathsf{R_{Cv}} = E_c \simeq 2\,V_T\,(p_0^* - p_W)\,\frac{p_0^* + p_W + 1}{p_0^* + p_W + 2}. \tag{2.20}$$

  The approximation is such that both for very small and for very large p_0^* and p_W it gives the correct results, while in the intermediate regime it is off by maximally 5%.

From $x_i/W_{\rm epi}$, $I_{C_1C_2}$, and p_W we can therefore calculate p_0^*, the hole density at the internal base-collector junction. The * is used to denote the difference between p_0^* calculated here and p_0 from the Kull model, calculated in Eq. (2.18).

- From p_0^* we can calculate the physical value of the internal base-collector bias $V^*_{B_2C_2}$.
- This physical internal bias is smooth and contains all effects we want to include. It can therefore be used for the main current I_N in Eq. (2.1), for the diffusion charge Q_{BC} and for the epilayer charge $Q_{\rm epi}$.

Summarizing, the epilayer resistance model takes into account:

- Ohmic current flow at low current densities.
- Space-charge limited current flow at high current densities.
- The decrease in resistance due to carriers injected from the base if only the internal base-collector junction is forward biased (quasi-saturation) and if both the internal and external base-collector junctions are forward biased (reverse mode of operation).

We have used a different formulation for reverse mode ($I_{C_1C_2} < 0$) and forward mode ($I_{C_1C_2} > 0$). This does not give discontinuities in the first and second derivative. The third derivative however is discontinuous. This is no real problem since normally the transistor is not biased in this region.

The model parameters are:

$\mathsf{V_{dc}}$	Built-in voltage of the base-collector junction (also used in the depletion capacitance Q_{t_C})
$\mathsf{I_{hc}}$	Critical current for hot carrier behaviour
$\mathsf{R_{Cv}}$	Ohmic resistance of the total epilayer
$\mathsf{SCR_{Cv}}$	Space-charge resistance of the epilayer
$\mathsf{a_{x_i}}$	Smoothing parameter for the onset of quasi-saturation

The model parameters can be given in physical quantities. Note that this is not part of the model itself, but rather of the scaling one should perform around the model. It is important to take current spreading into account [15]. Therefore we present the scaling formula here for the parameters of the epilayer model. Other parameters need to be scaled too of course. (See table 3 for the meaning of some of the quantities.)

$$\mathsf{V_{dc}} = V_T \, \ln\left(N_{\rm epi}^2/n_i^2\right), \tag{2.21}$$

$$\mathsf{I_{hc}} = qN_{\rm epi}A_{\rm em}v_{\rm sat}\,(1+S_{fL})^2, \tag{2.22}$$

$$\mathsf{R_{Cv}} = \frac{W_{\rm epi}}{qN_{\rm epi}\mu A_{\rm em}}\,\frac{1}{(1+S_{fL})^2}, \tag{2.23}$$

$$\mathsf{SCR_{Cv}} = \frac{W_{\rm epi}^2}{2\varepsilon v_{\rm sat}A_{\rm em}}\,\frac{1}{(1+S_{fH})^2}. \tag{2.24}$$

The emitter area and the low and high-current spreading factors can be given as function of the emitter length $L_{\rm em}$ and width $H_{\rm em}$:

$$A_{\rm em} = H_{\rm em} L_{\rm em}, \tag{2.25}$$

$$S_{fL} = \tan(\alpha_l)\ W_{\rm epi}\ \left(\frac{1}{H_{\rm em}} + \frac{1}{L_{\rm em}}\right), \tag{2.26}$$

$$S_{fH} = \tfrac{2}{3}\ \tan(\alpha_h)\ W_{\rm epi}\ \left(\frac{1}{H_{\rm em}} + \frac{1}{L_{\rm em}}\right). \tag{2.27}$$

Here α_l is the spreading angle at low current levels ($I_{C_1C_2} < \mathsf{I_{hc}}$) and α_h is the spreading angle at high current levels ($I_{C_1C_2} > \mathsf{I_{hc}}$). Note that S_{fH} is in principle equal to the current spreading factor $\mathsf{S_{fH}}$ used in the high-current avalanche model.

2.2.4 Diffusion charge of the epilayer

The diffusion charge of the epilayer can be derived easily by applying the ICCR [7] to the injection region only:

$$I_{C_1C_2} = \mathsf{I_s}\ \left(e^{V^*_{B_2C_2}/V_T} - e^{\mathcal{V}_{\rm B_2C_1}/V_T}\right)\ \frac{Q_{B0}}{Q_{\rm epi}}. \tag{2.28}$$

Using the expressions from the epilayer current model this can be rewritten to

$$Q_{\rm epi} = \tau_{\mathsf{epi}}\ \frac{2\,V_T}{\mathsf{R_{Cv}}}\ \frac{x_i}{W_{\rm epi}}\ (p_0^* + p_W + 2). \tag{2.29}$$

The transit time can also be given in terms of other quantities.

$$\tau_{\mathsf{epi}} = \frac{W_{\rm epi}^2}{4\,D_n} = \mathsf{I_s}\ Q_{B0}\ \left(\frac{\mathsf{R_{Cv}}}{2\,V_T}\right)^2\ e^{\mathsf{V_{dC}}/V_T}. \tag{2.30}$$

This can be used as an initial guess in the parameter extraction (and was implicitely used in Mextram 503).

τ_{epi} Transit time of the epilayer

2.2.5 Avalanche multiplication model

Due to the high-electric field in the space-charge region avalanche currents will be generated. This generation of avalanche currents strongly depends on the maximum electric field. For low currents the maximum of the electric field will be at the base-collector junction. In the model of Ref. [18] the avalanche current is only a function of the electric field at the internal base-collector junction. Therefore the validity of this model is restricted to low current densities ($I_{C_1C_2} < \mathsf{I_{hc}}$). Our avalanche model [**?**] is based on Ref. [18], but does take this current dependence into account.

As an optional feature (using the flag EXAVL) the model is extended to current levels exceeding $\mathsf{I_{hc}}$, taking into account that the maximum of the electric field might reside

at the buried layer. Snap-back behaviour is then modelled as well, which gives a better physical description. For these high current densities current spreading in the collector region changes the electric-field distribution and decreases the maximum electric-field. Because the generation of avalanche current is very sensitive to the maximum electric-field it is difficult to make an accurate and still simple model for high collector current densities, so we have chosen an emperical solution [**?**]. Because this operating area (high voltages, high current levels) is not of very practical interest (due to power dissipation) and, more importantly, the convergency behaviour of the model degrades considerably (the output resistance can become negative), we have made it an optional feature. Without using the extended model the output resistance can be very small but it is always positive.

The generation of avalanche current is based on Chynoweth's empirical law for the ionization coefficient [**?**]. The probability P_n of the generation of an electron-hole pair per unit of length is

$$P_n = A_n \ \exp\left(\frac{-B_n}{|E|}\right). \tag{2.31}$$

Because only weak-avalanche multiplication is considered, the generated avalanche current is proportional with the main current $I_{C_1C_2}$ through the epilayer

$$I_{\text{avl}} = I_{C_1C_2} \int_{x=0}^{x=x_d} A_n \ \exp\left(\frac{-B_n}{|E(x)|}\right) \ \mathrm{d}x, \tag{2.32}$$

where x_d is the boundary of the space-charge region. To calculate the avalanche current we have to evaluate the integral of Eq. (2.32) in the space-charge region. This integral is strongly determined by the maximum electric field. We make a suitable approximation around this maximum electric field

$$E(x) \simeq E_M \ \left(1 - \frac{x}{\lambda}\right) \simeq \frac{E_M}{1 + x/\lambda}, \tag{2.33}$$

where λ is the point where the extrapolation of the electric-field is zero. The generated avalanche current becomes:

$$\frac{I_{\text{avl}}}{I_{C_1C_2}} = \frac{A_n}{B_n} \ E_m \ \lambda \ \left\{\exp\left[\frac{-B_n}{E_M}\right] - \exp\left[\frac{-B_n}{E_M} \ \left(1 + \frac{x_d}{\lambda}\right)\right]\right\}. \tag{2.34}$$

The maximum electric field E_M, the depletion layer thickness x_d, and the intersection point λ are calculated using the simple model for the capacitance of an abrupt junction. In the high current model also quasi-saturation and the Kirk effect are included.

The parameters are

$\mathsf{W_{avl}}$	The effective thickness of the epilayer for avalanche
$\mathsf{V_{avl}}$	A voltage describing the derivative of the electric field at low currents
$\mathsf{S_{fH}}$	High current spreading factor [see Eq. (2.27); used only when EXAVL=1]

2.3 Extrinsic regions

2.3.1 Reverse base current

The reverse base current, similar to I_{B_1}, is affected by high injection and partitioned over the two external base-collector branches (with parameter $\mathsf{X_{ext}}$). It uses the electron density $n_{B\mathrm{ex}}$ in the external region of the base

$$I_{\mathrm{ex}} = \frac{1}{2\beta_{\mathsf{ri}}}\, \mathsf{I_k}\, n_{B\mathrm{ex}}(\mathcal{V}_{\mathrm{B_1C_4}}) \quad . \tag{2.35}$$

The current XI_{ex} is calculated in a similar way using the density $Xn_{B\mathrm{ex}}(\mathcal{V}_{\mathrm{BC_3}})$. As the convergency may be affected by this partitioning, it is an optional feature (with flag EXMOD).

β_{ri}	Ideal reverse current gain
$\mathsf{X_{ext}}$	Partitioning factor of the extrinsic regions

2.3.2 Non-ideal reverse base current

The non-ideal reverse base current originates from the recombination in the depleted base-collector region:

$$I_{B_3} = \mathsf{I_{Br}}\, \frac{e^{\mathcal{V}_{\mathrm{B_1C_4}}/V_T} - 1}{e^{\mathcal{V}_{\mathrm{B_1C_4}}/2V_T} + e^{\mathsf{V_{Lr}}/2V_T}}. \tag{2.36}$$

The formulation of this non-ideal base current differs from the Gummel-Poon model. It is meant to describe a transition from ideality factor 1 ($\mathcal{V}_{\mathrm{B_1C_4}} < \mathsf{V_{Lr}}$) to ideality factor 2 ($\mathcal{V}_{\mathrm{B_1C_4}} > \mathsf{V_{Lr}}$).

$\mathsf{I_{Br}}$	Saturation current of the non-ideal reverse base current.
$\mathsf{V_{Lr}}$	Cross-over voltage of the non-ideal reverse base current.

2.3.3 Extrinsic base-collector depletion capacitance

The base-collector depletion capacitance of the extrinsic region is divided over the external-base node (charge: XQ_{tex}), and the internal-base node B_1 (charge: Q_{tex}). The partitioning is important for the output conductance Y_{12} at high frequencies. The model formulation is obtained by omitting the current modulation term in the formulation of Q_{t_C} in Eq. (2.10)

$$C_{\mathrm{tex}} = \frac{\mathrm{d}Q_{\mathrm{tex}}}{\mathrm{d}\mathcal{V}_{\mathrm{B_1C_4}}} = (1-\mathsf{X_{ext}})(1-\mathsf{XC_{jc}})\mathsf{C_{jc}} \left(\frac{1-\mathsf{X_p}}{(1-\mathcal{V}_{\mathrm{B_1C_4}}/\mathsf{V_{dc}})^{\mathsf{pc}}} + \mathsf{X_p} \right), \tag{2.37}$$

$$XC_{\mathrm{tex}} = \frac{\mathrm{d}XQ_{\mathrm{tex}}}{\mathrm{d}\mathcal{V}_{\mathrm{BC_3}}} = \mathsf{X_{ext}}\, (1-\mathsf{XC_{jc}})\, \mathsf{C_{jc}} \left(\frac{1-\mathsf{X_p}}{(1-\mathcal{V}_{\mathrm{BC_3}}/\mathsf{V_{dc}})^{\mathsf{pc}}} + \mathsf{X_p} \right). \tag{2.38}$$

Parameter used:

$\mathsf{X_{ext}}$	Partitioning factor for the extrinsic region

2.3.4 Diffusion charge of the extrinsic region

These charges are formulated in the same way as Q_{BC} and $Q_{\rm epi}$, and depend on the biases $\mathcal{V}_{\rm B_1C_4}$ and $\mathcal{V}_{\rm BC_3}$. The corresponding transit time should be the sum of $\tau_{\sf B}$ and $\tau_{\sf epi}$ multiplied by the ratio of the corresponding surfaces.

$\tau_{\sf R}$	Reverse transit time of the extrinsic regions

2.3.5 Parasitic Base-Collector-Substrate (BCS) transistor

The description of the main current of the parasitic Base-Collector-Substrate (BCS) transistor includes high injection of the forward main current.

$$I_{\rm sub} = \frac{2\,{\sf I_{SsT}}\,\left(e^{\mathcal{V}_{\rm B_1C_4}/V_T} - e^{\mathcal{V}_{\rm SC_4}/V_T}\right)}{1+\sqrt{1+4\,\dfrac{\sf I_{sT}}{\sf I_{ksT}}\,e^{\mathcal{V}_{\rm B_1C_4}/V_T}}} \quad ({\sf EXSUB}=1)\,. \tag{2.39}$$

Note that in this expression $4\,{\sf I_{sT}}/{\sf I_{ksT}}$ is used instead of $4\,{\sf I_{SsT}}/{\sf I_{ksT}}$ which simplifies parameter extraction [3].

When ${\sf EXMOD} = 1$ the substrate current is partitioned over the constant base resistance, just as $I_{\rm ex}$.

Up until and including Mextram 504.8, the reverse behaviour of the parasitic BCS was not modelled. Only a simple diode current $I_{\rm Sf}$ used to be present that was meant to act as a signal to designers. Therefore in backwards compatibility mode, when ${\sf I_{CSs}}$ has its default value -1.0, the collector-substrate junction current model reduces to this mode. From level 504.9 onwards, for physical values of ${\sf I_{CSs}}$, ${\sf I_{CSs}} \geq 0$, the substrate-collector junction is modeled by an ideal diode current $I_{\rm Sf}$; this model has a physics-based temperature scaling with a mobility temperature scaling parameter ${\sf A_{sub}}$.

Up until and including Mextram 504.9, Mextram did not contain a full description of the reverse main current of the BCS since it was believed not to be relevant to circuit designers. Mextram 504.10 introduced a reverse (SB) component of the main current of the parasitic transistor; this is the current component on $\mathcal{V}_{\rm SC_4}$ in Eqn. (4.62a). The counterpart in $XI_{\rm sub}$ depends on $\mathcal{V}_{\rm SC_3}$. Early- and reverse high current effects are not taken into account in the parasitic BCS transistor. For reasons of backwards compatibility, the $\mathcal{V}_{\rm SC_4}$- and $\mathcal{V}_{\rm SC_3}$- dependent components of the substrate currents are present only when ${\sf EXSUB} = 1$ (default: ${\sf EXSUB} = 0$).

EXSUB	Flag for extended modelling of substrate currents
${\sf I_{Ss}}$	Substrate saturation current.
${\sf I_{ks}}$	Knee in the substrate current, projected on ${\sf I_s}$
${\sf I_{CSs}}$	Collector-substrate ideal saturation current
${\sf A_{sub}}$	Temperature coefficient of ${\sf I_{CSs}}$

2.3.6 Collector-substrate depletion capacitance.

The collector-substrate capacitance C_{t_S} is modelled in the usual way

$$C_{t_S} = \frac{\mathrm{d}Q_{t_S}}{\mathrm{d}\mathcal{V}_{\mathrm{SC_1}}} = \frac{\mathsf{C_{js}}}{(1 - \mathcal{V}_{\mathrm{SC_1}}/\mathsf{V_{ds}})^{\mathsf{ps}}}. \tag{2.40}$$

The parameters used are

$\mathsf{C_{js}}$	Zero bias collector-substrate depletion capacitance
$\mathsf{V_{ds}}$	Collector-substrate built-in voltage
$\mathsf{p_S}$	Collector-substrate grading coefficient.

2.3.7 Constant overlap capacitances

The model has two constant overlap capacitances.

$\mathsf{C_{BEO}}$	Base-emitter overlap capacitance
$\mathsf{C_{BCO}}$	Base-collector overlap capacitance

2.4 Resistances

2.4.1 Constant series resistances

The model contains constant, though temperature dependent, series resistors at the base, emitter and collector terminals. The resistances of the burried layer underneath the transistor are represented by two constant, temperature dependent resistances $\mathsf{R_{Cblx}}$and $\mathsf{R_{Cbli}}$; see also ref. [20] . Note that the substrate resistance is not incorporated in the model itself but should be added in a macro model or sub-circuit since it depends on the layout.

$\mathsf{R_E}$	Constant emitter resistance
$\mathsf{R_{Bc}}$	Constant base resistance
$\mathsf{R_{Cc}}$	Collector Contact resistance
$\mathsf{R_{Cblx}}$	Resistance Collector Buried Layer: extrinstic part
$\mathsf{R_{Cbli}}$	Resistance Collector Buried Layer: intrinstic part

The buried layer resistances were introduced in Mextram 504.7, in a backwards compatibe way. This implies that the default values of these resistances is zero. Because values of $0\,\Omega$ thus are allowed for resistances $\mathsf{R_{Cblx}}$ and $\mathsf{R_{Cbli}}$, the lower clipping value of the resistances is zero and very small values of the resistances $\mathsf{R_{Cblx}}$ and $\mathsf{R_{Cbli}}$ are formally allowed. Resistance values very close to zero are known to form a potential threat to convergence however. In order to exclude the possibility that the resistances of the buried layer take such small values during the convergence process due to temperature effects, the lower clipping value for the temperature coefficient $\mathsf{A_{Cbl}}$ of the resistances $\mathsf{R_{Cblx}}$ and $\mathsf{R_{Cbli}}$ has been set to zero.

In case one of both of the $\mathsf{R_{Cblx}}$ and $\mathsf{R_{Cbli}}$ resistances vanish, the corresponding node (C_3 and or C_4) effectively disappears from the equivalent circuit. Hence the circuit topology

depends on parameter values. Special attention has to be paid to this in implementation of the model.

2.4.2 Variable base resistance

The base resistance is divided in a constant part $\mathsf{R_{Bc}}$ (see previous section) and a variable part, loosely denoted by R_{Bv} but formally given by $I_{B_1B_2}$. The parameter $\mathsf{R_{Bv}}$ is the resistance of the variable part at zero base-emitter and base-collector bias. The variable (bias-dependent) part is modulated by the base width variation (Early effect) and at high current densities it decreases due to the diffusion charges Q_{BE} and Q_{BC}, just as the main current:

$$R_b = \mathsf{R_{Bv}}/q_B. \tag{2.41}$$

The resistance model also takes into account DC current crowding. The resistances decreases at high base currents when $\mathcal{V}_{\mathrm{B_1B_2}}$ is positive and it increases when $\mathcal{V}_{\mathrm{B_1B_2}}$ is negative (reversal of the base current):

$$I_{B_1B_2} = \frac{2\,V_T}{3\,R_b}\,\left(e^{\mathcal{V}_{\mathrm{B_1B_2}}/V_T} - 1\right) + \frac{\mathcal{V}_{\mathrm{B_1B_2}}}{3\,R_b}. \tag{2.42}$$

The AC current crowding is an optional feature of the model ($\mathsf{EXPHI} = 1$) and has been described earlier.

$\mathsf{R_{Bv}}$ zero bias value of the variable base resistance

2.5 Modelling of SiGe and possibly other HBT's

The most important difference between SiGe and pure-Si transistors is the difference between the total base hole charge (used for charges and for R_{Bv}) and the Gummel number (used in the main current). Its precise behaviour is important when the gradient of the bandgap is non-zero. In that case we have a different normalized base 'charge' q_B^I for the current:

$$q_B^I = \frac{\exp\left(\left[\frac{V_{t_E}}{\mathsf{V_{er}}} + 1\right]\,\frac{\mathsf{dE_g}}{V_T}\right) - \exp\left(\frac{-V_{t_C}}{\mathsf{V_{ef}}}\,\frac{\mathsf{dE_g}}{V_T}\right)}{\exp\left(\frac{\mathsf{dE_g}}{V_T}\right) - 1}. \tag{2.43}$$

Normally one would write $\mathsf{dE_g}/kT$ in these formulas. However, the value of $\mathsf{dE_g}$ is given in electron-Volt. This means we need to correct with q, the unity charge. It is then correct (at least in value) to divide $\mathsf{dE_g}$ by V_T.

In some cases SiGe transistors show neutral-base recombination. This means that the base current is dependent on the base-collector voltage. We have added a formulation that

describes this effect and also the increase of the base current in quasi-saturation, due to Auger recombination. The ideal base current then is:

$$I_{B_1} = \frac{\mathsf{I_s}}{\beta_\mathsf{f}}\left(1-\mathsf{XI_{B_1}}\right)\left[\left(1-\mathsf{X_{rec}}\right)\ \left(e^{\mathcal{V}_{\mathrm{B_2E_1}}/V_T}-1\right)\right.$$
$$\left.+\ \mathsf{X_{rec}}\left(e^{\mathcal{V}_{\mathrm{B_2E_1}}/V_T}+e^{V^*_{B_2C_2}/V_T}-2\right)\left(1+\frac{V_{t_C}}{\mathsf{V_{ef}}}\right)\right]. \tag{2.44}$$

Note that the parameter $\mathsf{X_{rec}}$ can be larger than 1.

$\mathsf{dE_g}$	Gradient of the bandgap in the intrinsic base times its width
$\mathsf{X_{rec}}$	Pre-factor of the recombination part of the ideal base current

2.6 Miscellaneous

2.6.1 Temperature scaling rules

The Mextram model contains extensive temperature scaling rules (see section 4.6). The parameters in the temperature scaling rules are:

$\mathsf{V_{g_B}}$, $\mathsf{V_{g_C}}$, $\mathsf{V_{g_S}}$, $\mathsf{V_{g_j}}$, $\mathsf{dV_{g\beta f}}$, $\mathsf{dV_{g\beta r}}$, $\mathsf{dV_{g\tau_E}}$	Bandgap voltages or differences
$\mathsf{A_E}$, $\mathsf{A_B}$, $\mathsf{A_{epi}}$, $\mathsf{A_{ex}}$, $\mathsf{A_C}$, $\mathsf{A_{CBl}}$, $\mathsf{A_S}$, $\mathsf{A_{sub}}$	Mobility exponents
$\mathsf{A_{Q_{B0}}}$	Exponent of zero bias base charge
$\mathsf{A_{th}}$	Exponent of thermal resistance

The temperature rules are applied to the avalanche constant B_n and to the following parameters:

Saturation and knee currents	$\mathsf{I_s}$, $\mathsf{I_{Ss}}$, $\mathsf{I_{CSs}}$, $\mathsf{I_k}$, $\mathsf{I_{ks}}$
Gain modelling	β_f, β_ri, $\mathsf{V_{er}}$, $\mathsf{V_{ef}}$, $\mathsf{I_{Bf}}$, $\mathsf{I_{Br}}$
Resistances	$\mathsf{R_E}$, $\mathsf{R_{Bc}}$, $\mathsf{R_{Bv}}$, $\mathsf{R_{Cc}}$, $\mathsf{R_{CBlx}}$, $\mathsf{R_{CBli}}$, $\mathsf{R_{Cv}}$
Capacitances	$\mathsf{C_{jE}}$, $\mathsf{C_{jC}}$, $\mathsf{C_{js}}$, $\mathsf{V_{d_E}}$, $\mathsf{V_{d_C}}$, $\mathsf{V_{d_S}}$, $\mathsf{X_p}$
Transit times	τ_E, τ_B, τ_epi, τ_R
Thermal resistance	$\mathsf{R_{th}}$

2.6.2 Self-heating

Self-heating is part of the model (see section 4.13). It is defined in the usual way by adding a self-heating network containing a current source describing the dissipated power and both a thermal resistance and a thermal capacitance. The total dissipated power is a sum of the dissipated power of each branch of the equivalent circuit.

Note that the effect of the parameter DTA and dynamic selfheating are independent. This is discussed in Ref. [4]. The local ambient temperature is increased as:

$$T_{\text{local ambient}} = T_{\text{global ambient}} + \mathsf{DTA}.$$

Dynamic self-heating gives an extra and independent contribution:

$$T_{\text{device}} = T_{\text{local ambient}} + (\Delta T)_{\text{dynamic heating}},$$

where $(\Delta T)_{\text{dynamic heating}}$ is given by $\mathcal{V}_{\text{dT}}$, the voltage at the temperature node of the self-heating network shown in Fig. 11.

The temperature dependence of the thermal resistance is taken into account. At large dissipation, the relation between dissipation and temperature increase becomes non-linear. This can be implemented in a sub-circuit [21].

$\mathsf{R_{th}}$	Thermal resistance
$\mathsf{C_{th}}$	Thermal capacitance

2.6.3 Noise model

Noise is included in various branches of the model:

Thermal noise	:	resistances $\mathsf{R_E}$, $\mathsf{R_{Bc}}$, $\mathsf{R_{Cc}}$, $\mathsf{R_{Cblx}}$, $\mathsf{R_{Cbli}}$, and variable resistance R_{Bv} [22]
Shot noise	:	I_N, I_{B_1}, $I^S_{B_1}$, I_{B_2}, I_{B_3}, I_{ex}, XI_{ex}, I_{sub}, and XI_{sub}
$1/f$ noise [23]	:	I_{B_1}, $I^S_{B_1}$, I_{B_2}, I_{B_3}, I_{ex} and XI_{ex}

Avalanche multiplication (due to impact-ionization) also adds noise [24]. This effect can be switched on or off by using the parameter $\mathsf{K_{avl}}$. Physically, it should be on: $\mathsf{K_{avl}} = 1$. For increased flexibility $\mathsf{K_{avl}}$ is allowed to have other values between 0 and 1; values greater than 1 are excluded because those could lead to a noise-correlation coefficient, for collector and base current noise, greater than 1.

$\mathsf{A_f}$	Exponent of the current dependence of the $1/f$ noise
$\mathsf{K_f}$	Pre-factor of the $1/f$ noise
$\mathsf{K_{fN}}$	Pre-factor of the $1/f$ noise in the non-ideal base current
$\mathsf{K_{avl}}$	Pre-factor (switch) for the noise due to avalanche

2.6.4 Number of transistor parameters

The parameters used in the Mextram model can be divided in:

Forward current modelling	:	28
Reverse current modelling (including BCS)	:	8
Extra parameters used only in charge modelling	:	14
Temperature scaling model	:	19
Self-heating	:	2
Noise model	:	4
HBT options	:	2
General parameters (level, flags, reference temperature)	:	7
Total	:	79

Of the total parameters mentioned above 4 parameters ($\mathsf{XC_{jE}}$, $\mathsf{XC_{jc}}$, $\mathsf{XI_{B_1}}$, and $\mathsf{X_{ext}}$) are specially dedicated to geometrical scaling (other parameters scale too of course). A scaling

model itself, however, is not part of Mextram.

2.7 Comments about the Mextram model

2.7.1 Convergency and computation time

Mextram is a more complex model than Gummel-Poon. Therefore, the computing time is larger, especially when self-heating is included. For the same reason the convergency will be less, although we cannot give any quantitative comparison. The computation time of Mextram 504 is comparable to that of Mextram 503. However, tests show that Mextram 504 has better convergency than Mextram 503. This is probably mainly due to improved smoothness of the model.

2.7.2 Not modelled within the model

Mextram does not contain a substrate resistance. We know that this substrate resistance can have an influence on transistor characteristics. This is mainly seen in the real part of Y_{22}. For optimimum flexibility we did not make it a part of the model itself, because in the technology it is also not part of the transistor itself. It depends very much on the layout. The layout in a final design might be different from the layout used in parameter extraction. Also complicated substrate resistance/capacitance networks are sometimes needed. Therefore we chose to let the substrate resistance not be part of the model.

2.7.3 Possible improvements

The forward current of the parasitic Base-Collector-Substrate (BCS) transistor is modelled.

Up until and including Mextram 504.9, Mextram did not contain a full description of the reverse current of the BCS since it was believed not to be relevant to circuit designers. Mextram 504.10 introduced a reverse (SB) component of the main current of the parasitic transistor. Early- and reverse high current effects are not taken into account in the parasitic BCS transistor.

The output conductance $\mathrm{d}I_C/\mathrm{d}\mathcal{V}_{\mathrm{CE}}$ at the point where hard saturation starts seems to be too abrupt for high current levels, compared to measurements. At present it is not possible to improve this, without losing some of the other features of the model.

The clarity of the extrinsic current model describing XI_{ex} and XI_{sub} could be improved by adding an extra node and an extra contact base resistance. Since the quality of the description does not improve, the parameter extraction would be more difficult, and the model topology would become dependent on a parameter (EXMOD) we choose not to do this.

3 Introduction to parameter extraction

The accuracy of circuit simulation depends not only on the performance of the transistor model itself, but also on the model parameters used. The use of a very sophisticated model with poorly determined parameters will result in an inaccurate simulation of the electronic circuit. The determination of the model-parameter extraction methodology is an important task in the development of a compact model.

A strong correlation between model parameters hampers unambiguous determination of individual parameters. Most parameters are extracted directly from measured data. Therefore we need depletion capacitance (CV), terminal currents versus voltages (DC) and high-frequency measurements (S-parameters). Important is that these measurements are done over a large range of collector, base and emitter biasing conditions. This greatly improves the accuracy of the parameters. The number of data points in an interval is of minor importance.

To extract Mextram model parameters the model is implemented in the characterization and analysis program ICCAP of Agilent. Previous work on parameter extraction methodology has shown that accurate extraction of all Mextram parameters is feasible without evaluation of the full model equations in a circuit simulator [25]. This method greatly enhances the efficiency and user-friendliness of parameter extraction.

The general extraction strategy [25] is to put the parameters in small groups (typical 1–3) and extract these parameters simultaneously out of measured data sensitive to these parameters. The composition of each individual group depends on the technology. However, it is possible to give general guide lines. A more thorough documentation on parameter extraction for Mextram 504, including temperature and geometric scaling, is given in Ref. [3].

A typical grouping of Mextram parameters is given in the following table:

Base-emitter capacitance	:	$\mathsf{C_{jE}}$, $\mathsf{V_{d_E}}$, $\mathsf{p_E}$
Base-collector capacitance	:	$\mathsf{C_{jC}}$, $\mathsf{p_C}$, $\mathsf{X_p}$
Collector-substrate capacitance	:	$\mathsf{C_{jS}}$, $\mathsf{V_{d_S}}$, $\mathsf{p_S}$
Zener tunneling current parameters: reverse biased EB junction, $V_{CB} = 0$	:	$\mathsf{I_{zEB}}$, $\mathsf{N_{zEB}}$
Avalanche at small collector currents, high V_{CB}	:	$\mathsf{W_{avl}}$, $\mathsf{V_{avl}}$
Reverse Early effect	:	$\mathsf{V_{er}}$
Forward Early effect	:	$\mathsf{V_{ef}}$
Forward Gummel plot small V_{BE}	:	$\mathsf{I_s}$
Substrate current small V_{BC}	:	$\mathsf{I_{Ss}}$, $\mathsf{I_{CSs}}$
Forward current gain up to medium current levels	:	β_f, $\mathsf{I_{Bf}}$, $\mathsf{m_{Lf}}$
Reverse current gain up to medium current levels	:	β_ri, $\mathsf{I_{Br}}$, $\mathsf{V_{Lr}}$, $\mathsf{I_{ks}}$

Giacoletto method	:	R_E
From forward Gummel plot at large V_{BE}, Y-parameters, or scaling	:	R_{Bc}, R_{Bv}
Substrate current in hard saturation	:	R_{Cc}
Geometry scaling	:	XC_{jE}, XC_{jC}, XI_{B_1}
Temperature scaling	:	Temperature parameters.
Decrease of V_{BE} for constant I_B at high V_{CE}	:	R_{th}
Collector current up to high V_{CE}	:	I_k
From the fall-of of $h_{\rm fe}$ and f_T at high currents	:	R_{Cv}, V_{dc}
From the f_T vs. I_C	:	SCR_{Cv}, I_{hc}, τ_E, τ_B, τ_{epi}, (m_τ, m_C, a_{x_i})
Reverse Gummel plot at large V_{BC}	:	X_{ext}
Output conductance as function of frequency	:	C_{th}

The first step in the determination of parameters is to generate an initial parameter set. An accurate calculation of the epilayer related parameters [see Eqs. (2.21)–(2.27)] prevents a lot of trouble and improves the convergency of the parameter extraction.

It is not possible to extract all the Mextram model parameters from one measured transistor. For example the scaling parameters XC_{jE}, XC_{jC} and XI_{B_1} are determined from geometrical scaling rules. The same is true for the overlap capacitances C_{BEO} and C_{BCO}.

It helps if the parameters are extracted in the sequence given in the table given above.

The extraction of the emitter and base resistances will give only satisfactory results when the current gain in this region is accurately modeled. It is nearly impossible to get accurate results for the variable part of the base resistance from DC measurements. Therefore either R_{Bv} is calculated from scaling information, or the resistances are extracted from S-parameters [26].

At high collector currents and voltages the measurements often become distorted by rise of the device temperature due to self heating. This complicates the extraction of R_{Cv}, SCR_{Cv}, I_{hc}, I_k and the transit time parameters. Self-heating should therefore be included. When doing this, the temperature scaling parameters should be known or estimated. First I_k is extracted from the collector current at high $\mathcal{V}_{CE}$ in the output characteristic (I_C versus $\mathcal{V}_{CE}$ at constant I_B). At sufficient high $\mathcal{V}_{CE}$ the transistor comes out of quasi-saturation and therefore the epilayer resistance is of minor importance at these bias points.

Next at small values of $\mathcal{V}_{CE}$ the DC current gain is optimised by extracting R_{Cv} and V_{dc}. We can use the measured output characteristics or I_C and I_B from the Gummel plot of the S-parameter measurement setup. The latter has the advantage that the high current parameters and transit times parameters are extracted from the same device.

In the final step SCR_{Cv}, I_{hc} and the transit times parameters are extracted from f_T. The hot-carrier current I_{hc} should be the collector current beyond the top of the f_T. The spacing between the different maxima of the f_T curves for currents around I_{hc} is determined by

R_{Cv} and SCR_{Cv}. These three extraction steps have to be repeated once or twice to get a stable parameter set.

To extract S_{fH} one needs to measure the avalanche effect at high currents (at least I_{hc}) and voltages and fit the model to the measurements. It is very important to take self-heating into account.

The reverse transit time can only be accurately determined from reverse high-frequency measurements. These are not normally done, since they need dedicated structures. As an alternative one can use the forward high-frequency measurements in or close to hard saturation ($\mathcal{V}_{CE} = 0.2\,\mathrm{V}$), or one can calculate it according to Eq. (5.41).

The two SiGe parameters can be determined as follows. The bandgap difference dE_g in the base between collector-edge and emitter-edge can be estimated from the process. The Early-effect on the base-current in the forward Early measurement can be used to determine X_{rec}.

Zener tunneling current model

The model for Zener tunneling current in the emitter base junction shares a model for the electric field with the emitter base depletion capacitance model. Therefore the Zener tunneling current has dedicated parameters I_{zEB} and N_{zEB}, but shares the parameters V_{d_E}, p_E with the depletion capacitance model. Depletion capacitance parameters should therefore be extracted before extraction of the dedicated Zener tunneling current parameters I_{zEB} and N_{zEB}.

4 Formal model formulation

In this section the formal definition of the model is given. We have given the description that includes a substrate node and self-heating. It is also possible to use Mextram without the substrate node, self-heating or both.

We will start with the structural elements of Mextram, the notation, the parameters and the equivalent circuit. Then a few model constants are defined and the temperature rules are given. The major part of this section consists of the description of the currents and of the charges. Then some extra modelling features are discussed, such as the extended modelling of the reverse current gain, the distributed high-frequency effects and hetero-junction features. The noise model, MULT-scaling and self-heating are next. At last some implementation issues, the embedding of PNP transistors and operating point information are discussed.

4.1 Structural elements of Mextram

Mextram has the following somewhat independent parts.

Parameters

The set of parameters consists of the following classes: the model-definition parameters like LEVEL and the three flags; the electrical parameters; the temperature scaling parameters; the noise parameters; and the self-heating parameters.

The model-definition parameters determine exactly which model is used. For some parts of the model we provide some extended features. These can be included or excluded using the three flags. The main part of the model is the description of currents and charges. For this description we need a set of electrical parameters. These parameters vary with temperature. In the parameter set itself only the values of the electrical parameters at the reference temperature are given. The temperature scaling parameters are used to calculate the actual values of the electrical parameters from their value at the reference temperature. This temperature scaling can in general be performed in preprocessing. The noise parameters are extra parameters use to calculate the various noise-sources.

Geometric scaling is not part of the model. The parameter MULT gives the possibility of putting several transistors in parallel. In this sense it is a very simple geometric scaling parameter. The model parameters can be scaling dependent (some are even especially made for this purpose, like the X-parameters). The scaling itself has to be done outside the model.

Self-heating

Self-heating increases the local temperature of the transistor w.r.t. the ambient temperature. This is due to power dissipation of the transistor itself. When taking self-heating

into account (this is an optional feature) the actual temperature depends on the actual bias conditions. This means that temperature scaling must be performed at every bias-point, and not only in preprocessing.

Clipping

After temperature-scaling it is possible that some parameters are outside a physically realistic range, or in a range that might create difficulties in the numerical evaluation of the model, for example a division by zero. In order to prevent this, some parameters are limited to a pre-specified range directly after scaling. This procedure is called clipping.

Equivalent circuit

The equivalent circuit describes how the various circuit elements of the model (currents, charges and noise-sources) are connected to each other. From the equivalent circuit and all the electrical equations it is also possible to derive a small-signal equivalent circuit.

Current and charge equations

The current and charge equations are the main part of the model. They are needed to calculate the various currents and charges defined in the equivalent circuit. The currents are those through common resistances, diode-like currents or more complicated voltage controlled current sources. The charges are the various depletion charges and diffusion charges in the model. The charges are only needed in AC and transient simulation, but not in DC simulations. Therefore some parameters have no influence on the DC model. However a part of the charge formulation is needed in the DC model, e.g. the curvature of the depletion charges determines the bias-dependent Early effect.

Noise equations

The noise equations describe the current noise sources that are parallel to some of the equivalent circuit elements. Only shot-noise, thermal noise and $1/f$-noise is modeled.

Operating point information

When the transistor is biased in a certain way, it is sometimes convenient to gain some insight in the internal state of the model. This is possible via the operating point information. This information contains all the internal biases, currents and charges, all the elements of the complete small-signal circuit, the elements of a very simplified small-signal circuit, and some characteristic values like f_T.

Embedding for PNP transistors

All the equations that will be given are for NPN transistors. For PNP transistors the same equations can be used after some embedding. This only consists of changing signs of biases before currents and charges are calculated and changing signs of currents and charges afterwards.

4.2 Notation

We used different fonts for different kind of quantities to clarify the structure of the equations:

$\mathsf{V_{d_E}}$, $\mathsf{R_{Cv}}$	Parameters
$\mathsf{V_{d_ET}}$, $\mathsf{R_{CvT}}$	Parameters after temperature scaling
$\mathcal{V}_{\mathrm{B_2E_1}}$, $\mathcal{V}_{\mathrm{B_2C_2}}$	Node voltages as given by the circuit simulator
$I_{C_1C_2}$, $V^*_{B_2C_2}$	Calculated quantities

When a previously calculated quantity needs to be changed this is denoted as

$$(\text{new value}) \rightarrow (\text{expression using previous values}) \tag{4.1}$$

4.3 Parameters

The following table gives all the parameters of Mextram. This includes the extra parameters needed when a substrate is present and the extra parameters needed when using a version with self-heating. The table contains the parameter name as used in the implementation as well as the symbol used in the formulas. Furthermore the unit of the parameter and a short description are given. The parameters are sorted in a logical way. First we have some general parameters like the level and the flags. Next the current parameters of the basic model, the parameters of the avalanche model, the resistances and epilayer parameters, the parameters of the depletion capacitances and the transit times are given. Then we have the parameters for the SiGe model features, followed by those of the temperature model (mobility exponents and bandgap voltages) and the noise parameters. The parameters specific for the four-terminal device are next. At last we have the self-heating parameters.

The parameters denoted with a '$*$' are not used in the DC model.

#	symbol	name	units	description
1	LEVEL	LEVEL	—	Model level, must be set to 504
2	$\mathsf{T_{ref}}$	TREF	°C	Reference temperature. Default is $25°\mathrm{C}$
3	DTA	DTA	°C	Difference between the local ambient and global ambient temperatures: $T_{\text{local ambient}} = T_{\text{global ambient}} + \mathsf{DTA}$
4	EXMOD	EXMOD	—	Flag for extended modelling of the reverse current gain
5	EXPHI	EXPHI	—	$*$Flag for the distributed high-frequency effects in transient
6	EXAVL	EXAVL	—	Flag for extended modelling of avalanche currents
7	EXSUB	EXSUB	—	Flag for extended modelling of substrate currents

#	symbol	name	units	description
8	I_s	IS	A	Collector-emitter saturation current
9	I_k	IK	A	Collector-emitter high injection knee current
10	V_{er}	VER	V	Reverse Early voltage
11	V_{ef}	VEF	V	Forward Early voltage
12	β_f	BF	—	Ideal forward current gain
13	I_{Bf}	IBF	A	Saturation current of the non-ideal forward base current
14	m_{Lf}	MLF	—	Non-ideality factor of the non-ideal forward base current
15	XI_{B_1}	XIBI	—	Part of ideal base current that belongs to the sidewall
16	I_{zEB}	IZEB	A	Pre-factor of emitter-base Zener tunneling current
17	N_{zEB}	NZEB	—	Coefficient of emitter-base Zener tunneling current
18	β_{ri}	BRI	—	Ideal reverse current gain
19	I_{Br}	IBR	A	Saturation current of the non-ideal reverse base current
20	V_{Lr}	VLR	V	Cross-over voltage of the non-ideal reverse base current
21	X_{ext}	XEXT	—	Part of I_{ex}, Q_{tex}, Q_{ex} and I_{sub} that depends on $\mathcal{V}_{BC_3}$ instead of $\mathcal{V}_{B_1C_4}$
22	W_{avl}	WAVL	m	Epilayer thickness used in weak-avalanche model
23	V_{avl}	VAVL	V	Voltage determining curvature of avalanche current
24	S_{fH}	SFH	—	Current spreading factor of avalanche model (when $\mathsf{EXAVL} = 1$)
25	R_E	RE	Ω	Emitter resistance
26	R_{Bc}	RBC	Ω	Constant part of the base resistance
27	R_{Bv}	RBV	Ω	Zero-bias value of the variable part of the base resistance
28	R_{Cc}	RCC	Ω	Collector Contact resistance
29	R_{Cblx}	RCBLX	Ω	Resistance of the Collector Buried Layer: eXtrinsic part
30	R_{Cbli}	RCBLI	Ω	Resistance of the Collector Buried Layer: Intrinsic part
31	R_{Cv}	RCV	Ω	Resistance of the un-modulated epilayer
32	SCR_{Cv}	SCRCV	Ω	Space charge resistance of the epilayer
33	I_{hc}	IHC	A	Critical current for velocity saturation in the epilayer
34	a_{x_i}	AXI	—	Smoothness parameter for the onset of quasi-saturation
35	C_{j_E}	CJE	F	∗Zero-bias emitter-base depletion capacitance
36	V_{d_E}	VDE	V	Emitter-base diffusion voltage
37	p_E	PE	—	Emitter-base grading coefficient
38	XC_{j_E}	XCJE	—	∗Fraction of the emitter-base depletion capacitance that belongs to the sidewall
39	C_{BEO}	CBEO	—	∗Emitter-base overlap capacitance
40	C_{jc}	CJC	F	∗Zero-bias collector-base depletion capacitance
41	V_{d_C}	VDC	V	Collector-base diffusion voltage
42	p_C	PC	—	Collector-base grading coefficient
43	X_p	XP	—	Constant part of C_{jc}
44	m_C	MC	—	Coefficient for the current modulation of the collector-base depletion capacitance
45	XC_{j_C}	XCJC	—	∗Fraction of the collector-base depletion capacitance under the emitter
46	C_{BCO}	CBCO	—	∗Collector-base overlap capacitance

#	symbol	name	units	description
47	m_τ	MTAU	—	∗Non-ideality factor of the emitter stored charge
48	τ_E	TAUE	s	∗Minimum transit time of stored emitter charge
49	τ_B	TAUB	s	∗Transit time of stored base charge
50	τ_{epi}	TEPI	s	∗Transit time of stored epilayer charge
51	τ_R	TAUR	s	∗Transit time of reverse extrinsic stored base charge
52	dE_g	DEG	eV	Bandgap difference over the base
53	X_{rec}	XREC	—	Pre-factor of the recombination part of I_{B_1}
54	X_{Q_B}	XQB	—	Fraction of the total base charge supplied by the collector instead of the base (Base charge partitioning)
55	$A_{Q_{B0}}$	AQBO	—	Temperature coefficient of the zero-bias base charge
56	A_E	AE	—	Temperature coefficient of the resistivity of the emitter
57	A_B	AB	—	Temperature coefficient of the resistivity of the base
58	A_{epi}	AEPI	—	Temperature coefficient of the resistivity of the epilayer
59	A_{ex}	AEX	—	Temperature coefficient of the resistivity of the extrinsic base
60	A_C	AC	—	Temperature coefficient of the resistivity of the collector contact
61	A_{Cbl}	ACBL	—	Temperature coefficient of the resistivity of the collector buried layer
62	dA_{I_s}	DAIS	—	Parameter for fine tuning of temperature dependence of collector-emitter saturation current
63	$dV_{g\beta f}$	DVGBF	V	Band-gap voltage difference of forward current gain
64	$dV_{g\beta r}$	DVGBR	V	Band-gap voltage difference of reverse current gain
65	V_{g_B}	VGB	V	Band-gap voltage of the base
66	V_{g_C}	VGC	V	Band-gap voltage of the collector
67	V_{g_j}	VGJ	V	Band-gap voltage recombination emitter-base junction
68	V_{gZEB}	VGZEB	V	Band-gap at reference temperature relevant to the Zener effect in the emitter-base junction
69	A_{VgEB}	AVGEB	$\mathrm{V/K}$	Temperature scaling coefficient of emitter-base Zener tunneling current
70	T_{VgEB}	TVGEB	K	Temperature scaling coefficient of emitter-base Zener tunneling current
71	$dV_{g\tau_E}$	DVGTE	V	∗Band-gap voltage difference of emitter stored charge

#	symbol	name	units	description
72	A_f	AF	—	∗Exponent of the Flicker-noise
73	K_f	KF	—	∗Flicker-noise coefficient of the ideal base current
74	K_{fN}	KFN	—	∗Flicker-noise coefficient of the non-ideal base current
75	K_{avl}	KAVL	—	∗Switch for white noise contribution due to avalanche
76	K_C	KC	—	∗Switch for RF correlation noise model selection
77	K_E	KE	—	∗Fraction of Q_E in excess phase shift
78	F_{taun}	FTAUN	—	∗Fraction of noise transit time to total transit time
79	I_{Ss}	ISS	A	Base-substrate saturation current
80	I_{CSs}	ICSS	A	Collector-substrate ideal saturation current
81	I_{ks}	IKS	A	Base-substrate high injection knee current
82	C_{js}	CJS	F	∗Zero-bias collector-substrate depletion capacitance
83	V_{ds}	VDS	V	∗Collector-substrate diffusion voltage
84	p_S	PS	—	∗Collector-substrate grading coefficient
85	V_{gs}	VGS	V	Band-gap voltage of the substrate
86	A_S	AS	—	For a closed buried layer: $A_S = A_C$, and for an open buried layer: $A_S = A_{epi}$
87	A_{sub}	ASUB	—	Temperature coefficient for mobility of minorities in the substrate
88	R_{th}	RTH	°C/W	Thermal resistance
89	C_{th}	CTH	J/°C	∗Thermal capacitance
90	A_{th}	ATH	—	Temperature coefficient of the thermal resistance
91	MULT	MULT	—	Multiplication factor

The following table gives the **default** values and the **clipping values** of the parameters. These values should not be circuit simulator dependent. The default values come from a realistic transistor and are therefore a good indication of typical values.

#	symbol	name	default	clip low	clip high
1	LEVEL	LEVEL	504	–	–
2	T_{ref}	TREF	25.0	−273	–
3	DTA	DTA	0.0	–	–
4	EXMOD	EXMOD	1.0	0.0	2.0
5	EXPHI	EXPHI	1.0	0.0	1.0
6	EXAVL	EXAVL	0.0	0.0	1.0
7	EXSUB	EXSUB	0.0	0.0	1.0
8	I_s	IS	$22.0 \cdot 10^{-18}$	0.0	–
9	I_k	IK	0.1	$1.0 \cdot 10^{-12}$	–
10	V_{er}	VER	2.5	0.01	–
11	V_{ef}	VEF	44.0	0.01	–
12	β_f	BF	215.0	$1.0 \cdot 10^{-4}$	–
13	I_{Bf}	IBF	$2.7 \cdot 10^{-15}$	0.0	–
14	m_{Lf}	MLF	2.0	0.1	–
15	XI_{B_1}	XIBI	0.0	0.0	1.0
16	I_{zEB}	IZEB	0.0	0.0	–
17	N_{zEB}	NZEB	22.0	0.0	–
18	β_{ri}	BRI	7.0	$1.0 \cdot 10^{-10}$	–
19	I_{Br}	IBR	$1.0 \cdot 10^{-15}$	0.0	–
20	V_{Lr}	VLR	0.2	–	–
21	X_{ext}	XEXT	0.63	0.0	1.0
22	W_{avl}	WAVL	$1.1 \cdot 10^{-6}$	$1.0 \cdot 10^{-9}$	–
23	V_{avl}	VAVL	3.0	0.01	–
24	S_{fH}	SFH	0.3	0.0	–
25	R_E	RE	5.0	$1.0 \cdot 10^{-3}$	–
26	R_{Bc}	RBC	23.0	$1.0 \cdot 10^{-3}$	–
27	R_{Bv}	RBV	18.0	$1.0 \cdot 10^{-3}$	–
28	R_{Cc}	RCC	12.0	$1.0 \cdot 10^{-3}$	–
29	R_{Cblx}	RCBLX	0.0	0.0	–
30	R_{Cbli}	RCBLI	0.0	0.0	–
31	R_{Cv}	RCV	150.0	$1.0 \cdot 10^{-3}$	–
32	SCR_{Cv}	SCRCV	1250.0	$1.0 \cdot 10^{-3}$	–
33	I_{hc}	IHC	$4.0 \cdot 10^{-3}$	$1.0 \cdot 10^{-12}$	–
34	a_{x_i}	AXI	0.3	0.02	–
35	C_{j_E}	CJE	$73.0 \cdot 10^{-15}$	0.0	–
36	V_{d_E}	VDE	0.95	0.05	–
37	p_E	PE	0.4	0.01	0.99
38	XC_{j_E}	XCJE	0.4	0.0	1.0
39	C_{BEO}	CBEO	0.0	0.0	–

#	symbol	name	default	clip low	clip high
40	C_{jc}	CJC	$78.0 \cdot 10^{-15}$	0.0	–
41	V_{dc}	VDC	0.68	0.05	–
42	p_C	PC	0.5	0.01	0.99
43	X_p	XP	0.35	0.0	0.99
44	m_C	MC	0.5	0.0	1.0
45	XC_{jc}	XCJC	$32.0 \cdot 10^{-3}$	0.0	1.0
46	C_{BCO}	CBCO	0.0	0.0	–
47	m_τ	MTAU	1.0	0.1	–
48	τ_E	TAUE	$2.0 \cdot 10^{-12}$	0.0	–
49	τ_B	TAUB	$4.2 \cdot 10^{-12}$	0.0	–
50	τ_{epi}	TEPI	$41.0 \cdot 10^{-12}$	0.0	–
51	τ_R	TAUR	$520.0 \cdot 10^{-12}$	0.0	–
52	dE_g	DEG	0.0	–	–
53	X_{rec}	XREC	0.0	0.0	–
54	X_{Q_B}	XQB	$1/3$	0.0	1.0
55	$A_{Q_{B0}}$	AQBO	0.3	–	–
56	A_E	AE	0.0	–	–
57	A_B	AB	1.0	–	–
58	A_{epi}	AEPI	2.5	–	–
59	A_{ex}	AEX	0.62	–	–
60	A_C	AC	2.0	–	–
61	A_{Cbl}	ACBL	2.0	0.0	–
62	dA_{I_s}	DAIS	0.0	–	–
63	$dV_{g\beta f}$	DVGBF	$50.0 \cdot 10^{-3}$	–	–
64	$dV_{g\beta r}$	DVGBR	$45.0 \cdot 10^{-3}$	–	–
65	V_{g_B}	VGB	1.17	0.1	–
66	V_{g_C}	VGC	1.18	0.1	–
67	V_{g_j}	VGJ	1.15	0.1	–
68	$V_{g_{ZEB}}$	VGZEB	1.15	0.1	–
69	A_{VgEB}	AVGEB	$4.73 \cdot 10^{-4}$	–	–
70	T_{VgEB}	TVGEB	636.0	0.0	–
71	$dV_{g\tau_E}$	DVGTE	0.05	–	–

#	symbol	name	default	clip low	clip high
72	A_f	AF	2.0	0.01	–
73	K_f	KF	$20.0 \cdot 10^{-12}$	0.0	–
74	K_{fN}	KFN	$20.0 \cdot 10^{-12}$	0.0	–
75	K_{avl}	KAVL	0.0‡	0.0‡	1.0
76	K_C	KC	0.0	0.0	2.0
77	K_E	KE	0.0	0.0	1.0
78	FTAUN	FTAUN	0.0	0.0	1.0
79	I_{Ss}	ISS	$48.0 \cdot 10^{-18}$	0.0	–
80	I_{CSs}	ICSS	-1.0§	–	–
81	I_{ks}	IKS	$250.0 \cdot 10^{-6}$	$1.0 \cdot 10^{-12}$	–
82	C_{js}	CJS	$315.0 \cdot 10^{-15}$	0.0	–
83	V_{ds}	VDS	0.62	0.05	–
84	p_S	PS	0.34	0.01	0.99
85	V_{gs}	VGS	1.20	0.1	–
86	A_S	AS	1.58	–	–
87	A_{sub}	ASUB	2.0	–	–
88	R_{th}	RTH	300.0	0.0	–
89	C_{th}	CTH	$3.0 \cdot 10^{-9}$	0.0¶	–
90	A_{th}	ATH	0.0	–	–
91	MULT	MULT	1.0	0.0	–

‡The physical and therefore recommended value is $K_{avl} = 1$.

§For $I_{CSs} < 0$ (default), the substrate-collector current I_{Sf} reduces to backwards compatibility mode.

¶Please note that a value of $C_{th} = 0$ often leads to incorrect results, see Sec. 4.13.

4.4 Model constants

$$k = 1.3806226 \cdot 10^{-23}\,\mathrm{JK}^{-1} \tag{4.2}$$
$$q = 1.6021918 \cdot 10^{-19}\,\mathrm{C} \tag{4.3}$$
$$\left(\frac{k}{q}\right) = 0.86171 \cdot 10^{-4}\,\mathrm{V/K} \tag{4.4}$$
$$V_{\mathrm{d,low}} = 0.05\,\mathrm{V} \tag{4.5}$$
$$a_{j_E} = 3.0 \tag{4.6}$$
$$a_{j_C} = 2.0 \tag{4.7}$$
$$a_{j_S} = 2.0 \tag{4.8}$$

Constants A_n and B_n for impact ionization depend on the transistor type:
For NPN:

$$A_n = 7.03 \cdot 10^{7}\,\mathrm{m}^{-1} \tag{4.9}$$

$$B_n = 1.23 \cdot 10^{8}\,\mathrm{V\,m}^{-1} \tag{4.10}$$

For PNP:

$$A_n = 1.58 \cdot 10^{8}\,\mathrm{m}^{-1} \tag{4.11}$$

$$B_n = 2.04 \cdot 10^{8}\,\mathrm{V\,m}^{-1} \tag{4.12}$$

The default reference temperature $\mathsf{T_{ref}}$ for parameter determination is $25\,^{\circ}\mathrm{C}$.

4.5 MULT-scaling

The parameter MULT may be used to put several transistors in parallel. This means that all currents, charges, and noise-current sources should be multiplied by MULT. It is however much easier to implement this by scaling some of the parameters up front. MULT is allowed to be non-integer for increased flexibility. To scale the geometry of a transistor the use of a process-block is preferable over using this feature.

The following parameters are multiplied by MULT

$$\begin{aligned}&\mathsf{I_s},\quad \mathsf{I_k},\quad \mathsf{I_{Bf}},\quad \mathsf{I_{Br}},\quad \mathsf{I_{hc}},\quad \mathsf{I_{Ss}},\quad \mathsf{I_{CSs}},\quad \mathsf{I_{ks}},\quad \mathsf{I_{zEB}}\\ &\mathsf{C_{j_E}},\quad \mathsf{C_{j_C}},\quad \mathsf{C_{j_S}},\quad \mathsf{C_{BEO}},\quad \mathsf{C_{BCO}},\quad \mathsf{C_{th}}\end{aligned} \tag{4.13}$$

The following parameters are divided by MULT

$$\mathsf{R_E},\quad \mathsf{R_{Bc}},\quad \mathsf{R_{Bv}},\quad \mathsf{R_{Cc}},\quad \mathsf{R_{Cblx}},\quad \mathsf{R_{Cbli}},\quad \mathsf{R_{Cv}},\quad \mathsf{SCR_{Cv}},\quad \mathsf{R_{th}} \tag{4.14}$$

The flicker-noise coefficients are scaled as

$$\mathsf{K_f} \rightarrow \mathsf{K_f} \cdot \mathsf{MULT}^{1-\mathsf{A_f}} \tag{4.15}$$
$$\mathsf{K_{fN}} \rightarrow \mathsf{K_{fN}} \cdot \mathsf{MULT}^{1-[2(\mathsf{m_{Lf}}-1)+\mathsf{A_f}(2-\mathsf{m_{Lf}})]} \tag{4.16}$$

4.6 Temperature scaling

The actual simulation temperature is denoted by TEMP (in $^\circ$C). The temperature at which the parameters are determined is $\mathsf{T_{ref}}$ (also in $^\circ$C).

Conversion to Kelvin

Note the addition of the voltage $\mathcal{V}_{\rm dT}$ of the thermal node (see Sec. 4.13).

$$T_K = \mathsf{TEMP} + \mathsf{DTA} + 273.15 + \mathcal{V}_{\rm dT} \tag{4.17a}$$

$$T_{\rm amb} = \mathsf{TEMP} + \mathsf{DTA} + 273.15 \tag{4.17b}$$

$$T_{RK} = \mathsf{T_{ref}} + 273.15 \tag{4.18}$$

$$t_N = \frac{T_K}{T_{RK}} \tag{4.19}$$

Thermal voltage

$$V_T = \left(\frac{k}{q}\right)\ T_K \tag{4.20}$$

$$V_{T_R} = \left(\frac{k}{q}\right)\ T_{RK} \tag{4.21}$$

$$\frac{1}{V_{\Delta T}} = \frac{1}{V_T} - \frac{1}{V_{T_R}} \tag{4.22}$$

Depletion capacitances

The junction diffusion voltages $\mathsf{V_{dE}}$, $\mathsf{V_{dC}}$, and $\mathsf{V_{dS}}$ with respect to temperature are

$$U_{d_E T} = -3\,V_T\ \ln t_N + \mathsf{V_{dE}}\ t_N + (1 - t_N)\ \mathsf{V_{gB}} \tag{4.23a}$$

$$\mathsf{V_{dE}T} = U_{d_E T} + V_T \ln\{1 + \exp[(V_{\rm d,low} - U_{d_E T})/V_T]\} \tag{4.23b}$$

$$U_{d_C T} = -3\,V_T\ \ln t_N + \mathsf{V_{dc}}\ t_N + (1 - t_N)\ \mathsf{V_{gc}} \tag{4.24a}$$

$$\mathsf{V_{dcT}} = U_{d_C T} + V_T \ln\{1 + \exp[(V_{\mathrm{d,low}} - U_{d_C T})/V_T]\} \tag{4.24b}$$

$$U_{d_S T} = -3\,V_T\ \ln t_N + \mathsf{V_{ds}}\ t_N + (1 - t_N)\ \mathsf{V_{gs}} \tag{4.25a}$$

$$\mathsf{V_{dsT}} = U_{d_S T} + V_T \ln\{1 + \exp[(V_{\mathrm{d,low}} - U_{d_S T})/V_T]\} \tag{4.25b}$$

The zero-bias capacitances scale with temperature as

$$\mathsf{C_{jeT}} = \mathsf{C_{je}}\ \left(\frac{\mathsf{V_{de}}}{\mathsf{V_{deT}}}\right)^{\mathsf{pe}} \tag{4.26}$$

$$\mathsf{C_{jsT}} = \mathsf{C_{js}}\ \left(\frac{\mathsf{V_{ds}}}{\mathsf{V_{dsT}}}\right)^{\mathsf{ps}} \tag{4.27}$$

The collector depletion capacitance is divided in a variable and a constant part. The constant part is temperature independent.

$$\mathsf{C_{jcT}} = \mathsf{C_{jc}}\ \left[(1 - \mathsf{X_p})\ \left(\frac{\mathsf{V_{dc}}}{\mathsf{V_{dcT}}}\right)^{\mathsf{pc}} + \mathsf{X_p}\right] \tag{4.28}$$

$$\mathsf{X_{pT}} = \mathsf{X_p}\ \left[(1 - \mathsf{X_p})\ \left(\frac{\mathsf{V_{dc}}}{\mathsf{V_{dcT}}}\right)^{\mathsf{pc}} + \mathsf{X_p}\right]^{-1} \tag{4.29}$$

Resistances

The various parameters A describe the mobility of the corresponding regions: $\mu \propto t_N^{-\mathsf{A}}$. The temperature dependence of the zero-bias base charge goes as $Q_{B0\mathrm{T}}/Q_{B0} = t_N^{\mathsf{A_{QB0}}}$.

$$\mathsf{R_{eT}} = \mathsf{R_e}\ t_N^{\mathsf{Ae}} \tag{4.30}$$

$$\mathsf{R_{BvT}} = \mathsf{R_{Bv}}\ t_N^{\mathsf{A_B} - \mathsf{A_{QB0}}} \tag{4.31}$$

$$\mathsf{R_{BcT}} = \mathsf{R_{Bc}}\ t_N^{\mathsf{Aex}} \tag{4.32}$$

$$\mathsf{R_{CvT}} = \mathsf{R_{Cv}}\; t_N^{\mathsf{A_{epi}}} \tag{4.33}$$

$$\mathsf{R_{CcT}} = \mathsf{R_{Cc}}\; t_N^{\mathsf{A_C}} \tag{4.34a}$$

$$\mathsf{R_{CblxT}} = \mathsf{R_{Cblx}}\; t_N^{\mathsf{A_{Cbl}}} \tag{4.34b}$$

$$\mathsf{R_{CbliT}} = \mathsf{R_{Cbli}}\; t_N^{\mathsf{A_{Cbl}}} \tag{4.34c}$$

Conductances

With the parasitic collector resistances, conductances are associated. These are to be used in the noise model and for the calculation of dissipated power. For those contexts, for the cases in which one or more of the resistances is zero, the appropriate value for the corresponding conductance is zero. In cases of vanishing resistance values, the topology of the equiavalent circuit is effectively changed. This is to be taken into account in implementations of the model.

$$\begin{array}{lll} \text{if} & \mathsf{R_{Cc}} > 0 & \text{then} \quad \mathsf{G_{CcT}} = 1/\mathsf{R_{CcT}} \;\; , \\ & & \text{else} \quad \mathsf{G_{CcT}} = 0 \;\; . \end{array} \tag{4.34d}$$

$$\begin{array}{lll} \text{if} & \mathsf{R_{Cblx}} > 0 & \text{then} \quad \mathsf{G_{CblxT}} = 1/\mathsf{R_{CblxT}} \;\; , \\ & & \text{else} \quad \mathsf{G_{CblxT}} = 0 \;\; . \end{array} \tag{4.34e}$$

$$\begin{array}{lll} \text{if} & \mathsf{R_{Cbli}} > 0 & \text{then} \quad \mathsf{G_{CbliT}} = 1/\mathsf{R_{CbliT}} \;\; , \\ & & \text{else} \quad \mathsf{G_{CbliT}} = 0 \;\; . \end{array} \tag{4.34f}$$

Current gains

$$\beta_{\mathsf{fT}} = \beta_{\mathsf{f}}\; t_N^{\mathsf{A_E}-\mathsf{A_B}-\mathsf{A_{Q_{B0}}}}\; \exp[-\mathsf{dV_{g\beta f}}/V_{\Delta T}] \tag{4.35}$$

$$\beta_{\mathsf{riT}} = \beta_{\mathsf{ri}}\; \exp[-\mathsf{dV_{g\beta r}}/V_{\Delta T}] \tag{4.36}$$

Currents and voltages

$$\mathsf{I_{sT}} = \mathsf{I_s}\ t_N^{4-\mathsf{A_B}-\mathsf{A_{Q_{B0}}}+\mathsf{dA_{I_s}}}\ \exp[-\mathsf{V_{g_B}}/V_{\Delta T}] \tag{4.37}$$

$$\mathsf{I_{kT}} = \mathsf{I_k}\ t_N^{1-\mathsf{A_B}} \tag{4.38}$$

$$\mathsf{I_{BfT}} = \mathsf{I_{Bf}}\ t_N^{(6-2\mathsf{m_{Lf}})}\ \exp[-\mathsf{V_{g_j}}/\mathsf{m_{Lf}}\ V_{\Delta T}] \tag{4.39}$$

$$\mathsf{I_{BrT}} = \mathsf{I_{Br}}\ t_N^2\ \exp[-\mathsf{V_{g_C}}/2V_{\Delta T}] \tag{4.40}$$

$$\mathsf{V_{efT}} = \mathsf{V_{ef}}\ t_N^{\mathsf{A_{Q_{B0}}}}\ \left[(1-\mathsf{X_p})\ \left(\frac{\mathsf{V_{d_C}}}{\mathsf{V_{d_CT}}}\right)^{\mathsf{p_C}} + \mathsf{X_p}\right]^{-1} \tag{4.41}$$

$$\mathsf{V_{erT}} = \mathsf{V_{er}}\ t_N^{\mathsf{A_{Q_{B0}}}}\ \left(\frac{\mathsf{V_{d_E}}}{\mathsf{V_{d_ET}}}\right)^{-\mathsf{p_E}} \tag{4.42}$$

The temperature dependence of $\mathsf{I_{Ss}}$ and $\mathsf{I_{ks}}$ is given by $\mathsf{A_S}$ and $\mathsf{V_{g_S}}$.
$\mathsf{A_S}$ equals $\mathsf{A_C}$ for a closed buried layer (BN) and $\mathsf{A_S}$ equals $\mathsf{A_{epi}}$ for an open buried layer.

$$\mathsf{I_{SsT}} = \mathsf{I_{Ss}}\ t_N^{4-\mathsf{A_S}}\ \exp[-\mathsf{V_{g_S}}/V_{\Delta T}] \tag{4.43}$$

$$\mathsf{I_{CSsT}} = \mathsf{I_{CSs}}\ t_N^{3.5-0.5\mathsf{A_{sub}}}\ \exp[-\mathsf{V_{g_S}}/V_{\Delta T}] \tag{4.44}$$

$$\mathsf{I_{ksT}} = \mathsf{I_{ks}}\ t_N^{1-\mathsf{A_S}}\ \frac{\mathsf{I_{sT}}}{\mathsf{I_s}}\ \frac{\mathsf{I_{Ss}}}{\mathsf{I_{SsT}}} \tag{4.45}$$

When either $\mathsf{I_s} = 0$ or $\mathsf{I_{SsT}} = 0$ we take $\mathsf{I_{ksT}} = \mathsf{I_{ks}}\ t_N^{1-\mathsf{A_S}}$.

Transit times

$$\tau_{\mathsf{ET}} = \tau_{\mathsf{E}}\ t_N^{(\mathsf{A_B}-2)}\ \exp[-\mathsf{dV_{g\tau_E}}/V_{\Delta T}] \tag{4.46}$$

$$\tau_{\mathsf{BT}} = \tau_{\mathsf{B}}\ t_N^{\mathsf{A_{Q_{B0}}}+\mathsf{A_B}-1} \tag{4.47}$$

$$\tau_{\mathsf{epiT}} = \tau_{\mathsf{epi}}\ t_N^{\mathsf{A_{epi}}-1} \tag{4.48}$$

$$\tau_{\mathsf{RT}} = \tau_{\mathsf{R}}\ \frac{\tau_{\mathsf{BT}} + \tau_{\mathsf{epiT}}}{\tau_{\mathsf{B}} + \tau_{\mathsf{epi}}} \tag{4.49}$$

Avalanche constant

Note that this temperature rule is independent of $\mathsf{T_{ref}}$ since we take B_n as a material constant. For $T_K < 525.0K$ we have

$$B_{n\mathrm{T}} = B_n \left[1 + 7.2 \cdot 10^{-4} \left(T_K - 300\right) - 1.6 \cdot 10^{-6} \left(T_K - 300\right)^2\right] \tag{4.50a}$$

whereas for $T_K \geq 525.0K$

$$B_{n\mathrm{T}} = B_n \ * 1.081 \tag{4.50b}$$

Heterojunction features

$$\mathsf{dE_{gT}} = \mathsf{dE_g}\ t_N^{\mathsf{A_{QB0}}} \tag{4.51a}$$

EB Zener tunneling current model

Temperature scaling of the Zener tunneling current model for the emitter-base junction is partially based on the following well-known temperature dependence of the bandgap:

$$\mathsf{V_{gz0K}} = \max{}_{\mathtt{logexp}}(\mathsf{V_{gzEB}} + \frac{\mathsf{A_{VgEB}} * T_{RK}^2}{T_{RK} + T_{\mathsf{VgEB}}}, 0.05; 0.1) \tag{4.51b}$$

$$\mathsf{V_{gzEBT}} = \max{}_{\mathtt{logexp}}(\mathsf{V_{gz0K}} - \frac{\mathsf{A_{VgEB}} * T_K^2}{T_K + T_{\mathsf{VgEB}}}, 0.05; 0.1) \tag{4.51c}$$

The function $\max{}_{\mathtt{logexp}}(x, x_0; a)$, which is defined in expression (4.205) on page 73, is used to set a lower bound of $0.05\mathrm{V}$ to the bandgaps $\mathsf{V_{gz0K}}$ and $\mathsf{V_{gzEBT}}$.

Expression (4.51c) models a material property and the parameters of this expression, $\mathsf{V_{gz0K}}$, $\mathsf{A_{VgEB}}$ and T_{VgEB}, are material constants. Values of these are tabulated in table 4. The default values in Mextram correspond to the silicon values tabulated in table 4.

Note that $\mathsf{A_{VgEB}}$ and T_{VgEB} are also model parameters of the Mextram model, but $\mathsf{V_{gz0K}}$ is not. In Mextram, $\mathsf{V_{gz0K}}$ is an internal model variable, the value of which is calculated according to expression (4.51b). The parameter $\mathsf{V_{gzEB}}$ of this expression is also a Mextram model parameter.

In practice, bandgap will depend on material composition (alloys, SiGe) and doping concentration. Therefore, in practice the actual values of the quantities tabulated in table 4 may deviate from the tabulated values. Therefore, and in anticipation of application of Mextram to transistors in different materials, the parameters $\mathsf{V_{gzEB}}$, $\mathsf{A_{VgEB}}$ and T_{VgEB} are accessible in Mextram as model parameters. Because the Zener effect is relatively insensitive to temperature however, we expect that the default values of these parameters will suffice in practice and no parameter extraction for these parameters will be needed.

Table 4: *Example values of the material constants for temperature dependence of the bandgap of various semiconducting materials (see relation 4.51c).*

material	$\mathsf{V_{gz0K}}(\mathrm{eV})$	$\mathsf{A_{VgEB}}(10^{-4}\mathrm{eV/K})$	$T_{\mathsf{VgEB}}(\mathrm{K})$
GaAs	1.519	5.405	204
Si	1.170	4.730	636
Ge	0.7437	4.774	235

The following T-scaling rules for the Zener current model do not introduce any new parameter:

$$\mathsf{N_{zEBT}} = \mathsf{N_{zEB}} \left(\frac{\mathsf{V_{gzEBT}}}{\mathsf{V_{gzEB}}} \right)^{3/2} \left(\frac{\mathsf{V_{d_E}T}}{\mathsf{V_{d_E}}} \right)^{\mathsf{p_E}-1} \tag{4.51d}$$

$$\mathsf{I_{zEBT}} = \mathsf{I_{zEB}} \left(\frac{\mathsf{V_{gzEBT}}}{\mathsf{V_{gzEB}}} \right)^{-1/2} \left(\frac{\mathsf{V_{d_E}T}}{\mathsf{V_{d_E}}} \right)^{2-\mathsf{p_E}} \exp(\mathsf{N_{zEB}} - \mathsf{N_{zEBT}}) \tag{4.51e}$$

Self-heating

$$\mathsf{R_{th,Tamb}} = \mathsf{R_{th}} \cdot \left(\frac{T_{\mathrm{amb}}}{T_{RK}} \right)^{\mathsf{A_{th}}} \tag{4.51f}$$

4.7 Description of currents

4.7.1 Main current

Ideal forward and reverse current:

$$I_f = \mathsf{I_{sT}}\, e^{\mathcal{V}_{\mathrm{B_2E_1}}/V_T} \tag{4.52}$$

$$I_r = \mathsf{I_{sT}}\, e^{V^*_{B_2C_2}/V_T} \tag{4.53}$$

The value of $V^*_{B_2C_2}$ is not always the same as the node voltage $\mathcal{V}_{\mathrm{B_2C_2}}$. The expression for $e^{V^*_{B_2C_2}/V_T}$ is given in Eqs. (4.109) and (4.111).

The Moll-Ross or integral charge-control relation is used to take high injection in the base into account. To avoid dividing by zero at punch-through in Eq. (4.57) the depletion charge term q_0 is modified. (Note that for SiGe transistors q_0^I might differ from q_0^Q, defined in Eq. (4.89). See Sec. 4.11).

$$q_0^I = 1 + \frac{V_{t_E}}{\mathsf{V_{erT}}} + \frac{V_{t_C}}{\mathsf{V_{efT}}} \tag{4.54}$$

$$q_1^I = \frac{q_0^I + \sqrt{(q_0^I)^2 + 0.01}}{2} \tag{4.55}$$

$$q_B^I = q_1^I \ (1 + \tfrac{1}{2}\, n_0 + \tfrac{1}{2}\, n_B) \tag{4.56}$$

$$I_N = \frac{I_f - I_r}{q_B^I} \tag{4.57}$$

The expressions for V_{t_E}, V_{t_C}, n_0, and n_B are given by Eqs. (4.117b), (4.133), (4.148), and (4.151), respectively.

4.7.2 Forward base currents

The total ideal base current is separated into a bulk and a sidewall component. The bulk component depends on the voltage $\mathcal{V}_{\mathrm{B_2E_1}}$ and the sidewall component on the voltage $\mathcal{V}_{\mathrm{B_1E_1}}$. The separation is given by the parameter $\mathsf{XI_{B_1}}$. (Note that I_{B_1} becomes more complicated when $\mathsf{X_{rec}} \neq 0$. See Sec. 4.11).

Bulk component:

$$I_{B_1} = (1 - \mathsf{XI_{B_1}})\, \frac{\mathsf{I_{sT}}}{\boldsymbol{\beta}_{\mathsf{fT}}}\ \left(e^{\mathcal{V}_{\mathrm{B_2E_1}}/V_T} - 1\right) \tag{4.58}$$

Sidewall component:

$$I_{B_1}^S = \mathsf{XI_{B_1}}\, \frac{\mathsf{I_{sT}}}{\boldsymbol{\beta}_{\mathsf{fT}}}\ \left(e^{\mathcal{V}_{\mathrm{B_1E_1}}/V_T} - 1\right) \tag{4.59}$$

The non-ideal base current is given by:

$$I_{B_2} = \mathsf{I_{BfT}}\ \left(e^{\mathcal{V}_{\mathrm{B_2E_1}}/\mathsf{m_{Lf}}V_T} - 1\right) \tag{4.60}$$

See section 4.14.1 for a discussion about $G_{\min}$-based convergence aid for Eqn. (4.60).

4.7.3 Reverse base currents

In Mextram the non-ideal reverse base current is

$$I_{B_3} = \mathsf{I_{BrT}}\ \frac{e^{\mathcal{V}_{\mathrm{B_1C_4}}/V_T} - 1}{e^{\mathcal{V}_{\mathrm{B_1C_4}}/2V_T} + e^{\mathsf{V_{Lr}}/2V_T}} \tag{4.61}$$

See section 4.14.1 for a discussion about $G_{\min}$-based convergence aid for Eqn. (4.61).

When $\mathsf{EXSUB} = 1$, the $\mathcal{V}_{\mathrm{SC_4}}$- dependent component of the main current of the parasitic BCS transistor is included, by default ($\mathsf{EXSUB} = 0$) it is not:

$$I_{\mathrm{sub}} = \frac{2\,\mathsf{I_{SsT}}\,\left(e^{\mathcal{V}_{\mathrm{B_1C_4}}/V_T} - 1\right)}{1 + \sqrt{1 + 4\,\dfrac{\mathsf{I_{sT}}}{\mathsf{I_{ksT}}}\,e^{\mathcal{V}_{\mathrm{B_1C_4}}/V_T}}} \quad (\mathsf{EXSUB} = 0)\ . \tag{4.62a}$$

$$I_{\mathrm{sub}} = \frac{2\,\mathsf{I_{SsT}}\,\left(e^{\mathcal{V}_{\mathrm{B_1C_4}}/V_T} - e^{\mathcal{V}_{\mathrm{SC_4}}/V_T}\right)}{1 + \sqrt{1 + 4\,\dfrac{\mathsf{I_{sT}}}{\mathsf{I_{ksT}}}\,e^{\mathcal{V}_{\mathrm{B_1C_4}}/V_T}}} \quad (\mathsf{EXSUB} = 1)\ . \tag{4.62b}$$

which includes high injection for the $\mathcal{V}_{\mathrm{B_1C_4}}$- driven component of I_{sub}. Note that in this expression $4\,\mathsf{I_{sT}}/\mathsf{I_{ksT}}$ is used instead of $4\,\mathsf{I_{SsT}}/\mathsf{I_{ksT}}$ which simplifies parameter extraction [3].

In backwards compatibility mode ($\mathsf{I_{CSs}} < 0$), the current with substrate bias in forward is only included as a signal to the designer. In this mode, no physical meaning should be attached to I_{Sf}:

$$I_{\mathrm{Sf}} = \mathsf{I_{SsT}}\,\left(e^{\mathcal{V}_{\mathrm{SC_1}}/V_T} - 1\right) \tag{4.63}$$

For physical values of $\mathsf{I_{CSs}}$ ($\mathsf{I_{CSs}} \geq 0$), the substrate-collector current is described by an ideal diode model that has a physics based temperature scaling rule:

$$I_{\mathrm{Sf}} = \mathsf{I_{CSsT}}\,\left(e^{\mathcal{V}_{\mathrm{SC_1}}/V_T} - 1\right) \tag{4.64}$$

The extrinsic base current (electrons injected from collector to extrinsic base, similar to I_{B_1}) is given by

$$g_1 = \frac{4\,\mathsf{I_{sT}}}{\mathsf{I_{kT}}}\,e^{\mathcal{V}_{\mathrm{B_1C_4}}/V_T} \tag{4.65}$$

$$n_{B\mathrm{ex}} = \frac{4\,\mathsf{I_{sT}}}{\mathsf{I_{kT}}}\,\frac{e^{\mathcal{V}_{\mathrm{B_1C_4}}/V_T} - 1}{1 + \sqrt{1 + g_1}} \tag{4.66}$$

$$I_{\mathrm{ex}} = \frac{\mathsf{I_{kT}}}{2\,\boldsymbol{\beta}_{\mathsf{riT}}}\,n_{B\mathrm{ex}} \tag{4.67}$$

4.7.4 Weak-avalanche current

In reverse mode ($I_{C_1C_2} \leq 0$) or hard saturation ($\mathcal{V}_{\mathrm{B_2C_1}} \geq \mathsf{V_{dcT}}$) both the avalanche current $I_{\mathrm{avl}} = 0$ and the generation factor G_{EM} are zero

$$I_{\mathrm{avl}} = 0\ ,\ G_{\mathrm{EM}} = 0 \tag{4.68}$$

In forward mode we have the following gradient of the electric field for zero bias

$$dEdx_0 = \frac{2\,\mathsf{V_{avl}}}{\mathsf{W_{avl}}^2} \tag{4.69}$$

The depletion layer thickness becomes

$$x_D = \sqrt{\frac{2}{dEdx_0}}\,\sqrt{\frac{\mathsf{V_{dcT}} - \mathcal{V}_{\mathrm{B_2C_1}}}{1 - I_{\mathrm{cap}}/\mathsf{I_{hc}}}} \tag{4.70}$$

The current I_{cap} will be given in Eq. (4.130).

The generation of avalanche current increases at high current levels. This is only taken into account when flag $\mathsf{EXAVL} = 1$.

When $\mathsf{EXAVL} = 0$, then the effective thickness of the epilayer is

$$W_{\mathrm{eff}} = \mathsf{W_{avl}} \tag{4.71}$$

When $\mathsf{EXAVL} = 1$, then

$$W_{\mathrm{eff}} = \mathsf{W_{avl}}\,\left(1 - \frac{x_i}{2\,W_{\mathrm{epi}}}\right)^2 \tag{4.72}$$

For either value of EXAVL the thickness over which the electric field is important is

$$W_D = \frac{x_D\,W_{\mathrm{eff}}}{\sqrt{x_D^2 + W_{\mathrm{eff}}^2}} \tag{4.73}$$

The average electric field and the field at the base-collector junction are

$$E_{\mathrm{av}} = \frac{\mathsf{V_{dcT}} - \mathcal{V}_{\mathrm{B_2C_1}}}{W_D} \tag{4.74}$$

$$E_0 = E_{\mathrm{av}} + \tfrac{1}{2}W_D\;dEdx_0\;\left(1 - \frac{I_{\mathrm{cap}}}{\mathsf{I_{hc}}}\right) \tag{4.75}$$

When $\mathsf{EXAVL} = 0$, then the maximum of the electric field is

$$E_M = E_0 \tag{4.76}$$

When $\mathsf{EXAVL} = 1$, then

$$SH_W = 1 + 2\,\mathsf{S_{fH}}\;\left(1 + 2\,\frac{x_i}{W_{\mathrm{epi}}}\right) \tag{4.77}$$

$$E_{fi} = \frac{1 + \mathsf{S_{fH}}}{1 + 2\,\mathsf{S_{fH}}} \tag{4.78}$$

$$E_W = E_{\rm av} - \tfrac{1}{2}\, W_D\; dEdx_0 \left(E_{fi} - \frac{I_{C_1C_2}}{\mathsf{I_{hc}}\; SH_W} \right) \tag{4.79}$$

$$E_M = \tfrac{1}{2} \left(E_W + E_0 + \sqrt{(E_W - E_0)^2 + 0.1\; E_{\rm av}^2\; I_{\rm cap}/\mathsf{I_{hc}}} \right) \tag{4.80}$$

The injection thickness $x_i/W_{\rm epi}$ is given in Eq. (4.106).

For either value of EXAVL the intersection point λ_D and the generation factor $G_{\rm EM}$ are

$$\lambda_D = \frac{E_M\; W_D}{2\,(E_M - E_{\rm av})} \tag{4.81}$$

$$G_{\rm EM} = \frac{A_n}{B_{n\rm T}}\; E_M\; \lambda_D \left\{ \exp\left[-\frac{B_{n\rm T}}{E_M} \right] - \exp\left[-\frac{B_{n\rm T}}{E_M} \left(1 + \frac{W_{\rm eff}}{\lambda_D} \right) \right] \right\} \tag{4.82}$$

When $E_M \simeq E_{\rm av}$ the expression for λ_D will diverge. Hence for $(1 - E_{\rm av}/E_M) < 10^{-7}$ we need to take the appropriate analytical limit and get:

$$G_{\rm EM} = A_n\; W_{\rm eff} \exp\left[-\frac{B_{n\rm T}}{E_M} \right] \tag{4.83}$$

The generation factor may not exceed 1 and may not exceed

$$G_{\rm max} = \frac{V_T}{I_{C_1C_2}\; (\mathsf{R_{BcT}} + R_{B_2})} + \frac{q_B^I}{\beta_{\rm fT}} + \frac{\mathsf{R_{ET}}}{\mathsf{R_{BcT}} + R_{B_2}} \tag{4.84}$$

The variable base resistance R_{B_2} is given by Eq. (4.92). The base charge terms q_B^I is given by Eq. (4.56). The current $I_{C_1C_2}$ is given by Eq. (4.98). The avalanche current then is

$$I_{\rm avl} = I_{C_1C_2}\; \frac{G_{\rm EM}\; G_{\rm max}}{G_{\rm EM}\; G_{\rm max} + G_{\rm EM} + G_{\rm max}} \tag{4.85}$$

4.7.5 Emitter-base Zener tunneling current

In Mextram 504.12, the contribution to the current across the emitter-base junction due to Zener tunneling effects is assumed to be always negligible in forward mode; hence $I_{\rm ztEB} = 0$ whenever $0 \le V_{B_2E_1}$. In reverse mode, $V_{B_2E_1} < 0$, it is modeled by the expressions below. Note that the transition at $V_{B_2E_1} = 0$ is non-trivial, yet the model for Zener tunneling current is C^∞: all derivatives of the Zener tunneling current $I_{\rm ztEB}$ are continuous everywhere, including $V_{B_2E_1} = 0$.

$$x_z = \frac{\mathcal{V}_{\rm B_2E_1}}{\mathsf{V_{dET}}} \tag{4.86a}$$

$$\tilde{E}_{0\mathrm{EB}} = \frac{1}{6\,(-x_z)^{2+\mathsf{p_E}}}\left(\mathsf{p_E}\left(1-{\mathsf{p_E}}^2-3x_z\,(\mathsf{p_E}-1)\right)-6x_z^2\,(\mathsf{p_E}-1+x_z)\right) \quad (4.86b)$$

$$D_{\mathrm{zEB}} = -\mathcal{V}_{\mathrm{B_2E_1}} - \frac{\mathsf{V_{gzEBT}}}{2^{2-\mathsf{p_E}}\,\mathsf{N_{zEBT}}}\,\tilde{E}_{0\mathrm{EB}}\left(1-\exp\left(\frac{2^{2-\mathsf{p_E}}\mathsf{N_{zEBT}}\,\mathcal{V}_{\mathrm{B_2E_1}}}{\mathsf{V_{gzEBT}}\,\tilde{E}_{0\mathrm{EB}}}\right)\right) \quad (4.87)$$

The Zener tunneling current I_{ztEB} is defined to be positive if it runs from node E_1 to node B_2.

$$I_{\mathrm{ztEB}} = \frac{\mathsf{I_{zEBT}}}{2^{1-\mathsf{p_E}}\,\mathsf{V_{d_ET}}}\,D_{\mathrm{zEB}}\,E_{0\mathrm{EB}}\exp\left(\mathsf{N_{zEBT}}\left(1-\frac{2^{1-\mathsf{p_E}}}{E_{0\mathrm{EB}}}\right)\right) \quad (4.88)$$

where $E_{0\mathrm{EB}}$ is as defined by expression (4.117a) on page 59.

4.7.6 Resistances

The parasitic resistances for the emitter ($\mathsf{R_{ET}}$), the base ($\mathsf{R_{BcT}}$) and the collector ($\mathsf{R_{CcT}}$, $\mathsf{R_{CblxT}}$ and $\mathsf{R_{CbliT}}$) depend only on temperature.

4.7.7 Variable base resistance

The variable part of the base resistance is modulated by the base charges and takes into account current crowding.

$$q_0^Q = 1 + \frac{V_{t_E}}{\mathsf{V_{erT}}} + \frac{V_{t_C}}{\mathsf{V_{efT}}} \quad (4.89)$$

$$q_1^Q = \frac{q_0^Q + \sqrt{(q_0^Q)^2 + 0.01}}{2} \quad (4.90)$$

$$q_B^Q = q_1^Q\,(1 + \tfrac{1}{2}\,n_0 + \tfrac{1}{2}\,n_B) \quad (4.91)$$

$$R_{B_2} = \frac{3\,\mathsf{R_{BvT}}}{q_B^Q} \quad (4.92)$$

$$I_{B_1B_2} = \frac{2V_T}{R_{B_2}}\left(e^{\mathcal{V}_{\mathrm{B_1B_2}}/V_T}-1\right) + \frac{\mathcal{V}_{\mathrm{B_1B_2}}}{R_{B_2}} \quad (4.93)$$

Note the correspondance and differences between R_{B_2} and I_N from Eq. (4.57).

4.7.8 Variable collector resistance: the epilayer model

This model of the epilayer resistance takes into account:
– The decrease in resistance due to carriers injected from the base if only the internal base-collector is forward biased (quasi-saturation) and if both the internal and external base-collector junctions are forward biased (hard saturation and reverse mode of operation).
– Ohmic current flow at low current densities.
– Space charge limited current flow at high current densities (Kirk effect; only in forward mode).

The current through the epilayer is given by

$$K_0 = \sqrt{1 + 4\, e^{(\mathcal{V}_{\mathrm{B_2C_2}} - \mathsf{V_{dCT}})/V_T}}, \tag{4.94}$$

$$K_W = \sqrt{1 + 4\, e^{(\mathcal{V}_{\mathrm{B_2C_1}} - \mathsf{V_{dCT}})/V_T}}, \tag{4.95}$$

$$p_W = \frac{2\, e^{(\mathcal{V}_{\mathrm{B_2C_1}} - \mathsf{V_{dCT}})/V_T}}{1 + K_W}. \tag{4.96}$$

$$E_c = V_T \left[K_0 - K_W - \ln\left(\frac{K_0 + 1}{K_W + 1} \right) \right], \tag{4.97}$$

$$I_{C_1C_2} = \frac{E_c + \mathcal{V}_{\mathrm{C_1C_2}}}{\mathsf{R_{CvT}}}. \tag{4.98}$$

In reverse mode the node voltage difference $\mathcal{V}_{\mathrm{B_2C_2}}$ is the quantity that we use in further calculations. In forward mode the relation between the voltage difference $\mathcal{V}_{\mathrm{B_2C_2}}$ and the current $I_{C_1C_2}$ is not smooth enough. We will instead calculate $V^*_{B_2C_2}$ that is to be used in subsequent calculations. It has smoother properties than $\mathcal{V}_{\mathrm{B_2C_2}}$ itself. In forward mode the node voltage $\mathcal{V}_{\mathrm{C_2}}$ is *only* used for Eqs. (4.94) and (4.98).

For the rest of the quantities in the epilayer model a distinction must be made between forward and reverse mode.

Forward mode ($I_{C_1C_2} > 0$)

The voltage and current at which quasi-saturation or Kirk effect start are given by

$$V^{th}_{qs} = \mathsf{V_{dCT}} + 2\, V_T \ln\left(\frac{I_{C_1C_2}\, \mathsf{R_{CvT}}}{2V_T} + 1 \right) - \mathcal{V}_{\mathrm{B_2C_1}}, \tag{4.99}$$

$$V_{qs} = \tfrac{1}{2} \left(V^{th}_{qs} + \sqrt{(V^{th}_{qs})^2 + 4\, (0.1\, \mathsf{V_{dCT}})^2} \right), \tag{4.100}$$

$$I_{qs} = \frac{V_{qs}}{\mathsf{SCR_{Cv}}} \frac{V_{qs} + \mathsf{I_{hc}}\ \mathsf{SCR_{Cv}}}{V_{qs} + \mathsf{I_{hc}}\ \mathsf{R_{CvT}}}. \tag{4.101}$$

From this we calculate

$$\alpha = \frac{1 + \mathsf{a_{x_i}}\ \ln\{1 + \exp[(I_{C_1C_2}/I_{qs} - 1)/\mathsf{a_{x_i}}]\}}{1 + \mathsf{a_{x_i}}\ \ln\{1 + \exp[-1/\mathsf{a_{x_i}}]\}} \tag{4.102}$$

We need to solve

$$\alpha\ I_{qs} = \frac{V_{qs}}{\mathsf{SCR_{Cv}}\ y_i^2} \frac{V_{qs} + \mathsf{SCR_{Cv}}\ \mathsf{I_{hc}}\ y_i}{V_{qs} + \mathsf{R_{CvT}}\ \mathsf{I_{hc}}} \tag{4.103}$$

which leads to

$$v = \frac{V_{qs}}{\mathsf{I_{hc}}\ \mathsf{SCR_{Cv}}} \tag{4.104}$$

$$y_i = \frac{1 + \sqrt{1 + 4\,\alpha\,v\,(1+v)}}{2\,\alpha\,(1+v)} \tag{4.105}$$

The injection thickness is given by

$$\frac{x_i}{W_{\mathrm{epi}}} = 1 - \frac{y_i}{1 + p_W y_i} \tag{4.106}$$

The hole density p_0^* at the base-collector junction is given by

$$g = \frac{I_{C_1C_2}\ \mathsf{R_{CvT}}}{2V_T} \frac{x_i}{W_{\mathrm{epi}}} \tag{4.107}$$

$$p_0^* = \frac{g-1}{2} + \sqrt{\left(\frac{g-1}{2}\right)^2 + 2g + p_W(p_W + g + 1)} \tag{4.108}$$

For numerical reasons: when $p_0^* < e^{-40}$ we take $p_0^* \to 0$.

$$e^{V^*_{B_2C_2}/V_T} = p_0^*(p_0^* + 1)\ e^{\mathsf{V_{dCT}}/V_T} \tag{4.109}$$

Reverse mode ($I_{C_1C_2} \le 0$)

The hole density at the base-collector junction is given by

$$p_0^* = \frac{2\,e^{(\mathcal{V}_{\mathrm{B_2C_2}} - \mathsf{V_{dCT}})/V_T}}{1 + K_0} \tag{4.110}$$

$$e^{V^*_{B_2C_2}/V_T} = e^{\mathcal{V}_{\mathrm{B_2C_2}}/V_T} \tag{4.111}$$

The injection thickness is

$$\frac{x_i}{W_{\mathrm{epi}}} = \frac{E_c}{E_c + \mathcal{V}_{\mathrm{B_2C_2}} - \mathcal{V}_{\mathrm{B_2C_1}}} \tag{4.112}$$

Numerical problems might arise for $I_{C_1C_2} \simeq 0$. When $|\mathcal{V}_{\mathrm{C_1C_2}}| < 10^{-5}\, V_T$ or $|E_c| < e^{-40}\, V_T\, (K_0 + K_W)$ we approximate

$$p_{\mathrm{av}} = \frac{p_0^* + p_W}{2} \tag{4.113}$$

$$\frac{x_i}{W_{\mathrm{epi}}} = \frac{p_{\mathrm{av}}}{p_{\mathrm{av}} + 1} \tag{4.114}$$

4.8 Description of charges

4.8.1 Emitter depletion charges

The total base-emitter depletion capacitance is separated into a bulk and as sidewall component. The bulk component is located between nodes E_1 and B_2 and the sidewall component between nodes E_1 and B_1 (see Fig. 1)

The bulk component is

$$V_{FE} = \mathsf{V_{dE}T}\left(1 - a_{j_E}^{-1/\mathsf{pE}}\right) \tag{4.115}$$

$$V_{jE} = \mathcal{V}_{\mathrm{B_2E_1}} - 0.1\mathsf{V_{dE}T}\ln\{1 + \exp[(\mathcal{V}_{\mathrm{B_2E_1}} - V_{FE})/0.1\mathsf{V_{dE}T}]\} \tag{4.116}$$

$$E_{0}\mathrm{EB} = (1 - V_{jE}/\mathsf{V_{dE}T})^{1-\mathsf{pE}} \tag{4.117a}$$

$$V_{t_E} = \frac{\mathsf{V_{dE}T}}{1-\mathsf{pE}}\left[1 - E_{0}\mathrm{EB}\right] + a_{j_E}(\mathcal{V}_{\mathrm{B_2E_1}} - V_{jE}) \tag{4.117b}$$

$$Q_{t_E} = (1 - \mathsf{XC_{jE}})\ \mathsf{C_{jE}T}\ V_{t_E} \tag{4.118}$$

The sidewall component is

$$V_{jE}^{S} = \mathcal{V}_{\mathrm{B_1E_1}} - 0.1\mathsf{V_{dE}T}\ln\{1 + \exp[(\mathcal{V}_{\mathrm{B_1E_1}} - V_{FE})/0.1\mathsf{V_{dE}T}]\} \tag{4.119}$$

$$Q_{t_E}^{S} = \mathsf{XC_{jE}}\ \mathsf{C_{jE}T}\left(\frac{\mathsf{V_{dE}T}}{1-\mathsf{pE}}\left[1 - (1-V_{jE}^{S}/\mathsf{V_{dE}T})^{1-\mathsf{pE}}\right] + a_{j_E}(\mathcal{V}_{\mathrm{B_1E_1}} - V_{jE}^{S})\right) \tag{4.120}$$

4.8.2 Intrinsic collector depletion charge

In forward mode ($I_{C_1C_2} > 0$)

$$B_1 = \tfrac{1}{2}\mathsf{SCR_{Cv}}(I_{C_1C_2} - \mathsf{I_{hc}}) \tag{4.121}$$

$$B_2 = \mathsf{SCR_{Cv}}\ \mathsf{R_{CvT}}\ \mathsf{I_{hc}}\ I_{C_1C_2} \tag{4.122}$$

$$V_{x_i=0} = B_1 + \sqrt{B_1^2 + B_2} \tag{4.123}$$

In reverse mode ($I_{C_1C_2} \leq 0$)

$$V_{x_i=0} = \mathcal{V}_{\mathrm{C_1C_2}} \tag{4.124}$$

The junction voltage for the capacitance is given by

$$V_{\mathrm{junc}} = \mathcal{V}_{\mathrm{B_2C_1}} + V_{x_i=0} \tag{4.125}$$

The capacitance can now be calculated using

$$V_{ch} = \begin{cases} 0.1\ \mathsf{V_{dcT}} & \text{for } I_{C_1C_2} \leq 0 \\ \mathsf{V_{dcT}} \left(0.1 + 2\ \dfrac{I_{C_1C_2}}{I_{C_1C_2} + I_{qs}}\right) & \text{for } I_{C_1C_2} > 0 \end{cases} \tag{4.126}$$

$$b_{j_C} = \frac{a_{j_C} - \mathsf{X_{pT}}}{1 - \mathsf{X_{pT}}} \tag{4.127}$$

$$V_{FC} = \mathsf{V_{dcT}} \left(1 - b_{j_C}^{-1/\mathsf{pc}}\right) \tag{4.128}$$

$$V_{jC} = V_{\mathrm{junc}} - V_{ch} \ln\{1 + \exp[(V_{\mathrm{junc}} - V_{FC})/V_{ch}]\} \tag{4.129}$$

The current dependence is given by

$$I_{\mathrm{cap}} = \begin{cases} \dfrac{\mathsf{I_{hc}}\ I_{C_1C_2}}{\mathsf{I_{hc}} + I_{C_1C_2}} & \text{for } I_{C_1C_2} > 0 \\ I_{C_1C_2} & \text{for } I_{C_1C_2} \leq 0 \end{cases} \tag{4.130}$$

$$f_I = \left(1 - \frac{I_{\mathrm{cap}}}{\mathsf{I_{hc}}}\right)^{\mathsf{mc}} \tag{4.131}$$

The charge is now given by

$$V_{C_V} = \frac{\mathsf{V_{dcT}}}{1 - \mathsf{pc}} \left[1 - f_I\ (1 - V_{jC}/\mathsf{V_{dcT}})^{1-\mathsf{pc}}\right] + f_I\ b_{j_C}(V_{\mathrm{junc}} - V_{jC}) \tag{4.132}$$

$$V_{t_C} = (1 - \mathsf{X_{pT}})\ V_{C_V} + \mathsf{X_{pT}} \mathcal{V}_{\mathrm{B_2C_1}} \tag{4.133}$$

$$Q_{t_C} = \mathsf{XC_{jc}}\ \mathsf{C_{jcT}}\ V_{t_C} \tag{4.134}$$

4.8.3 Extrinsic collector depletion charges

The extrinsic collector depletion charge is partitioned between nodes C_1 and B_1 and nodes C_1 and B respectively, independent of the flag EXMOD.

$$V_{jC_{\rm ex}} = \mathcal{V}_{\rm B_1C_4} - 0.1\mathsf{V_{d_CT}} \ln\{1+\exp[(\mathcal{V}_{\rm B_1C_4} - V_{FC})/0.1\mathsf{V_{d_CT}}]\} \tag{4.135}$$

$$V_{\rm tex_V} = \frac{\mathsf{V_{d_CT}}}{1-\mathsf{p_C}}\left[1-(1-V_{jC_{\rm ex}}/\mathsf{V_{d_CT}})^{1-\mathsf{p_C}}\right] + b_{j_C}(\mathcal{V}_{\rm B_1C_4} - V_{jC_{\rm ex}}) \tag{4.136}$$

$$Q_{\rm tex} = \mathsf{C_{j_CT}}\ [(1-\mathsf{X_{pT}})\ V_{\rm tex_V} + \mathsf{X_{pT}}\mathcal{V}_{\rm B_1C_4}]\,(1-\mathsf{XC_{j_C}})\ (1-\mathsf{X_{ext}}) \tag{4.137}$$

$$XV_{jC_{\rm ex}} = \mathcal{V}_{\rm BC_3} - 0.1\mathsf{V_{d_CT}} \ln\{1+\exp[(\mathcal{V}_{\rm BC_3} - V_{FC})/0.1\mathsf{V_{d_CT}}]\} \tag{4.138}$$

$$XV_{\rm tex_V} = \frac{\mathsf{V_{d_CT}}}{1-\mathsf{p_C}}\left[1-(1-XV_{jC_{\rm ex}}/\mathsf{V_{d_CT}})^{1-\mathsf{p_C}}\right] + b_{j_C}(\mathcal{V}_{\rm BC_3} - XV_{jC_{\rm ex}}) \tag{4.139}$$

$$XQ_{\rm tex} = \mathsf{C_{j_CT}}\ [(1-\mathsf{X_{pT}})\ XV_{\rm tex_V} + \mathsf{X_{pT}}\mathcal{V}_{\rm BC_3}]\,(1-\mathsf{XC_{j_C}})\ \mathsf{X_{ext}} \tag{4.140}$$

4.8.4 Substrate depletion charge

$$V_{FS} = \mathsf{V_{d_ST}}\left(1-a_{j_S}^{-1/\mathsf{p_S}}\right) \tag{4.141}$$

$$V_{jS} = \mathcal{V}_{\rm SC_1} - 0.1\mathsf{V_{d_ST}} \ln\{1+\exp[(\mathcal{V}_{\rm SC_1} - V_{FS})/0.1\mathsf{V_{d_ST}}]\} \tag{4.142}$$

$$Q_{t_S} = \mathsf{C_{j_ST}}\ \left(\frac{\mathsf{V_{d_ST}}}{1-\mathsf{p_S}}\left[1-(1-V_{jS}/\mathsf{V_{d_ST}})^{1-\mathsf{p_S}}\right] + a_{j_S}(\mathcal{V}_{\rm SC_1} - V_{jS})\right) \tag{4.143}$$

4.8.5 Stored emitter charge

$$Q_{E0} = \boldsymbol{\tau}_{\mathsf{ET}}\ \mathsf{I_{kT}}\left(\frac{\mathsf{I_{sT}}}{\mathsf{I_{kT}}}\right)^{1/\mathsf{m_\tau}} \tag{4.144}$$

$$Q_E = Q_{E0}\ e^{\mathcal{V}_{\rm B_2E_1}/\mathsf{m_\tau}\,V_T} \tag{4.145}$$

4.8.6 Stored base charges

$$Q_{B0} = \tau_{\mathrm{BT}}\ \mathsf{I}_{\mathrm{kT}} \tag{4.146}$$

Base-emitter part

$$f_1 = \frac{4\,\mathsf{I}_{\mathrm{sT}}}{\mathsf{I}_{\mathrm{kT}}}\ e^{\mathcal{V}_{\mathrm{B_2E_1}}/V_T} \tag{4.147}$$

$$n_0 = \frac{f_1}{1+\sqrt{1+f_1}} \tag{4.148}$$

$$Q_{BE} = \tfrac{1}{2}\,Q_{B0}\ n_0\ q_1^Q \tag{4.149}$$

Base-collector part

$$f_2 = \frac{4\,\mathsf{I}_{\mathrm{sT}}}{\mathsf{I}_{\mathrm{kT}}}\ e^{V^*_{B_2C_2}/V_T} \tag{4.150}$$

$$n_B = \frac{f_2}{1+\sqrt{1+f_2}} \tag{4.151}$$

$$Q_{BC} = \tfrac{1}{2}\,Q_{B0}\ n_B\ q_1^Q \tag{4.152}$$

The expression for $e^{V^*_{B_2C_2}/V_T}$ is given in Eqs. (4.109) and (4.111).

4.8.7 Stored epilayer charge

$$Q_{\mathrm{epi0}} = \frac{4\,\tau_{\mathrm{epiT}}\ V_T}{\mathsf{R}_{\mathrm{CvT}}} \tag{4.153}$$

$$Q_{\mathrm{epi}} = \tfrac{1}{2}\ Q_{\mathrm{epi0}}\ \frac{x_i}{W_{\mathrm{epi}}}\ (p_0^* + p_W + 2) \tag{4.154}$$

4.8.8 Stored extrinsic charges

$$g_2 = 4\,e^{(\mathcal{V}_{\mathrm{B_1C_4}} - \mathsf{V}_{\mathsf{dC}\mathrm{T}})/V_T} \tag{4.155}$$

$$p_{W\mathrm{ex}} = \frac{g_2}{1+\sqrt{1+g_2}} \tag{4.156}$$

$$Q_{\mathrm{ex}} = \frac{\tau_{\mathrm{RT}}}{\tau_{\mathrm{BT}} + \tau_{\mathrm{epiT}}}\ \left(\tfrac{1}{2}\,Q_{B0}\ n_{B\mathrm{ex}} + \tfrac{1}{2}\,Q_{\mathrm{epi0}}\ p_{W\mathrm{ex}}\right) \tag{4.157}$$

The electron density $n_{B\mathrm{ex}}$ is given in Eq. (4.66).

4.8.9 Overlap charges

The overlap capacitances C_{BEO} and C_{BCO} are constant.

4.9 Extended modelling of the reverse current gain: EXMOD>1

4.9.1 Currents

The reverse currents $I_{\rm ex}$ and $I_{\rm sub}$ are redefined

$$I_{\rm ex} \rightarrow (1 - \mathsf{X_{ext}})\ I_{\rm ex} \tag{4.158}$$

$$I_{\rm sub} \rightarrow (1 - \mathsf{X_{ext}})\ I_{\rm sub} \tag{4.159}$$

The part $\mathsf{X_{ext}}$ of the reverse currents in the extrinsic transistor are connected to the external base node

$$Xg_1 = \frac{4\,\mathsf{I_{sT}}}{\mathsf{I_{kT}}}\, e^{\mathcal{V}_{\rm BC_3}/V_T} \tag{4.160}$$

$$Xn_{B\rm ex} = \frac{4\,\mathsf{I_{sT}}}{\mathsf{I_{kT}}}\, \frac{e^{\mathcal{V}_{\rm BC_3}/V_T} - 1}{1 + \sqrt{1 + Xg_1}} \tag{4.161}$$

$$XIM_{\rm ex} = \mathsf{X_{ext}}\, \frac{\mathsf{I_{kT}}}{2\,\beta_{\rm riT}}\, Xn_{B\rm ex} \tag{4.162}$$

When $\mathsf{EXSUB} = 1$, the $\mathcal{V}_{\rm SC_3}$- dependent component of the main current of the parasitic BCS transistor is included, by default ($\mathsf{EXSUB} = 0$) it is not:

$$XIM_{\rm sub} = \mathsf{X_{ext}}\, \frac{2\,\mathsf{I_{SsT}}\, \left(e^{\mathcal{V}_{\rm BC_3}/V_T} - 1\right)}{1 + \sqrt{1 + 4\, \dfrac{\mathsf{I_{sT}}}{\mathsf{I_{ksT}}}\, e^{\mathcal{V}_{\rm BC_3}/V_T}}} \quad (\mathsf{EXSUB} = 0)\ . \tag{4.163a}$$

$$XIM_{\rm sub} = \mathsf{X_{ext}}\, \frac{2\,\mathsf{I_{SsT}}\, \left(e^{\mathcal{V}_{\rm BC_3}/V_T} - e^{\mathcal{V}_{\rm SC_3}/V_T}\right)}{1 + \sqrt{1 + 4\, \dfrac{\mathsf{I_{sT}}}{\mathsf{I_{ksT}}}\, e^{\mathcal{V}_{\rm BC_3}/V_T}}} \quad (\mathsf{EXSUB} = 1)\ . \tag{4.163b}$$

If $\mathsf{EXMOD} = 1$, diode-like currents in the branch B-C_1 are limited by a resistance of value $\mathsf{R_{CcT}}$, for $\mathsf{EXMOD} = 2$ this is limiting is omitted[‖]

$$V_{\rm ex} = V_T\, \left\{2 - \ln\left[\frac{\mathsf{X_{ext}}\, (\mathsf{I_{sT}}/\beta_{\rm riT} + \mathsf{I_{SsT}})\, \mathsf{R_{CcT}}}{V_T}\right]\right\} \tag{4.164}$$

$$VB_{\rm ex} = \tfrac{1}{2}\left[(\mathcal{V}_{\rm BC_3} - V_{\rm ex}) + \sqrt{(\mathcal{V}_{\rm BC_3} - V_{\rm ex})^2 + 0.0121}\right] \tag{4.165}$$

[‖]For the sake of efficiency of implementation of the Mextram model, it is noted here that in case EXMOD = 2, the quantities $V_{\rm ex}$ and $VB_{\rm ex}$ need not be evaluated.

If $\mathsf{EXMOD} = 1$, then:

$$F_{\rm ex} = \frac{VB_{\rm ex}}{\mathsf{X_{ext}}\,(\mathsf{I_{sT}}/\beta_{\mathsf{ri}\rm T} + \mathsf{I_{SsT}})\,\mathsf{R_{CcT}} + (XIM_{\rm ex} + XIM_{\rm sub})\,\mathsf{R_{CcT}} + VB_{\rm ex}} \tag{4.166a}$$

If $\mathsf{EXMOD} = 2$, then:

$$F_{\rm ex} = 1 \tag{4.166b}$$

$$XI_{\rm ex} = F_{\rm ex}\; XIM_{\rm ex} \tag{4.167}$$

$$XI_{\rm sub} = F_{\rm ex}\; XIM_{\rm sub} \tag{4.168}$$

4.9.2 Charges

The charge $Q_{\rm ex}$ is redefined:

$$Q_{\rm ex} \rightarrow (1 - \mathsf{X_{ext}})\; Q_{\rm ex} \tag{4.169}$$

In case $\mathsf{EXMOD} = 1$, the charge in the branch B-C_3 is limited using $F_{\rm ex}$, analogous to the limiting of $XI_{\rm ex}$; in case $\mathsf{EXMOD} = 2$ this limiting is effectively omitted:

$$Xg_2 = 4\, e^{(\mathcal{V}_{\rm BC_3} - \mathsf{V_{dCT}})/V_T} \tag{4.170}$$

$$Xp_{W\rm ex} = \frac{Xg_2}{1 + \sqrt{1 + Xg_2}} \tag{4.171}$$

$$XQ_{\rm ex} = F_{\rm ex}\; \mathsf{X_{ext}}\; \frac{\tau_{\mathsf{R}\rm T}}{\tau_{\mathsf{B}\rm T} + \tau_{\mathsf{epi}\rm T}}\; \left(\tfrac{1}{2}\, Q_{B0}\; Xn_{B\rm ex} + \tfrac{1}{2}\, Q_{\rm epi0}\; Xp_{W\rm ex}\right) \tag{4.172}$$

4.10 Distributed high-frequency effects in the intrinsic base EXPHI=1

Distributed high-frequency effects are modelled, in first order approximation, both in lateral direction (current crowding) and in vertical direction (excess phase-shift). The distributed effects are an optional part of the Mextram model and can be switched on and off by a flag (on: $\mathsf{EXPHI} = 1$ and off: $\mathsf{EXPHI} = 0$).

The high-frequency current crowding is modelled by

$$Q_{B_1B_2} = \tfrac{1}{5}\; \mathcal{V}_{\rm B_1B_2}\; \left(\frac{{\rm d}Q_{t_E}}{{\rm d}\mathcal{V}_{\rm B_2E_1}} + \tfrac{1}{2}\, Q_{B0}\, q_1^Q\, \frac{{\rm d}n_0}{{\rm d}\mathcal{V}_{\rm B_2E_1}} + \frac{{\rm d}Q_E}{{\rm d}\mathcal{V}_{\rm B_2E_1}}\right) \tag{4.173}$$

For simplicity reasons only the forward depletion and diffusion charges are taken into account. (Note that the second term is the derivative of $Q_{BE} = \frac{1}{2} Q_{B0}\, q_1^Q\, n_0$, but with the derivative of q_1^Q neglected).

In vertical direction (excess phase-shift) base-charge partitioning is used. For simplicity reasons it is only implemented for high level injection. Now Q_{BE} from Eq. (4.149) and Q_{BC} from Eq. (4.152) are redefined according to

$$Q_{BC} \rightarrow \mathsf{X_{Q_B}} \cdot (Q_{BE} + \mathsf{K_E} Q_E) + Q_{BC} \tag{4.175}$$

$$Q_{BE} \rightarrow (1 - \mathsf{X_{Q_B}}) \cdot (Q_{BE} + \mathsf{K_E} Q_E) \tag{4.176}$$

Where $\mathsf{K_E} = 1$ (default value is zero), the charges Q_{BE} and Q_E are considered to form an inseparable whole; in turn it is this whole that is redistributed over the emitter-base and collector-base junction, the ratio of this distribution being controlled by the parameter $\mathsf{X_{Q_B}}$. The value of $\mathsf{X_{Q_B}}$ in Mextram is set to $\frac{1}{3}$ by default.

In terms of the Equivalent circuit of Fig. 1: whenever $\mathsf{EXPHI} = 1$ and $\mathsf{K_E} = 1$, the charge Q_E is considered to be absorbed in charge Q_{BE} and it is not to be taken into account separately in e.g. the calculation of dynamic currents or capacitances. In general, the total charge $Q_{B_2E_1}$ between nodes B_2 and E_1 therefore amounts to

$$Q_{B_2E_1} = Q_{t_E} + Q_{BE} + Q_E * (1 - \mathsf{K_E} * \mathsf{EXPHI}). \tag{4.177}$$

4.11 Heterojunction features

The most important difference between SiGe and pure Si transistors is the functional difference between hole charges and Gummel number. When the Ge concentration has a non-zero slope ($\mathsf{dE_g} \neq 0$) we redefine the q_0^I describing the Early effect for the currents (the q_0^Q remains unchanged):

$$q_0^I \rightarrow \frac{\exp\left(\left[\dfrac{V_{t_E}}{\mathsf{V_{erT}}} + 1\right] \dfrac{\mathsf{dE_{gT}}}{V_T}\right) - \exp\left(\dfrac{-V_{t_C}}{\mathsf{V_{efT}}} \dfrac{\mathsf{dE_{gT}}}{V_T}\right)}{\exp\left(\dfrac{\mathsf{dE_{gT}}}{V_T}\right) - 1}. \tag{4.178}$$

Another feature that might be needed for SiGe transistors is recombination in the base. This changes the forward ideal base current (when $\mathsf{X_{rec}} \neq 0$)

$$I_{B_1} \rightarrow \frac{\mathsf{I_{sT}}}{\boldsymbol{\beta}_{\mathsf{fT}}} (1 - \mathsf{XI_{B_1}}) \left[(1 - \mathsf{X_{rec}}) \left(e^{\mathcal{V}_{\mathrm{B_2E_1}}/V_T} - 1 \right) + \mathsf{X_{rec}} \left(e^{\mathcal{V}_{\mathrm{B_2E_1}}/V_T} + e^{V^*_{B_2C_2}/V_T} - 2 \right) \left(1 + \frac{V_{t_C}}{\mathsf{V_{efT}}} \right) \right] . \tag{4.179}$$

The last term also describes Auger recombination in high injection.

4.12 Noise model

For noise analysis, noise sources are added to various components of the equivalent circuit in the form of current sources. The types of noise supported include:

- Thermal noise of resistive components resulting from majority carrier Brownian motion.
- Transistor $1/f$ noise resulting from carrier trapping, primarily in the base current.
- Transistor "shot" noise which physically results from minority carrier Brownian motion.
- Additional high frequency transistor correlation noise resulting from frequency dependence of the propagation of minority carrier Brownian motion towards transistor terminals.
- Avalanche multiplication noises.

Coupling of correlation noise and avalanche noises are not accounted for as it is not important, at least for present applications.

Below the mean square power is given for each independent noise source. Noise correlation is produced using dependent sources with proper control coefficients.

We will use f for operation frequency, Δf for bandwidth. When Δf is taken as $1\,\mathrm{Hz}$, a noise power spectral density (PSD) is obtained.

4.12.1 Thermal noise

For each resistor in Fig. 1 on page 4, a thermal noise current source is placed in parallel with it. The mean square values are:

$$\overline{iN^2_{R_E}} = \frac{4\,kT_K}{\mathsf{R_{ET}}}\,\Delta f. \tag{4.180}$$

$$\overline{iN^2_{R_{Bc}}} = \frac{4\,kT_K}{\mathsf{R_{BcT}}}\,\Delta f. \tag{4.181}$$

$$\overline{iN^2_{R_{Cc}}} = 4\,kT_K\,\mathsf{G_{CcT}}\,\Delta f, \tag{4.182a}$$
$$\overline{iN^2_{\mathsf{R_{Cblx}}}} = 4\,kT_K\,\mathsf{G_{CblxT}}\,\Delta f, \tag{4.182b}$$
$$\overline{iN^2_{\mathsf{R_{Cbli}}}} = 4\,kT_K\,\mathsf{G_{CbliT}}\,\Delta f. \tag{4.182c}$$

For the variable part of the base resistance a different formula is used, taking into account the effect of current crowding on noise behaviour [22]

$$\overline{iN^2_{R_{Bv}}} = \frac{4\,kT_K}{R_{B_2}}\,\frac{4\,e^{\mathcal{V}_{\mathrm{B_1B_2}}/V_T}+5}{3}\,\Delta f, \tag{4.183}$$

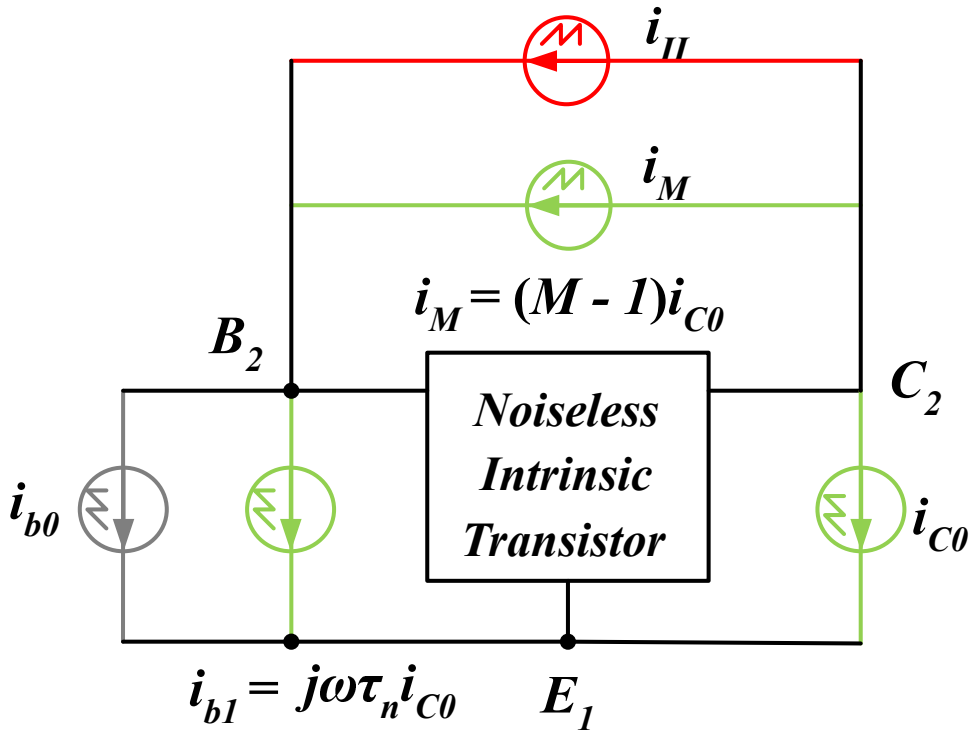

Figure 10: *Noise sources of the intrinsic transistor.*

4.12.2 Intrinsic transistor noise

The intrinsic transistor noise model is depicted in Fig. 10.

i_{b0} includes base current shot noise and $1/f$ noise:

$$\overline{i_{b0}i_{b0}^*} = \left\{ 2q \left(|I_{B_1}| + |I_{B_2}| + |I_{\mathrm{ztEB}}| \right) + \frac{\mathsf{K_f}}{f} \left(1 - \mathsf{XI_{B_1}}\right) \left(\frac{|I_{B_1}|}{1 - \mathsf{XI_{B_1}}} \right)^{\mathsf{A_f}} + \frac{\mathsf{K_{fN}}}{f} |I_{B_2}|^{2(\mathsf{m_{Lf}}-1)+\mathsf{A_f}(2-\mathsf{m_{Lf}})} \right\} \Delta f. \tag{4.184}$$

i_{C0} is collector current shot noise:

$$\overline{i_{C0}i_{C0}^*} = 2qI_{C0}\Delta f, \tag{4.185a}$$

$$I_{C0} = \frac{I_f + I_r}{q_B^I}, \tag{4.185b}$$

where I_{C0} is essentially the main current, or current transported from the emitter in forward mode operation.

i_{b1} in Fig. 10 is a base current noise correlated with i_{C0} as follows:

$$i_{b1} = j\omega\tau_n i_{C0}, \tag{4.186}$$

where τ_n is called noise transit time, and evaluated according to the value of noise correlation switch $\mathsf{K_C}$:

$$\tau_n = \begin{cases} 0 & \mathsf{K_C} = 0, \\ \mathsf{X_{QB}}\tau_{Bn} & \mathsf{K_C} = 1, \\ \mathsf{F_{taun}}\tau_{Bn} & \mathsf{K_C} = 2. \end{cases} \tag{4.187a}$$

The τ_{Bn} above is a version of the base transit time modified for noise purpose. $\mathsf{F_{taun}}$ is fraction of τ_n in τ_{Bn}. τ_{Bn} is evaluated as:

$$\tau_{Bn} = \begin{cases} \frac{Q_{BE}+Q_{BC}}{I_{C0}} & I_{C0} > 0, \\ \tau_{BT} q_1 q_B^I & I_{C0} = 0. \end{cases} \tag{4.188}$$

In forward mode, τ_{Bn} is essentially the effective base transit time accounting for high injection effects. In reverse mode, only base width modulation effect is considered.

i_{M} and i_{II} in Fig. 10 describe avalanche noise. i_{M} is direct result of the avalanche multiplication of the noise in the electron current entering collector-base junction, i_{C0}, and relates to i_{C0} the same way I_{avl} relates to $\mathsf{I_N}$:

$$i_{\mathrm{M}} = \mathsf{K_{avl}}(M-1)i_{C0}, \tag{4.189}$$

where M is avalanche multiplication factor and computed from the avalanche current as:

$$M - 1 = \frac{I_{avl}}{I_{C0}}. \tag{4.190}$$

i_{II} is due to the noise of the impact ionization process itself, which is independent of i_{M}

$$\overline{i_{\mathrm{II}} i_{\mathrm{II}}^*} = \mathsf{K_{avl}} \cdot 2q\ I_{C0}(M-1)M\Delta f. \tag{4.191}$$

4.12.3 Parasitic transistor noise

Emitter-base sidewall current has shot noise and $1/f$-noise:

$$\overline{iN_{BS}^2} = \left\{ 2q\ |I_{B_1}^S| + \frac{\mathsf{K_f}}{f}\ \mathsf{XI_{B_1}}\ \left(\frac{|I_{B_1}^S|}{\mathsf{XI_{B_1}}} \right)^{\mathsf{A_f}} \right\}\ \Delta f. \tag{4.192}$$

Reverse base current has shot noise and $1/f$-noise:

$$\overline{iN_{B_3}^2} = \left\{ 2q\ |I_{B_3}| + \frac{\mathsf{K_f}}{f}\ |I_{B_3}|^{\mathsf{A_f}} \right\}\ \Delta f. \tag{4.193}$$

Extrinsic current shot noise and $1/f$-noise are implemented as follows. When $\mathsf{EXMOD} = 0$ we have

$$\overline{iN^2_{I_{\rm ex}}} = \left\{ 2q\,|I_{\rm ex}| + \frac{\mathsf{K_f}}{f}\;|I_{\rm ex}|^{\mathsf{A_f}} \right\}\;\Delta f. \tag{4.194}$$

When $\mathsf{EXMOD} = 1$ we have

$$\overline{iN^2_{I_{\rm ex}}} = \left\{ 2q\,|I_{\rm ex}| + \frac{\mathsf{K_f}}{f}\;(1-\mathsf{X_{ext}})\;\left(\frac{|I_{\rm ex}|}{1-\mathsf{X_{ext}}}\right)^{\mathsf{A_f}} \right\}\;\Delta f. \tag{4.195}$$

$$\overline{iN^2_{XI_{\rm ex}}} = \left\{ 2q\,|XI_{\rm ex}| + \frac{\mathsf{K_f}}{f}\;\mathsf{X_{ext}}\;\left(\frac{|XI_{\rm ex}|}{\mathsf{X_{ext}}}\right)^{\mathsf{A_f}} \right\}\;\Delta f. \tag{4.196}$$

Substrate current has only shot noise:

$$\overline{iN^2_{I_{\rm sub}}} = 2q\,|I_{\rm sub}|\;\Delta f. \tag{4.197}$$

$$\overline{iN^2_{XI_{\rm sub}}} = 2q\,|XI_{\rm sub}|\;\Delta f. \tag{4.198}$$

4.13 Self-heating

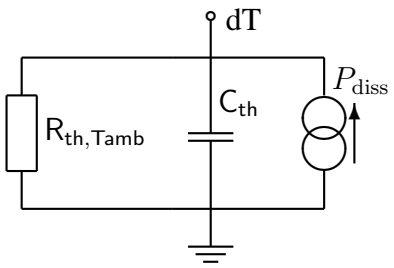

Material	$\mathsf{A_{th}}$
Si	1.3
Ge	1.25
GaAs	1.25
AlAs	1.37
InAs	1.1
InP	1.4
GaP	1.4
SiO_2	0.7

Figure 11: *On the left, the self-heating network. Note that for increased flexibility the node dT should be available to the user. On the right are parameter values that can be used for* $\mathsf{A_{th}}$.

For self-heating an extra network is introduced, see Fig. 11. It contains the self-heating resistance $\mathsf{R_{th,Tamb}}$ and capacitance $\mathsf{C_{th}}$, both connected between ground and the temperature node dT. The value of the voltage $\mathcal{V}_{\rm dT}$ at the temperature node gives the increase in local temperature. The dissipation is given by

$$\begin{aligned} P_{\rm diss} = {} & I_N\,(\mathcal{V}_{\rm B_2E_1} - V^*_{B_2C_2}) + I_{C_1C_2}\,(V^*_{B_2C_2} - \mathcal{V}_{\rm B_2C_1}) - I_{\rm avl}\,V^*_{B_2C_2} \\ & + \mathcal{V}^2_{\rm EE_1}/\mathsf{R_{ET}} + \mathcal{V}^2_{\rm BB_1}/\mathsf{R_{BcT}} \\ & + \mathcal{V}^2_{\rm CC_3}\,\mathsf{G_{CcT}} + \mathcal{V}^2_{\rm C_3C_4}\,\mathsf{G_{CblxT}} + \mathcal{V}^2_{\rm C_4C_1}\,\mathsf{G_{CbliT}} \\ & + I_{B_1B_2}\,\mathcal{V}_{\rm B_1B_2} + (I_{B_1} + I_{B_2} - I_{\rm ztEB})\mathcal{V}_{\rm B_2E_1} + I^S_{B_1}\,\mathcal{V}_{\rm B_1E_1} \\ & + (I_{\rm ex} + I_{B_3})\,\mathcal{V}_{\rm B_1C_4} + XI_{\rm ex}\,\mathcal{V}_{\rm BC_3} \\ & + I_{\rm sub}\mathcal{V}_{\rm B_1S} + XI_{\rm sub}\mathcal{V}_{\rm BS} - I_{\rm Sf}\,\mathcal{V}_{\rm C_1S}. \end{aligned} \tag{4.199}$$

Note that the effect of the parameter DTA and dynamic selfheating as discussed here are independent [4, 27], see Sec. 2.6.2. To use a more complicated self-heating network, one can increase $\mathsf{R_{th}}$ to very large values, make $\mathsf{C_{th}}$ zero, and add the wanted self-heating network externally to the node dT. Examples of how to use thermal networks are given in Ref. [27].

For the value of $\mathsf{A_{th}}$ we recommend using values from literature that describe the temperature scaling of the thermal conductivity. For the most important materials, the values are given in Figure 11, which is largely based on Ref. [28], see also [29].

Please note that taking $\mathsf{C_{th}} = 0$ in the self-heating model is *incorrect* for AC simulations (and hence also for transient simulations). The reason is that $\mathsf{C_{th}} = 0$ means that self-heating is infinitely fast. In reality, however, self-heating is much slower than the relevant time scales in most applications. Therefore, for simulations always a non-zero thermal capacitance should be used, even when the thermal capacitance has not been extracted. Since in practice the thermal time delay is of the order of $1\,\mu$s, a reasonable estimate for the thermal capitance can be given by $\mathsf{C_{th}} = 1\,\mu\mathrm{s}/\mathsf{R_{th}}$.

4.14 Implementation issues

4.14.1 Convergence aid: minimal conductance $G_{\min}$

Experience has learned that convergence of the model in circuit simulation is helped by addition of a conductance $G_{\min}$ to the forward- (4.60) and reverse non-ideal base currents (4.61). In practice, during simulation, the value of $G_{\min}$ is often controlled by the circuit simulator.

When we include this convergence aid, Eqn (4.60) is implemented as

$$I_{B_2} = \mathsf{I}_{\mathsf{BfT}} \left(e^{\mathcal{V}_{\mathrm{B_2E_1}}/\mathsf{m}_{\mathsf{Lf}} V_T} - 1\right) + G_{\min}\, \mathcal{V}_{\mathrm{B_2E_1}}, \tag{4.200}$$

while Eqn. (4.61) is implemented as:

$$I_{B_3} = \mathsf{I}_{\mathsf{BrT}} \frac{e^{\mathcal{V}_{\mathrm{B_1C_4}}/V_T} - 1}{e^{\mathcal{V}_{\mathrm{B_1C_4}}/2V_T} + e^{\mathsf{V}_{\mathsf{Lr}}/2V_T}} + G_{\min}\, \mathcal{V}_{\mathrm{B_1C_4}}. \tag{4.201}$$

We emphasize that the terms $G_{\min}$ are added in circuit simulators only to improve convergence: the physically correct behaviour of the model is established only in the limit $G_{\min} \to 0$.

If $G_{\min}$ is not zero, its influence can be seen on some characteristics. In the context of implementation testing and comparison, it is therefore important to give $G_{\min}$ a well-defined, prescribed value. Traditionally, Mextram has been tested with the above implementation – i.e. Eqns. (4.200) and (4.201) – of Equations (4.60) and (4.61), with a value $G_{\min} = 1.0 \cdot 10^{-13}\,\mathrm{A/V}$. In practical testing, specification of the value of $G_{\min}$ should be part of the test specification.

$G_{\min}$ is not included in the operating point information.

4.14.2 Transition functions

In several places in the code a transition function is used, like the `hyp`-functions and the `log-exp`-functions. These functions are the smoothed versions of the functions `min` and `max`. These functions must be programmed in a numerical stable way. This can be done in several ways. Here we only give the basic formulations.

For the depletion charges we use the function

$$\min{}_{\texttt{logexp}}(x, x_0; a) = x - a\ \ln\{1 + \exp[(x - x_0)/a]\} \tag{4.202}$$

In the implementation this is coded as

$$\min{}_{\texttt{logexp}}(x, x_0; a) = \begin{cases} x - a\ \ln\{1 + \exp[(x - x_0)/a]\} & \text{for } x < x_0 \\ x_0 - a\ \ln\{1 + \exp[(x_0 - x)/a]\} & \text{for } x \geq x_0 \end{cases} \tag{4.203}$$

In the epilayer model we calculate α using

$$\max{}_{\texttt{logexp}}(x, x_0; a) = x_0 + a\ \ln\{1 + \exp[(x - x_0)/a]\} \tag{4.204}$$

In the implementation this is coded as

$$\max{}_{\texttt{logexp}}(x,x_0;a)=\begin{cases}x_0+a\ \ln\{1+\exp[(x-x_0)/a]\} & \text{for } x<x_0\\ x+a\ \ln\{1+\exp[(x_0-x)/a]\} & \text{for } x\geq x_0\end{cases} \tag{4.205}$$

The same is used for the temperature scaling of the diffusion voltages. Real hyperbolic functions are used for the calculation of $q_1^{Q,I}$, V_{qs}, and $V_{B\mathrm{ex}}$:

$$\max{}_{\texttt{hyp}}(x,x_0;\epsilon)=\tfrac{1}{2}\left[\sqrt{(x-x_0)^2+4\epsilon^2}+x+x_0\right] \tag{4.206}$$

In the implementation this can be coded as

$$\max{}_{\texttt{hyp}}(x,x_0;\epsilon)=\begin{cases}x_0+\dfrac{2\epsilon^2}{\sqrt{(x-x_0)^2+4\epsilon^2}+x_0-x} & \text{for } x<x_0\\ x+\dfrac{2\epsilon^2}{\sqrt{(x-x_0)^2+4\epsilon^2}+x-x_0} & \text{for } x\geq x_0\end{cases} \tag{4.207}$$

One can also make a difference between the cases $|x|<2\epsilon$ and $|x|>2\epsilon$ to improve the stability.

4.14.3 Some derivatives

For some of the equations the derivatives can be simplified by using some math. For instance, for n_0 we have

$$n_0=\frac{f_1}{1+\sqrt{1+f_1}}=\sqrt{1+f_1}-1 \tag{4.208a}$$

For the implementation of n_0 we need the first expression, especially when f_1 is small. But for the derivative we can take the second expression. The same holds for

$$n_B=\frac{f_2}{1+\sqrt{1+f_2}}=\sqrt{1+f_2}-1 \tag{4.208b}$$

$$p_{W\mathrm{ex}}=\frac{g_2}{1+\sqrt{1+g_2}}=\sqrt{1+g_2}-1 \tag{4.208c}$$

$$Xp_{W\mathrm{ex}}=\frac{Xg_2}{1+\sqrt{1+Xg_2}}=\sqrt{1+Xg_2}-1 \tag{4.208d}$$

For the epilayer model we have similar equations, where again the second expression can be used for calculating derivatives:

$$p_W=\frac{2\,e^{(\mathcal{V}_{\mathrm{B_2C_1}}-\mathsf{V}_{\mathrm{d_CT}})/V_T}}{1+K_W}=\tfrac{1}{2}\,(K_W-1) \tag{4.208e}$$

$$p_0^*=\frac{2\,e^{(\mathcal{V}_{\mathrm{B_2C_2}}-\mathsf{V}_{\mathrm{d_CT}})/V_T}}{1+K_0}=\tfrac{1}{2}\,(K_0-1) \tag{4.208f}$$

The latter is needed only in reverse mode.

4.14.4 Numerical stability of p_0^*

For any root of a quadratic equation there are two ways of writing the solution. These differ in their numerical stability. Therefore, for p_0^*, we implement:

$$p_0^* = \begin{cases} \dfrac{g-1}{2} + \sqrt{\left(\dfrac{g-1}{2}\right)^2 + 2g + p_W(p_W+g+1)}, & \text{for } g > 1 \\ \dfrac{2g + p_W(p_W+g+1)}{\dfrac{1-g}{2} + \sqrt{\left(\dfrac{1-g}{2}\right)^2 + 2g + p_W(p_W+g+1)}}, & \text{for } g < 1 \end{cases} \tag{4.209}$$

4.15 Embedding of PNP transistors

Although NPN transistors are the most used bipolar transistors it is also necessary to be able to describe PNP-transistors. The equations given above are only for NPN transistors. It is however easy to map a PNP-device with its bias conditions onto an NPN model. To do this we need three steps:
• The model uses the following internal voltages:

$$\mathcal{V}_{\mathrm{B_2C_1}},\ \mathcal{V}_{\mathrm{B_2C_2}},\ \mathcal{V}_{\mathrm{B_2E_1}},\ \mathcal{V}_{\mathrm{B_1E_1}},\ \mathcal{V}_{\mathrm{B_1B_2}},\ \mathcal{V}_{\mathrm{B_1C_1}},\ \mathcal{V}_{\mathrm{BC_1}},\ \mathcal{V}_{\mathrm{SC_1}}$$

For a PNP the sign of these voltages must be changed ($V \rightarrow -V$). The value of $\mathcal{V}_{\mathrm{dT}}$ does *not* change sign.
• Calculate the currents, charges and noise densities with the equations for the NPN transistor. Note that the parameters are still like those for an NPN. For instance all currents like $\mathsf{I_s}$ must be taken positive.
• Change the sign of all resulting currents ($I \rightarrow -I$)

$$I_N,\ I_{B_1B_2},\ I_{C_1C_2},\ I_{\mathrm{avl}},\ I_{B_1},\ I_{B_1}^S,\ I_{B_2},\ I_{\mathrm{ztEB}},\ I_{B_3},\ I_{\mathrm{ex}},\ XI_{\mathrm{ex}},\ I_{\mathrm{sub}},\ XI_{\mathrm{sub}},\ I_{\mathrm{Sf}}$$

and charges ($Q \rightarrow -Q$)

$$Q_E,\ Q_{t_E},\ Q_{t_C},\ Q_{BE},\ Q_{BC},\ Q_{\mathrm{epi}},\ Q_{B_1B_2},\ Q_{\mathrm{ex}},\ XQ_{\mathrm{ex}},\ Q_{\mathrm{tex}},\ XQ_{\mathrm{tex}},\ Q_{t_S},\ Q_{BEO},\ Q_{BCO}$$

The noise current densities do not change sign. The power dissipation term P_{diss} and the thermal charge $\mathsf{C_{th}} \cdot V_{dT}$ do not change sign. The following derivatives *do* need an extra sign:

$$\frac{\partial P_{\mathrm{diss}}}{\partial \mathcal{V}_{\mathrm{B_2E_1}}}, \qquad \text{etc.}$$

All other derivatives $\partial I/\partial V$ and $\partial Q/\partial V$ do not need an extra sign.

Furthermore, note that the constants A_n and B_n for the avalanche model are different for NPN's and for PNP's.

4.16 Distribution of the collector resistance

The buried layer resistances were introduced in Mextram 504.7, in a backwards compatibe way. This implies that the default values of these resistances is zero. Because values of $0\,\Omega$ thus are allowed for resistances $\mathsf{R_{Cblx}}$ and $\mathsf{R_{Cbli}}$, the lower clipping value of the resistances is zero and very small values of the resistances $\mathsf{R_{Cblx}}$ and $\mathsf{R_{Cbli}}$ are formally allowed. Resistance values very close to zero are known to form a potential threat to convergence however. In order to exclude the possibility that the resistances of the buried layer take such small values during the convergence process due to temperature effects, the lower clipping value for the temperature coefficient $\mathsf{A_{Cbl}}$ of the resistances $\mathsf{R_{Cblx}}$ and $\mathsf{R_{Cbli}}$ has been set to zero.

In case one of both of the $\mathsf{R_{Cblx}}$ and $\mathsf{R_{Cbli}}$ resistances vanish, the corresponding node (C_3 and or C_4) effectively disappears from the equivalent circuit. Hence the circuit topology depends on parameter values. Special attention has to be paid to this in implementation of the model.

4.17 Operating point information

The operating point information is a list of quantities that describe the internal state of the transistor. When a circuit simulator is able to provide these, it might help the designer understand the behaviour of the transistor and the circuit. All of these values have the sign that belongs to NPN-transistors (so normally I_C and $\mathcal{V}_{\mathrm{B_2E_1}}$ will be positive, even for a PNP transistor).

The full list of operating point information consists of four parts. First the external collector currents, base current and current gain are given. Next we have all the branch biases, the currents and the charges. Then we have, as usual, the elements that can be used if a full small-signal equivalent circuit is needed. These are all the derivatives of the charges and currents. At last, and possibly the most informative, we have given approximations to the small-signal model which together form a hybrid-π model with similar behavior as the full Mextram model. In addition the cut-off frequency is included.

Note that $G_{\min}$ is not included in the expressions of the operating point information (see section 4.14).

The external currents and current gain:

I_E External DC emitter current
I_C External DC collector current
I_B External DC base current
I_S External DC substrate current
β_{dc} External DC current gain I_C/I_B

External voltage differences:

V_{BE} External base-emitter voltage
V_{BC} External base-collector voltage
V_{CE} External collector-emitter voltage
V_{SE} External substrate-emitter voltage
V_{BS} External base-substrate voltage
V_{SC} External substrate-collector voltage

Since we have 5 internal nodes we need 5 voltage differences to describe the bias at each internal node, given the external biases. We take those that are the most informative for the internal state of the transistor:

$\mathcal{V}_{\mathrm{B_2E_1}}$ Internal base-emitter bias
$\mathcal{V}_{\mathrm{B_2C_2}}$ Internal base-collector bias
$\mathcal{V}_{\mathrm{B_2C_1}}$ Internal base-collector bias including epilayer
$\mathcal{V}_{\mathrm{B_1C_1}}$ External base-collector bias without parasitic resistances
$\mathcal{V}_{\mathrm{C_4C_1}}$ Bias over intrinsic buried layer
$\mathcal{V}_{\mathrm{C_3C_4}}$ Bias over extrinsic buried layer
$\mathcal{V}_{\mathrm{E_1E}}$ Bias over emitter resistance

The actual currents are:

I_N Main current

$I_{C_1C_2}$	Epilayer current
$I_{B_1B_2}$	Pinched-base current
I_{B_1}	Ideal forward base current
$I_{B_1}^S$	Ideal side-wall base current
I_{ztEB}	Zener tunneling current in emitter-base junction
I_{B_2}	Non-ideal forward base current
I_{B_3}	Non-ideal reverse base current
I_{avl}	Avalanche current
I_{ex}	Extrinsic reverse base current
XI_{ex}	Extrinsic reverse base current
I_{sub}	Substrate current
XI_{sub}	Substrate current
I_{Sf}	Substrate-Collector current
I_{R_E}	Current through emitter resistance
$I_{R_{Bc}}$	Current through constant base resistance
$I_{R_{Cblx}}$	Current through extrinsic buried layer resistance
$I_{R_{Cbli}}$	Current through intrinsic buried layer resistance
$I_{R_{Cc}}$	Current through collector contact resistance

The actual charges are:

Q_E	Emitter charge or emitter neutral charge
Q_{t_E}	Base-emitter depletion charge
$Q_{t_E}^S$	Sidewall base-emitter depletion charge
Q_{BE}	Base-emitter diffusion charge
Q_{BC}	Base-collector diffusion charge
Q_{t_C}	Base-collector depletion charge
Q_{epi}	Epilayer diffusion charge
$Q_{B_1B_2}$	AC current crowding charge
Q_{tex}	Extrinsic base-collector depletion charge
XQ_{tex}	Extrinsic base-collector depletion charge
Q_{ex}	Extrinsic base-collector diffusion charge
XQ_{ex}	Extrinsic base-collector diffusion charge
Q_{t_S}	Collector-substrate depletion charge

The small-signal equivalent circuit contains the following conductances. In the terminology we use the notation A_x, A_y and A_z to denote derivatives of the quantity A to some voltage difference. We use x for base-emitter biases, y is the derivative w./r./t./ $\mathcal{V}_{\mathrm{B_2C_2}}$ and z is used for all other base-collector biases. The subindex π is used for base-emitter base currents, μ is used for base-collector base currents, Rbv for derivatives of $I_{B_1B_2}$ and Rcv for derivatives of $I_{C_1C_2}$.

Quantity	Equation	Description
g_x	$\partial I_N/\partial\mathcal{V}_{\mathrm{B_2E_1}}$	Forward transconductance
g_y	$\partial I_N/\partial\mathcal{V}_{\mathrm{B_2C_2}}$	Reverse transconductance
g_z	$\partial I_N/\partial\mathcal{V}_{\mathrm{B_2C_1}}$	Reverse transconductance
g_π^S	$\partial I_{B_1}^S/\partial\mathcal{V}_{\mathrm{B_1E_1}}$	Conductance sidewall b-e junction
$g_{\pi,x}$	$\partial(I_{B_1}+I_{B_2}-I_{\mathrm{ztEB}})/\partial\mathcal{V}_{\mathrm{B_2E_1}}$	Conductance floor b-e junction
$g_{\pi,y}$	$\partial I_{B_1}/\partial\mathcal{V}_{\mathrm{B_2C_2}}$	Early effect on recombination base current
$g_{\pi,z}$	$\partial I_{B_1}/\partial\mathcal{V}_{\mathrm{B_2C_1}}$	Early effect on recombination base current
$g_{\mu,x}$	$-\partial I_{\mathrm{avl}}/\partial\mathcal{V}_{\mathrm{B_2E_1}}$	Early effect on avalanche current limiting
$g_{\mu,y}$	$-\partial I_{\mathrm{avl}}/\partial\mathcal{V}_{\mathrm{B_2C_2}}$	Conductance of avalanche current
$g_{\mu,z}$	$-\partial I_{\mathrm{avl}}/\partial\mathcal{V}_{\mathrm{B_2C_1}}$	Conductance of avalanche current
$g_{\mu\mathrm{ex}}$	$\partial(I_{\mathrm{ex}}+I_{B_3})/\partial\mathcal{V}_{\mathrm{B_1C_4}}$	Conductance extrinsic b-c junction
$Xg_{\mu\mathrm{ex}}$	$\partial XI_{\mathrm{ex}}/\partial\mathcal{V}_{\mathrm{BC_3}}$	Conductance extrinsic b-c junction
$g_{Rcv,y}$	$\partial I_{C_1C_2}/\partial\mathcal{V}_{\mathrm{B_2C_2}}$	Conductance of epilayer current
$g_{Rcv,z}$	$\partial I_{C_1C_2}/\partial\mathcal{V}_{\mathrm{B_2C_1}}$	Conductance of epilayer current
r_{bv}	$1/(\partial I_{B_1B_2}/\partial\mathcal{V}_{\mathrm{B_1B_2}})$	Base resistance
$g_{Rbv,x}$	$\partial I_{B_1B_2}/\partial\mathcal{V}_{\mathrm{B_2E_1}}$	Early effect on base resistance
$g_{Rbv,y}$	$\partial I_{B_1B_2}/\partial\mathcal{V}_{\mathrm{B_2C_2}}$	Early effect on base resistance
$g_{Rbv,z}$	$\partial I_{B_1B_2}/\partial\mathcal{V}_{\mathrm{B_2C_1}}$	Early effect on base resistance
r_{bv}	$1/(\partial I_{B_1B_2}/\partial\mathcal{V}_{\mathrm{B_1B_2}})$	Base resistance
$g_{Rbv,x}$	$\partial I_{B_1B_2}/\partial\mathcal{V}_{\mathrm{B_2E_1}}$	Early effect on base resistance
$g_{Rbv,y}$	$\partial I_{B_1B_2}/\partial\mathcal{V}_{\mathrm{B_2C_2}}$	Early effect on base resistance
$g_{Rbv,z}$	$\partial I_{B_1B_2}/\partial\mathcal{V}_{\mathrm{B_2C_1}}$	Early effect on base resistance
r_{bv}	$1/(\partial I_{B_1B_2}/\partial\mathcal{V}_{\mathrm{B_1B_2}})$	Base resistance
$g_{Rbv,x}$	$\partial I_{B_1B_2}/\partial\mathcal{V}_{\mathrm{B_2E_1}}$	Early effect on base resistance
$g_{Rbv,y}$	$\partial I_{B_1B_2}/\partial\mathcal{V}_{\mathrm{B_2C_2}}$	Early effect on base resistance
$g_{Rbv,z}$	$\partial I_{B_1B_2}/\partial\mathcal{V}_{\mathrm{B_2C_1}}$	Early effect on base resistance
R_E	$\mathsf{R}_{\mathsf{E}\mathrm{T}}$	Emitter resistance
R_{Bc}	$\mathsf{R}_{\mathsf{Bc}\mathrm{T}}$	Constant base resistance
R_{Cc}	$\mathsf{R}_{\mathsf{Cc}\mathrm{T}}$	Collector contact resistance
R_{Cblx}	$\mathsf{R}_{\mathsf{Cblx}\mathrm{T}}$	Extrinsic buried layer resistance
R_{Cbli}	$\mathsf{R}_{\mathsf{Cbli}\mathrm{T}}$	Intrinsic buried layer resistance
g_S	$\partial I_{\mathrm{sub}}/\partial\mathcal{V}_{\mathrm{B_1C_1}}$	Conductance parasitic PNP transistor
Xg_S	$\partial XI_{\mathrm{sub}}/\partial\mathcal{V}_{\mathrm{BC_1}}$	Conductance parasitic PNP transistor
g_{Sf}	$\partial I_{\mathrm{Sf}}/\partial\mathcal{V}_{\mathrm{SC_1}}$	Conductance Substrate-Collector current

The small-signal equivalent circuit contains the following capacitances

Quantity	Equation	Description
C_{BE}^S	$\partial Q_{t_E}^S/\partial\mathcal{V}_{\mathrm{B_1E_1}}$	Capacitance sidewall b-e junction
$C_{BE,x}$	$\partial(Q_{t_E}+Q_{BE}+Q_E*(1-\mathsf{K_E}*\mathsf{EXPHI}))/\partial\mathcal{V}_{\mathrm{B_2E_1}}$	Capacitance floor b-e junction
$C_{BE,y}$	$\partial Q_{BE}/\partial\mathcal{V}_{\mathrm{B_2C_2}}$	Early effect on b-e diffusion charge
$C_{BE,z}$	$\partial Q_{BE}/\partial\mathcal{V}_{\mathrm{B_2C_1}}$	Early effect on b-e diffusion charge
$C_{BC,x}$	$\partial Q_{BC}/\partial\mathcal{V}_{\mathrm{B_2E_1}}$	Early effect on b-c diffusion charge
$C_{BC,y}$	$\partial(Q_{t_C}+Q_{BC}+Q_{\mathrm{epi}})/\partial\mathcal{V}_{\mathrm{B_2C_2}}$	Capacitance floor b-c junction

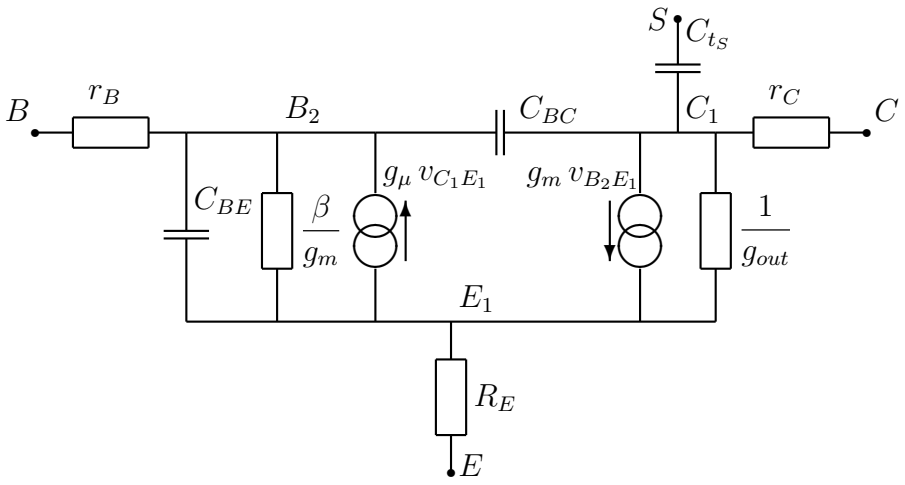

Figure 12: *Small-signal equivalent circuit describing the approximate behaviour of the Mextram model. The actual forward Early voltage can be found as* $V_{eaf} = I_C/g_{out} - \mathcal{V}_{\rm CE}$. *which can be different from the parameter value* $\mathsf{V_{ef}}$, *especially when* $\mathsf{dE_g} \neq 0$.

$C_{BC,z}$	$\partial(Q_{t_C} + Q_{BC} + Q_{\rm epi})/\partial\mathcal{V}_{\rm B_2C_1}$	Capacitance floor b-c junction
$C_{BC\rm ex}$	$\partial(Q_{\rm tex} + Q_{\rm ex})/\partial\mathcal{V}_{\rm B_1C_4}$	Capacitance extrinsic b-c junction
$XC_{BC\rm ex}$	$\partial(XQ_{\rm tex} + XQ_{\rm ex})/\partial\mathcal{V}_{\rm BC_3}$	Capacitance extrinsic b-c junction
$C_{B_1B_2}$	$\partial Q_{B_1B_2}/\partial\mathcal{V}_{\rm B_1B_2}$	Capacitance AC current crowding
$C_{B_1B_2,x}$	$\partial Q_{B_1B_2}/\partial\mathcal{V}_{\rm B_2E_1}$	Cross-capacitance AC current crowding
$C_{B_1B_2,y}$	$\partial Q_{B_1B_2}/\partial\mathcal{V}_{\rm B_2C_2}$	Cross-capacitance AC current crowding
$C_{B_1B_2,z}$	$\partial Q_{B_1B_2}/\partial\mathcal{V}_{\rm B_2C_1}$	Cross-capacitance AC current crowding
C_{t_S}	$\partial Q_{t_S}/\partial\mathcal{V}_{\rm SC_1}$	Capacitance s-c junction

The full small-signal circuit is in practice not very useful, since it is difficult to do hand-calculations with it. Mextram therefore provides the elements of an approximate small-signal model, shown in Fig. 12. This model contains the following elements:

g_m	Transconductance
β	Current amplification
g_{out}	Output conductance
g_μ	Feedback transconductance
R_E	Emitter resistance (already given above)
r_B	Base resistance
r_C	Collector resistance
C_{BE}	Base-emitter capacitance
C_{BC}	Base-collector capacitance
C_{t_S}	Collector-substrate capacitance (already given above)

We make a few assumptions by making this approximation. It is meant to work in forward mode. For use in reverse mode or for the equivalent hybrid-π version of the circuit we refer to Ref. [2]. To keep the model simple, the base-emitter and base-collector capacitances are a sum of various contributions that are in the full model between different nodes. The elements that have not been defined before can be calculated from the small

signal parameters of the full model. As help variables we use

$$\frac{\mathrm{d}y}{\mathrm{d}x} = \frac{g_x - g_{\mu,x}}{g_{Rcv,y} + g_{\mu,y} - g_y} \tag{4.210}$$

$$\frac{\mathrm{d}y}{\mathrm{d}z} = \frac{g_z - g_{Rcv,z} - g_{\mu,z}}{g_{Rcv,y} + g_{\mu,y} - g_y} \tag{4.211}$$

$$g_\pi = g_\pi^S + g_{\pi,x} + g_{\mu,x} + g_{\pi,z} + g_{\mu,z} + (g_{\pi,y} + g_{\mu,y}) \left[\frac{\mathrm{d}y}{\mathrm{d}x} + \frac{\mathrm{d}y}{\mathrm{d}z}\right] \tag{4.212}$$

The quantities in the small-signal circuit then are:

$$g_m = \frac{g_{Rcv,y}(g_x - g_{\mu,x} + g_z - g_{\mu,z}) - (g_{Rcv,z})(g_y - g_{\mu,y})}{g_{Rcv,y} + g_{\mu,y} - g_y} \tag{4.213}$$

$$\beta = g_m/g_\pi \tag{4.214}$$

$$g_{out} = \frac{(g_y - g_{\mu,y})g_{Rcv,z} - (g_z - g_{\mu,z})g_{Rcv,y}}{g_{Rcv,y} + g_{\mu,y} - g_y} \tag{4.215}$$

$$g_\mu = g_{\pi,z} + g_{\mu,z} + (g_{\pi,y} + g_{\mu,y})\frac{\mathrm{d}y}{\mathrm{d}z} + g_{\mu\mathrm{ex}} + Xg_{\mu\mathrm{ex}} \tag{4.216}$$

$$r_B = \mathsf{R_{BcT}} + r_{bv} \tag{4.217}$$

$$r_C = \mathsf{R_{CcT}} + \mathsf{R_{CblxT}} + \mathsf{R_{CbliT}} \tag{4.218}$$

$$C_{BE} = C_{BE,x} + C_{BE}^S + C_{BC,x} + (C_{BE,y} + C_{BC,y})\,\frac{\mathrm{d}y}{\mathrm{d}x} + \mathsf{C_{BEO}} \tag{4.219}$$

$$C_{BC} = (C_{BE,y} + C_{BC,y})\,\frac{\mathrm{d}y}{\mathrm{d}z} + C_{BC,z} + C_{BC\mathrm{ex}} + XC_{BC\mathrm{ex}} + \mathsf{C_{BCO}} \tag{4.220}$$

Note that we added the overlap capacitances to the internal capacitances for simplicity.

Apart from the small signal approximated hybrid-π model, we would also like to have a rather good estimate of f_T, the cut-off frequency. We neglect the substrate current, but we now do take into account that the capacitances have different positions in the equivalent circuit. The derivation [2] is based on $1/(2\pi f_T) = \mathrm{d}Q/\mathrm{d}I_C$ for constant V_{CE}. The formulas used to calculate f_T are:

$$\gamma_x = (g_{\pi,x} + g_{\mu,x} - g_{Rbv,x})\, r_{bv} \tag{4.221}$$
$$\gamma_y = (g_{\pi,y} + g_{\mu,y} - g_{Rbv,y})\, r_{bv} \tag{4.222}$$
$$\gamma_z = (g_{\pi,z} + g_{\mu,z} - g_{Rbv,z})\, r_{bv} \tag{4.223}$$
$$g_{Bf,x} = g_{\pi,x} + g_\pi^S\, (1+\gamma_x) \tag{4.224}$$
$$g_{Bf,y} = g_{\pi,y} + g_\pi^S\, \gamma_y \tag{4.225}$$
$$g_{Bf,z} = g_{\pi,z} + g_\pi^S\, \gamma_z \tag{4.226}$$
$$\alpha = \frac{1 + \left[g_{Rcv,y}\frac{\mathrm{d}y}{\mathrm{d}x}\right] r_C + \left[g_x + g_{Bf,x} + (g_y + g_{Bf,y})\frac{\mathrm{d}y}{\mathrm{d}x}\right] \mathsf{R_{ET}}}{1 - \left[g_{Rcv,z} + g_{Rcv,y}\frac{\mathrm{d}y}{\mathrm{d}z}\right] r_C - \left[g_z + g_{Bf,z} + (g_y + g_{Bf,y})\frac{\mathrm{d}y}{\mathrm{d}z}\right] \mathsf{R_{ET}}} \tag{4.227}$$
$$r_x = \left[g_{Rcv,y}\frac{\mathrm{d}y}{\mathrm{d}x} + \alpha\, \left(g_{Rcv,z} + g_{Rcv,y}\frac{\mathrm{d}y}{\mathrm{d}z} \right) \right]^{-1} \tag{4.228}$$
$$r_z = \alpha\, r_x \tag{4.229}$$
$$r_y = \frac{1 - g_{Rcv,z} r_z}{g_{Rcv,y}} \tag{4.230}$$
$$r_{b1b2} = \gamma_x\, r_x + \gamma_y\, r_y + \gamma_z\, r_z \tag{4.231}$$
$$r_{\mathrm{ex}} = r_z + r_{b1b2} - \mathsf{R_{CbliT}} \tag{4.232}$$
$$\begin{aligned} Xr_{\mathrm{ex}} = {} & r_z + r_{b1b2} + \mathsf{R_{BcT}}\, [(g_{Bf,x} + g_{\mu,x})\, r_x + (g_{Bf,y} + g_{\mu,y})\, r_y \\ & + (g_{Bf,z} + g_{\mu,z})\, r_z] - \mathsf{R_{CbliT}} - \mathsf{R_{CblxT}} \end{aligned} \tag{4.233}$$
$$\begin{aligned} \tau_T = {} & C_{BE}^S\, (r_x + r_{b1b2}) + (C_{BE,x} + C_{BC,x})\, r_x + (C_{BE,y} + C_{BC,y})\, r_y \\ & + (C_{BE,z} + C_{BC,z})\, r_z + C_{BC\mathrm{ex}}\, r_{\mathrm{ex}} + XC_{BC\mathrm{ex}}\, Xr_{\mathrm{ex}} \\ & + (\mathsf{C_{BEO}} + \mathsf{C_{BCO}})\, (Xr_{\mathrm{ex}} - \mathsf{R_{CcT}}) \end{aligned} \tag{4.234}$$

Apart from the cut-off frequency we also have some other quantities to describe the internal state of the model:

f_T	$1/(2\pi\,\tau_T)$	Good approximation for cut-off frequency
I_{qs}		Current at onset of quasi-saturation (please refer to note below)
x_i/W_{epi}		Thickness of injection layer
$V^*_{B_2C_2}$		Physical value of internal base-collector bias

Note on value of I_{qs}: In reverse mode ($I_{C1C2} \leq 0$), the variable I_{qs} is superfluous and its value is formally undefined; in the standard software implementation, this is implemented as I_{qs} = 0 whenever $I_{C1C2} \leq 0$.

Related to self-heating we have the following quantities

P_{diss}	Dissipation
T_K	Actual temperature

5 Going from 503 to 504

In general it is possible to do Mextram 504 simulations using Mextram 503 parameters as input, without losing much accuracy, even though Mextram 503 is not fully backward compatible with Mextram 504. Most of the Mextram 503 model equations have been modified to some extent. So even when the model parameters are not changed, like for the three depletion capacitances, the simulation results may differ slightly as a function of bias. To do Mextram 504 simulations with Mextram 503 parameters as input, we have developed a procedure to convert Mextram 503 parameters to Mextram 504 parameters. In this section we describe this conversion. These conversion rules have been checked over bias and temperature for transistors in several processes. A Pstar input deck is available upon request that contains all the conversion rules explained in this section.

5.1 Overview

The Mextram 503 model contains 62 parameters while Mextram 504 contains 75 parameters in total. In Mextram 504 new parameters are introduced for the Early effect, avalanche multiplication, the non-ideal base current, transit times, temperature scaling rules and self-heating. There are 22 new parameters and 9 parameters have been removed. The parameter τ_{NE} is renamed to τ_{E} for consistency reasons. In Table 5 below we have given an overview of the parameters that are new in Mextram 504 and those that have been removed compared to Mextram 503.

The value of some parameters can directly be given, as has been done in the table. For those parameters that do not have a fixed value we give the conversion rules below. Some of the parameters that are present in both Mextram 503 and Mextram 504 have to be changed slightly for use in Mextram 504. These are I_{Bf} for the non-ideal forward base current and the temperature parameters V_{g_B} and V_{g_S}.

Table 5: *Overview of the new parameters in Mextram 504 and the parameters removed compared to Mextram 503. For some of the parameters we have already given the value that should be used when converting from Mextram 503 to Mextram 504.*

Part of the model	New	Removed
Early Voltages	V_{er}	Q_{B0}
	V_{ef}	
Built-in field of the base		η
Non-ideal base current	m_{Lf}	V_{Lf}
Avalanche model	W_{avl}	AVL
	V_{avl}	E_{fi}
Epilayer model	$a_{x_i} = 0.3$	
Overlap capacitances	$C_{BEO} = 0$	
	$C_{BCO} = 0$	
Transit times	τ_{B}	
	τ_{epi}	
	τ_{R}	

Part of the model	New	Removed
Self-heating	$\mathsf{R_{th}} = 0$ $\mathsf{C_{th}} = 0$ $\mathsf{A_{th}} = 0$	
SiGe modelling	$\mathsf{dE_g} = 0$ $\mathsf{X_{rec}} = 0$	
Noise modelling	$\mathsf{K_{avl}} = 0$	
Temperature model:		
Emitter resistance	$\mathsf{A_E} = 0$	
Base width	$\mathsf{A_{Q_{B0}}}$	$\mathsf{N_A}$ $\mathsf{V_I}$
Forward current gain	$\mathsf{dV_{g\beta f}}$	$\mathsf{V_{g_E}}$
Reverse current gain	$\mathsf{dV_{g\beta r}} = 0$	
Emitter transit time	$\mathsf{dV_{g\tau_E}}$	
Non-ideal base currents		$\mathsf{E_R}$
Total	22	9

For the conversion rules a few quantities have to be given beforehand. These are the breakdown voltage $\mathrm{BV_{ceo}}$ for the avalanche model and the calibration temperature T_{cal} for the temperature rules. Since some of the temperature rules have been changed it is not possible to get exactly the same results for Mextram 503 and Mextram 504 for all temperatures. The calibration temperature T_{cal} is used below as the temperature where the Mextram 503 and the Mextram 504 temperature rules give the same result. A good value for T_{cal} is $100^{\circ}\mathrm{C}$, which is in general not too close to the temperature at which parameter extraction has been done but which gives a reasonable temperature range.

5.2 Temperature scaling

The Mextram 503 temperature scaling rules have been evaluated and many of them have been slightly adapted. This results in minor changes of the related parameters. We will calibrate the new model at a certain temperature T_{cal}. For the equations we need the following definitions, that closely follow the definitions in Sec. 4

$$T_{RK} = T_{\mathrm{ref}} + 273.15 \tag{5.1}$$

$$T_K = T_{\mathrm{cal}} + 273.15 \tag{5.2}$$

$$t_N = \frac{T_K}{T_{RK}} \tag{5.3}$$

$$V_T = \left(\frac{k}{q}\right) T_K \tag{5.4}$$

$$V_{T_R} = \left(\frac{k}{q}\right) T_{RK} \tag{5.5}$$

$$\frac{1}{V_{\Delta T}} = \frac{1}{V_T} - \frac{1}{V_{T_R}} \tag{5.6}$$

The temperature dependence of the neutral base charge $\mathsf{Q_{B0}}$ in Mextram 503 is quite complicated due to the base width modulation and therefore many parameters are involved (e.g. $\mathsf{V_{g_B}}$, $\mathsf{V_{g_C}}$, $\mathsf{N_A}$, and $\mathsf{V_l}$). We removed $\mathsf{Q_{B0}}$ from the parameter list. However, the temperature dependent ratio $\mathsf{Q_{B0T}}/\mathsf{Q_{B0}}$ is still needed in the model. We simplify it by using a power law $\mathsf{Q_{B0T}}/\mathsf{Q_{B0}} = t_N^{\mathsf{A_{Q_{B0}}}}$ with parameter $\mathsf{A_{Q_{B0}}}$. To determine this parameter we must repeat a part of the Mextram 503 temperature model:

$$\mathsf{V_{d_ET}} = -3\,V_T\,\ln t_N + \mathsf{V_{d_E}}\,t_N + (1-t_N)\,\mathsf{V_{g_B}} \tag{5.7}$$

$$\mathsf{V_{d_CT}} = -3\,V_T\,\ln t_N + \mathsf{V_{d_C}}\,t_N + (1-t_N)\,\mathsf{V_{g_C}} \tag{5.8}$$

$$\mathsf{C_{j_ET}} = \mathsf{C_{j_E}}\left(\frac{\mathsf{V_{d_E}}}{\mathsf{V_{d_ET}}}\right)^{\mathsf{p_E}} \tag{5.9}$$

$$\mathsf{C_{j_CT}} = \mathsf{C_{j_C}}\left[(1-\mathsf{X_p})\left(\frac{\mathsf{V_{d_C}}}{\mathsf{V_{d_CT}}}\right)^{\mathsf{p_C}} + \mathsf{X_p}\right] \tag{5.10}$$

$$\mathsf{X_{pT}} = \mathsf{X_p}\,\frac{\mathsf{C_{j_C}}}{\mathsf{C_{j_CT}}} \tag{5.11}$$

$$Q_E = \frac{1-\mathsf{XC_{j_E}}}{1-\mathsf{p_E}}\,\mathsf{C_{j_E}}\,\mathsf{V_{d_E}} \tag{5.12}$$

$$Q_C = \left(\frac{1-\mathsf{X_p}}{1-\mathsf{p_C}} + \mathsf{X_p}\right)\,\mathsf{XC_{j_C}}\,\mathsf{C_{j_C}}\,\mathsf{V_{d_C}} \tag{5.13}$$

$$g_i = 2\cdot\left[1+\sqrt{1+\frac{\mathsf{N_A}\,\exp\left(\mathsf{V_l}/V_{TR}\right)}{6.04\cdot 10^{14}\,T_{RK}^{1.5}}}\right]^{-1} \tag{5.14}$$

$$Q_{\mathrm{imp}} = \left(\mathsf{Q_{B0}} + Q_E + Q_C\right)/g_i \tag{5.15}$$

$$Q_{E\mathrm{T}} = \frac{1-\mathsf{XC_{j_E}}}{1-\mathsf{p_E}}\,\mathsf{C_{j_ET}}\,\mathsf{V_{d_ET}} \tag{5.16}$$

$$Q_{C\mathrm{T}} = \left(\frac{1-\mathsf{X_{pT}}}{1-\mathsf{p_C}} + \mathsf{X_{pT}}\right)\,\mathsf{XC_{j_C}}\,\mathsf{C_{j_CT}}\,\mathsf{V_{d_CT}} \tag{5.17}$$

$$g_{i\mathrm{T}} = 2\cdot\left[1+\sqrt{1+\frac{\mathsf{N_A}\,\exp\left(\mathsf{V_l}/V_T\right)}{6.04\cdot 10^{14}\,T_K^{1.5}}}\right]^{-1} \tag{5.18}$$

$$\mathsf{Q_{B0T}} = g_{i\mathrm{T}}\,Q_{\mathrm{imp}} - Q_{E\mathrm{T}} - Q_{C\mathrm{T}} \tag{5.19}$$

Finally the base charge temperature coefficient becomes

$$\mathsf{A_{Q_{B0}}} = \frac{\ln(\mathsf{Q_{B0T}}/\mathsf{Q_{B0}})}{\ln t_N} \tag{5.20}$$

Next the parameters $\mathsf{V_{g_B}}$ of the collector saturation current $\mathsf{I_s}$ and $\mathsf{V_{g_S}}$ of the substrate saturation current $\mathsf{I_{Ss}}$ are adapted. This is done by demanding that the temperature rules for Mextram 503 and Mextram 504 lead to the same saturation currents at temperature T_{cal}. This leads to

$$\mathsf{V_{g_B}}^{(504)} = \mathsf{V_{g_B}}^{(503)} + V_{\Delta T}\,(0.2 + 0.5\,\mathsf{A_B} - \mathsf{A_{Q_{B0}}})\,\ln t_N \tag{5.21}$$

$$\mathsf{V_{g_S}}^{(504)} = \mathsf{V_{g_S}}^{(503)} + V_{\Delta T}\,(0.5 - 2\,\mathsf{A_S})\,\ln t_N \tag{5.22}$$

In the same way we demand that the forward current gain of both models is the same at the calibration temperature. This leads to

$$\mathsf{dV_{g\beta f}} = \mathsf{V_{g_B}}^{(503)} - \mathsf{V_{g_E}} + V_{\Delta T}\ (0.5\,\mathsf{A_B} - \mathsf{A_{Q_{B0}}} - 0.03)\ \ln t_N \tag{5.23}$$

Parameter $\mathsf{V_{g_E}}$ is removed from the list. The last bandgap voltage difference we need to define is that of the emitter transit time. Again we demand that the emitter transit time is the same for both models at the calibration temperature, but we simplify the case where $\mathsf{m_\tau} \neq 1$

$$\mathsf{dV_{g\tau_E}} = \mathsf{V_{g_j}} - \mathsf{V_{g_B}}^{(503)}/\mathsf{m_\tau} \tag{5.24}$$

5.3 Early effect

In Mextram 503 the parameters $\mathsf{Q_{B0}}$ and $\mathsf{XC_{j_C}}$ are used to define the forward and reverse Early voltage. In Mextram 504 we directly have the Early voltages $\mathsf{V_{ef}}$ and $\mathsf{V_{er}}$ as parameters. The advantage is that the correlation of the Early effect with parameter $\mathsf{XC_{j_E}}$ is removed and that $\mathsf{XC_{j_C}}$ can be used solely to distribute the base-collector junction capacitance. In Mextram 504 the parameters $1 - \mathsf{XC_{j_E}}$ and $\mathsf{XC_{j_C}}$ are defined as the fraction of the base-emitter and base-collector depletion capacitance underneath the emitter and have to be obtained from geometrical scaling rules. Parameter $\mathsf{Q_{B0}}$ is removed from the list. The conversion rules for the new parameters are:

$$\mathsf{V_{er}} = \frac{\mathsf{Q_{B0}}}{(1 - \mathsf{XC_{j_E}})\ \mathsf{C_{j_E}}} \tag{5.25}$$

$$\mathsf{V_{ef}} = \frac{\mathsf{Q_{B0}}}{\mathsf{XC_{j_C}}\ \mathsf{C_{j_C}}} \tag{5.26}$$

These parameters are the Early voltages at zero base-emitter and base-collector bias. The real forward Early voltage increases with $\mathcal{V}_{\mathrm{BE}}$ and $\mathcal{V}_{\mathrm{BC}}$ and its maximum is usually about 2 times higher than the parameter value.

5.4 Avalanche multiplication

In Mextram 504 the avalanche multiplication model is basically the same as that of Mextram 503. The modelling of the base-collector depletion layer width W_D with collector voltage is simplified. In Mextram 503 the bias dependency of W_D with collector voltage and current is given by the base-collector depletion charge model. Therefore avalanche multiplication is apart from the avalanche parameter AVL also dependent on parameters $\mathsf{X_p}$ and $\mathsf{p_C}$ of the base-collector capacitance model. $\mathsf{X_p}$ and $\mathsf{p_C}$ define the increase of the avalanche current (slope) with collector voltage and they are average values of the total base-collector junction capacitance. Avalanche currents are generated only in the base-collector region underneath the emitter and $\mathsf{X_p}$ and $\mathsf{p_C}$ may be different there due to a selective implanted collector, additional implants in the extrinsic base regions or the sidewall base-collector junction capacitance. In Mextram 504 we take the effective thickness

$\mathsf{W_{avl}}$ and punch through voltage $\mathsf{V_{avl}}$ (defined by the dope and thickness) of the epilayer underneath the emitter as parameters. A relatively simple model of a one-sided step junction is used to calculate W_D as a function of collector voltage and current. In this way we decouple the avalanche model parameters from the base-collector capacitance model parameters. To calculate the new parameters $\mathsf{W_{avl}}$ and $\mathsf{V_{avl}}$ from the Mextram 503 parameter set we have to calibrate the avalanche current at a certain collector voltage. A suitable voltage is the collector-emitter breakdown voltage $\mathrm{BV_{ceo}}$. This is the voltage where the base current becomes zero with increasing collector voltage. Because this voltage is slightly bias and temperature dependent it has to be given as an input. At this given collector voltage the maximum electric field, and therefore the calculated avalanche current, will be made the same for both models. In Mextram 503 the gradient of the electric field $\partial E/\partial x$ under the condition $I_c \ll \mathsf{I_{hc}}$ and the depletion layer thickness W_D as a function of collector voltage are:

$$\frac{\partial E}{\partial x} = 2\,\mathsf{V_{dc}}\,\left(\frac{B_n}{\mathsf{AVL}}\right)^2 \tag{5.27}$$

$$f_c = \frac{1-\mathsf{X_p}}{(1+\mathrm{BV_{ceo}}/\mathsf{V_{dc}})^{\mathsf{pc}}} + \mathsf{X_p} \tag{5.28}$$

$$W_D = \frac{\mathsf{AVL}}{B_n\; f_c} \tag{5.29}$$

In Mextram 504 the depletion layer thickness x_D using the same bias condition is:

$$x_D = \sqrt{\frac{2\;(\mathsf{V_{dc}}+\mathrm{BV_{ceo}})}{\partial E/\partial x}} \tag{5.30}$$

The depletion layer thickness has to be the same in both models and therefore W_D also equals $x_D\;\mathsf{W_{avl}}/\sqrt{x_D^2+\mathsf{W_{avl}}^2}$. This leads to

$$\mathsf{W_{avl}} = \frac{x_D\,W_D}{\sqrt{x_D^2-W_D^2}} \tag{5.31}$$

$$\mathsf{V_{avl}} = \frac{\partial E}{\partial x}\;\frac{\mathsf{W_{avl}}^2}{2} \tag{5.32}$$

In the improbable case that the equation for $\mathsf{W_{avl}}$ leads to numerical problems ($x_D < W_D$) either the parameter set is unphysical or the process is not optimized. In both cases one needs to give a physical value for $\mathsf{W_{avl}}$ by hand.

5.5 Non-ideal forward base current

The non-ideal base current I_{B_2} has, in Mextram 503, a cross-over voltage $\mathsf{V_{Lf}}$ where the slope $1/m = V_T\;\partial \ln I_{B_2}/\partial \mathcal{V}_{\mathrm{BE}}$ decreases from 1 to $1/2$. In most cases $\mathsf{V_{Lf}}$ is small and in the bias range of interest the slope of I_{B_2} is constant (1/2). With this model it is difficult to

describe a steady increasing gain over several decades. To be more flexible in this sense we introduce in Mextram 504 a constant non-ideality factor $\mathsf{m_{Lf}}$. To keep the number of parameters the same we remove $\mathsf{V_{Lf}}$. In the conversion we define two base-emitter voltages where the non-ideal base current of both models are the same

$$V_1 = 0.45 \tag{5.33}$$

$$V_2 = 0.75 \tag{5.34}$$

$$I_1 = \mathsf{I_{Bf}}^{(503)} \frac{\exp(V_1/V_{T_R}) - 1}{\exp\left(V_1/2\,V_{T_R}\right) + \exp\left(\mathsf{V_{Lf}}/2\,V_{T_R}\right)} \tag{5.35}$$

$$I_2 = \mathsf{I_{Bf}}^{(503)} \frac{\exp(V_2/V_{T_R}) - 1}{\exp\left(V_2/2\,V_{T_R}\right) + \exp\left(\mathsf{V_{Lf}}/2\,V_{T_R}\right)} \tag{5.36}$$

$$\mathsf{m_{Lf}} = \frac{V_2 - V_1}{V_{T_R}\,\ln\left(I_2/I_1\right)} \tag{5.37}$$

$$\mathsf{I_{Bf}}^{(504)} = \frac{I_2}{\exp\left(V_2/\mathsf{m_{Lf}}\,V_{T_R}\right) - 1} \tag{5.38}$$

When $\mathsf{V_{Lf}} \lesssim 0.3$ we have $\mathsf{m_{Lf}} = 2$ and $\mathsf{I_{Bf}}^{(504)} = \mathsf{I_{Bf}}^{(503)}$.

5.6 Transit times

In Mextram 503 we have only the emitter transit time τ_{NE} (renamed to τ_{E} in Mextram 504) as parameter. All other transit times, like for the base and collector, are calculated from DC parameters. In Mextram 504 we introduce transit times for the base, collector and reverse mode. They can easily be calculated from the Mextram 503 parameter set.

$$\tau_{\mathsf{B}} = \frac{\mathsf{Q_{B0}}}{\mathsf{I_k}} \tag{5.39}$$

$$\tau_{\mathsf{epi}} = \frac{\mathsf{I_s}\,\mathsf{Q_{B0}}\,\mathsf{R_{Cv}}^2 \exp\left(\mathsf{V_{d_C}}/V_{T_R}\right)}{4\,V_{T_R}^2} \tag{5.40}$$

$$\tau_{\mathsf{R}} = \left(\tau_{\mathsf{B}} + \tau_{\mathsf{epi}}\right) \frac{1 - \mathsf{XC_{jc}}}{\mathsf{XC_{jc}}} \tag{5.41}$$

Because the cut-off frequency f_T is sensitive to many parameters in some cases it might be necessary to correct a transit time (e.g. τ_{E} or τ_{B}). This can be done by tuning the top of the f_T.

6 Numerical examples

In this section we provide some numerical examples, based on Pstar 4.2. These results can be used to check the correctness of a model implementation. More numerical examples can be generated using the solver on the web [1]. Here we used the values of the default parameter set given in Sec. 4.3, but with $\mathsf{dE_g} = 0.01$ and $\mathsf{X_{rec}} = 0.1$, to include also the SiGe expressions. Some flags were changed as indicated in the tables. Self-heating is not included, unless specifically stated. Substrate currents below $1\,\mathrm{fA}$ were disregarded.

6.1 Forward Gummel plot

In this example the base voltage is swept from 0.4 to $1.2\,\mathrm{V}$, with emitter and substrate voltages at $0\,\mathrm{V}$ and the collector voltage at $1\,\mathrm{V}$.

Device temperature $T = 25°\mathrm{C}$

$\mathcal{V}_{\mathrm{BE}}\,(\mathrm{V})$	$I_C\,(\mathrm{A})$	$I_B\,(\mathrm{A})$	$I_{\mathrm{sub}}\,(\mathrm{A})$
0.40	$1.0474 \cdot 10^{-10}$	$7.0562 \cdot 10^{-12}$	—
0.50	$4.8522 \cdot 10^{-09}$	$7.4371 \cdot 10^{-11}$	—
0.60	$2.2402 \cdot 10^{-07}$	$1.7371 \cdot 10^{-09}$	—
0.70	$1.0254 \cdot 10^{-05}$	$7.1660 \cdot 10^{-08}$	—
0.80	$4.2490 \cdot 10^{-04}$	$3.1412 \cdot 10^{-06}$	—
0.90	$5.5812 \cdot 10^{-03}$	$5.2923 \cdot 10^{-05}$	—
1.00	$1.5882 \cdot 10^{-02}$	$2.7185 \cdot 10^{-04}$	$-7.3559 \cdot 10^{-14}$
1.10	$2.7384 \cdot 10^{-02}$	$7.8543 \cdot 10^{-04}$	$-6.8642 \cdot 10^{-10}$
1.20	$3.8631 \cdot 10^{-02}$	$1.6447 \cdot 10^{-03}$	$-5.5645 \cdot 10^{-06}$

Device temperature $T = 100°\mathrm{C}$

$\mathcal{V}_{\mathrm{BE}}\,(\mathrm{V})$	$I_C\,(\mathrm{A})$	$I_B\,(\mathrm{A})$	$I_{\mathrm{sub}}\,(\mathrm{A})$
0.40	$8.0045 \cdot 10^{-08}$	$5.9427 \cdot 10^{-10}$	—
0.50	$1.6985 \cdot 10^{-06}$	$9.9748 \cdot 10^{-09}$	—
0.60	$3.5649 \cdot 10^{-05}$	$2.0657 \cdot 10^{-07}$	—
0.70	$6.6588 \cdot 10^{-04}$	$4.1113 \cdot 10^{-06}$	—
0.80	$5.2130 \cdot 10^{-03}$	$4.3737 \cdot 10^{-05}$	$-4.0795 \cdot 10^{-14}$
0.90	$1.3673 \cdot 10^{-02}$	$2.2102 \cdot 10^{-04}$	$-1.2225 \cdot 10^{-10}$
1.00	$2.3552 \cdot 10^{-02}$	$6.7151 \cdot 10^{-04}$	$-7.9106 \cdot 10^{-07}$
1.10	$3.2388 \cdot 10^{-02}$	$2.1960 \cdot 10^{-03}$	$-6.6654 \cdot 10^{-04}$
1.20	$3.5243 \cdot 10^{-02}$	$8.2877 \cdot 10^{-03}$	$-3.8786 \cdot 10^{-03}$

Device temperature $T = 25°\mathrm{C}$, with self-heating

$\mathcal{V}_{\mathrm{BE}}\,(\mathrm{V})$	$I_C\,(\mathrm{A})$	$I_B\,(\mathrm{A})$	$I_{\mathrm{sub}}\,(\mathrm{A})$	$T_K(°\mathrm{C})$
0.80	$4.2781 \cdot 10^{-04}$	$3.1619 \cdot 10^{-06}$	—	25.129
0.90	$5.7715 \cdot 10^{-03}$	$5.5125 \cdot 10^{-05}$	—	26.746
1.00	$1.6471 \cdot 10^{-02}$	$2.9026 \cdot 10^{-04}$	$-2.4797 \cdot 10^{-13}$	30.028
1.10	$2.8246 \cdot 10^{-02}$	$8.4606 \cdot 10^{-04}$	$-5.4441 \cdot 10^{-09}$	33.753
1.20	$3.9449 \cdot 10^{-02}$	$1.8510 \cdot 10^{-03}$	$-7.5766 \cdot 10^{-05}$	37.501

6.2 Reverse Gummel plot

In this example again the base voltage is swept from 0.4 to $1.2\,\mathrm{V}$, but now with collector and substrate voltages at $0\,\mathrm{V}$ and the emitter voltage at $1\,\mathrm{V}$.

Device temperature $T = 25°\mathrm{C}$, EXMOD $= 1$

$\mathcal{V}_{\mathrm{BC}}\,(\mathrm{V})$	$I_E\,(\mathrm{A})$	$I_B\,(\mathrm{A})$	$I_{\mathrm{sub}}\,(\mathrm{A})$
0.40	$1.6687 \cdot 10^{-10}$	$2.9777 \cdot 10^{-10}$	$-2.7723 \cdot 10^{-10}$
0.50	$7.7698 \cdot 10^{-09}$	$1.4499 \cdot 10^{-08}$	$-1.3590 \cdot 10^{-08}$
0.60	$3.6108 \cdot 10^{-07}$	$7.0890 \cdot 10^{-07}$	$-6.6504 \cdot 10^{-07}$
0.70	$1.5810 \cdot 10^{-05}$	$3.2360 \cdot 10^{-05}$	$-3.0260 \cdot 10^{-05}$
0.80	$3.9318 \cdot 10^{-04}$	$5.9320 \cdot 10^{-04}$	$-5.2275 \cdot 10^{-04}$
0.90	$2.2197 \cdot 10^{-03}$	$2.5994 \cdot 10^{-03}$	$-1.9150 \cdot 10^{-03}$
1.00	$4.8747 \cdot 10^{-03}$	$5.8002 \cdot 10^{-03}$	$-3.5480 \cdot 10^{-03}$
1.10	$7.6813 \cdot 10^{-03}$	$9.6108 \cdot 10^{-03}$	$-5.2096 \cdot 10^{-03}$
1.20	$1.0540 \cdot 10^{-02}$	$1.3724 \cdot 10^{-02}$	$-6.9400 \cdot 10^{-03}$

Device temperature $T = 100°\mathrm{C}$, EXMOD $= 1$

$\mathcal{V}_{\mathrm{BC}}\,(\mathrm{V})$	$I_E\,(\mathrm{A})$	$I_B\,(\mathrm{A})$	$I_{\mathrm{sub}}\,(\mathrm{A})$
0.40	$1.2362 \cdot 10^{-07}$	$2.5885 \cdot 10^{-07}$	$-2.4907 \cdot 10^{-07}$
0.50	$2.5916 \cdot 10^{-06}$	$5.7085 \cdot 10^{-06}$	$-5.4918 \cdot 10^{-06}$
0.60	$4.7158 \cdot 10^{-05}$	$9.9629 \cdot 10^{-05}$	$-9.5155 \cdot 10^{-05}$
0.70	$4.7495 \cdot 10^{-04}$	$6.7806 \cdot 10^{-04}$	$-6.1741 \cdot 10^{-04}$
0.80	$1.8123 \cdot 10^{-03}$	$2.0214 \cdot 10^{-03}$	$-1.6608 \cdot 10^{-03}$
0.90	$3.7155 \cdot 10^{-03}$	$3.9952 \cdot 10^{-03}$	$-2.9251 \cdot 10^{-03}$
1.00	$5.7889 \cdot 10^{-03}$	$6.3542 \cdot 10^{-03}$	$-4.2443 \cdot 10^{-03}$
1.10	$7.9240 \cdot 10^{-03}$	$8.9302 \cdot 10^{-03}$	$-5.6007 \cdot 10^{-03}$
1.20	$1.0097 \cdot 10^{-02}$	$1.1632 \cdot 10^{-02}$	$-6.9964 \cdot 10^{-03}$

Device temperature $T = 25°\mathrm{C}$, EXMOD $= 0$

$\mathcal{V}_{\mathrm{BC}}\,(\mathrm{V})$	$I_E\,(\mathrm{A})$	$I_B\,(\mathrm{A})$	$I_{\mathrm{sub}}\,(\mathrm{A})$
0.40	$1.6687 \cdot 10^{-10}$	$2.9777 \cdot 10^{-10}$	$-2.7723 \cdot 10^{-10}$
0.50	$7.7698 \cdot 10^{-09}$	$1.4499 \cdot 10^{-08}$	$-1.3590 \cdot 10^{-08}$
0.60	$3.6094 \cdot 10^{-07}$	$7.0873 \cdot 10^{-07}$	$-6.6488 \cdot 10^{-07}$
0.70	$1.5544 \cdot 10^{-05}$	$3.1916 \cdot 10^{-05}$	$-2.9848 \cdot 10^{-05}$
0.80	$3.2428 \cdot 10^{-04}$	$5.1459 \cdot 10^{-04}$	$-4.5927 \cdot 10^{-04}$
0.90	$1.5972 \cdot 10^{-03}$	$1.8906 \cdot 10^{-03}$	$-1.5217 \cdot 10^{-03}$
1.00	$3.5189 \cdot 10^{-03}$	$3.7361 \cdot 10^{-03}$	$-2.7309 \cdot 10^{-03}$
1.10	$5.6544 \cdot 10^{-03}$	$5.7762 \cdot 10^{-03}$	$-3.9166 \cdot 10^{-03}$
1.20	$7.8552 \cdot 10^{-03}$	$7.9157 \cdot 10^{-03}$	$-5.0659 \cdot 10^{-03}$

6.3 Output characteristics

In these two examples the base current is kept constant at $10\,\mu\mathrm{A}$. The collector current is swept from 0 to $20\,\mathrm{mA}$ (note the two different step sizes of the collector current). Emitter and substrate are grounded. In the second example extended avalanche is switched on which makes the collector-emitter voltage decrease again when $I_C > 8\,\mathrm{mA}$. This decrease is not observed in the first example.

Device temperature $T = 25°\mathrm{C}$, EXAVL $= 0$

$I_C\,(\mathrm{A})$	$\mathcal{V}_{\mathrm{CE}}\,(\mathrm{V})$	$\mathcal{V}_{\mathrm{BE}}\,(\mathrm{V})$	$I_{\mathrm{sub}}\,(\mathrm{A})$
$0.0 \cdot 10^{+00}$	$4.8992 \cdot 10^{-03}$	$6.7332 \cdot 10^{-01}$	$-9.3489 \cdot 10^{-06}$
$5.0 \cdot 10^{-04}$	$1.5574 \cdot 10^{-01}$	$8.0558 \cdot 10^{-01}$	$-5.7683 \cdot 10^{-06}$
$1.0 \cdot 10^{-03}$	$2.1013 \cdot 10^{-01}$	$8.2659 \cdot 10^{-01}$	$-2.0019 \cdot 10^{-06}$
$1.5 \cdot 10^{-03}$	$9.8664 \cdot 10^{+00}$	$8.3759 \cdot 10^{-01}$	—
$2.0 \cdot 10^{-03}$	$1.1711 \cdot 10^{+01}$	$8.4755 \cdot 10^{-01}$	—
$4.0 \cdot 10^{-03}$	$1.3321 \cdot 10^{+01}$	$8.7643 \cdot 10^{-01}$	—
$6.0 \cdot 10^{-03}$	$1.3922 \cdot 10^{+01}$	$8.9793 \cdot 10^{-01}$	—
$8.0 \cdot 10^{-03}$	$1.4297 \cdot 10^{+01}$	$9.1636 \cdot 10^{-01}$	—
$1.0 \cdot 10^{-02}$	$1.4575 \cdot 10^{+01}$	$9.3309 \cdot 10^{-01}$	—
$1.2 \cdot 10^{-02}$	$1.4802 \cdot 10^{+01}$	$9.4877 \cdot 10^{-01}$	—
$1.4 \cdot 10^{-02}$	$1.5003 \cdot 10^{+01}$	$9.6378 \cdot 10^{-01}$	—
$1.6 \cdot 10^{-02}$	$1.5208 \cdot 10^{+01}$	$9.7854 \cdot 10^{-01}$	—
$1.8 \cdot 10^{-02}$	$1.5414 \cdot 10^{+01}$	$9.9306 \cdot 10^{-01}$	—
$2.0 \cdot 10^{-02}$	$1.5612 \cdot 10^{+01}$	$1.0073 \cdot 10^{+00}$	—

Device temperature $T = 25°\mathrm{C}$, EXAVL $= 1$

$I_C\,(\mathrm{A})$	$\mathcal{V}_{\mathrm{CE}}\,(\mathrm{V})$	$\mathcal{V}_{\mathrm{BE}}\,(\mathrm{V})$	$I_{\mathrm{sub}}\,(\mathrm{A})$
$0.0 \cdot 10^{+00}$	$4.8992 \cdot 10^{-03}$	$6.7332 \cdot 10^{-01}$	$-9.3489 \cdot 10^{-06}$
$5.0 \cdot 10^{-04}$	$1.5574 \cdot 10^{-01}$	$8.0558 \cdot 10^{-01}$	$-5.7683 \cdot 10^{-06}$
$1.0 \cdot 10^{-03}$	$2.1013 \cdot 10^{-01}$	$8.2659 \cdot 10^{-01}$	$-2.0019 \cdot 10^{-06}$
$1.5 \cdot 10^{-03}$	$9.7462 \cdot 10^{+00}$	$8.3761 \cdot 10^{-01}$	—
$2.0 \cdot 10^{-03}$	$1.1520 \cdot 10^{+01}$	$8.4758 \cdot 10^{-01}$	—
$4.0 \cdot 10^{-03}$	$1.2909 \cdot 10^{+01}$	$8.7650 \cdot 10^{-01}$	—
$6.0 \cdot 10^{-03}$	$1.3240 \cdot 10^{+01}$	$8.9805 \cdot 10^{-01}$	—
$8.0 \cdot 10^{-03}$	$1.3256 \cdot 10^{+01}$	$9.1653 \cdot 10^{-01}$	—
$1.0 \cdot 10^{-02}$	$1.3073 \cdot 10^{+01}$	$9.3337 \cdot 10^{-01}$	—
$1.2 \cdot 10^{-02}$	$1.2748 \cdot 10^{+01}$	$9.4923 \cdot 10^{-01}$	—
$1.4 \cdot 10^{-02}$	$1.2354 \cdot 10^{+01}$	$9.6479 \cdot 10^{-01}$	—
$1.6 \cdot 10^{-02}$	$1.1927 \cdot 10^{+01}$	$9.8009 \cdot 10^{-01}$	—
$1.8 \cdot 10^{-02}$	$1.1497 \cdot 10^{+01}$	$9.9506 \cdot 10^{-01}$	—
$2.0 \cdot 10^{-02}$	$1.1103 \cdot 10^{+01}$	$1.0098 \cdot 10^{+00}$	—

Device temperature $T = 25°\mathrm{C}$, $\mathsf{EXAVL} = 0$, with self-heating

$I_C\,(\mathrm{A})$	$\mathcal{V}_{\mathrm{CE}}\,(\mathrm{V})$	$\mathcal{V}_{\mathrm{BE}}\,(\mathrm{V})$	$I_{\mathrm{sub}}\,(\mathrm{A})$	$T_K(°\mathrm{C})$
$0.0 \cdot 10^{+00}$	$4.8992 \cdot 10^{-03}$	$6.7331 \cdot 10^{-01}$	$-9.3489 \cdot 10^{-06}$	25.002
$5.0 \cdot 10^{-04}$	$1.5576 \cdot 10^{-01}$	$8.0554 \cdot 10^{-01}$	$-5.7687 \cdot 10^{-06}$	25.026
$1.0 \cdot 10^{-03}$	$2.1016 \cdot 10^{-01}$	$8.2650 \cdot 10^{-01}$	$-2.0036 \cdot 10^{-06}$	25.066
$1.5 \cdot 10^{-03}$	$9.6837 \cdot 10^{+00}$	$8.3146 \cdot 10^{-01}$	—	29.360
$2.0 \cdot 10^{-03}$	$1.1676 \cdot 10^{+01}$	$8.3782 \cdot 10^{-01}$	—	32.008
$4.0 \cdot 10^{-03}$	$1.3370 \cdot 10^{+01}$	$8.5510 \cdot 10^{-01}$	—	41.046
$6.0 \cdot 10^{-03}$	$1.4032 \cdot 10^{+01}$	$8.6521 \cdot 10^{-01}$	—	50.261
$8.0 \cdot 10^{-03}$	$1.4471 \cdot 10^{+01}$	$8.7219 \cdot 10^{-01}$	—	59.733
$1.0 \cdot 10^{-02}$	$1.4816 \cdot 10^{+01}$	$8.7738 \cdot 10^{-01}$	—	69.452
$1.2 \cdot 10^{-02}$	$1.5116 \cdot 10^{+01}$	$8.8139 \cdot 10^{-01}$	—	79.419
$1.4 \cdot 10^{-02}$	$1.5396 \cdot 10^{+01}$	$8.8458 \cdot 10^{-01}$	—	89.667
$1.6 \cdot 10^{-02}$	$1.5698 \cdot 10^{+01}$	$8.8735 \cdot 10^{-01}$	—	100.35
$1.8 \cdot 10^{-02}$	$1.6014 \cdot 10^{+01}$	$8.8966 \cdot 10^{-01}$	—	111.48
$2.0 \cdot 10^{-02}$	$1.6339 \cdot 10^{+01}$	$8.9147 \cdot 10^{-01}$	—	123.04

6.4 Small-signal characteristics

In the next example the cut-off frequency f_T is calculated. The emitter and substrate are at $0\,\mathrm{V}$ and the collector is at $1\,\mathrm{V}$. The DC base voltage is swept and the amplitude of the AC base voltage is $1\,\mathrm{mV}$. We give the absolute values of the small-signal base and collector currents, as well as $f_T = f \cdot i_C/i_B$ with $f = 1\,\mathrm{GHz}$.

Device temperature $T = 25°\mathrm{C}$

$\mathcal{V}_{\mathrm{BE}}\,(\mathrm{V})$	$\lvert i_C\rvert\,(\mathrm{A})$	$\lvert i_B\rvert\,(\mathrm{A})$	$f_T\,(\mathrm{Hz})$
0.70	$5.9997 \cdot 10^{-07}$	$1.3075 \cdot 10^{-06}$	$4.5887 \cdot 10^{+08}$
0.72	$9.6236 \cdot 10^{-07}$	$1.3790 \cdot 10^{-06}$	$6.9789 \cdot 10^{+08}$
0.74	$1.8469 \cdot 10^{-06}$	$1.4944 \cdot 10^{-06}$	$1.2359 \cdot 10^{+09}$
0.76	$3.7588 \cdot 10^{-06}$	$1.6993 \cdot 10^{-06}$	$2.2120 \cdot 10^{+09}$
0.78	$7.6130 \cdot 10^{-06}$	$2.0818 \cdot 10^{-06}$	$3.6568 \cdot 10^{+09}$
0.80	$1.4783 \cdot 10^{-05}$	$2.7966 \cdot 10^{-06}$	$5.2861 \cdot 10^{+09}$
0.82	$2.6511 \cdot 10^{-05}$	$4.0416 \cdot 10^{-06}$	$6.5596 \cdot 10^{+09}$
0.84	$4.2265 \cdot 10^{-05}$	$6.0608 \cdot 10^{-06}$	$6.9735 \cdot 10^{+09}$
0.86	$5.7134 \cdot 10^{-05}$	$9.8903 \cdot 10^{-06}$	$5.7768 \cdot 10^{+09}$
0.88	$5.9762 \cdot 10^{-05}$	$1.6082 \cdot 10^{-05}$	$3.7161 \cdot 10^{+09}$
0.90	$5.6033 \cdot 10^{-05}$	$2.0063 \cdot 10^{-05}$	$2.7928 \cdot 10^{+09}$
0.92	$5.3789 \cdot 10^{-05}$	$2.2275 \cdot 10^{-05}$	$2.4148 \cdot 10^{+09}$
0.94	$5.1755 \cdot 10^{-05}$	$2.3876 \cdot 10^{-05}$	$2.1677 \cdot 10^{+09}$
0.96	$4.9648 \cdot 10^{-05}$	$2.5173 \cdot 10^{-05}$	$1.9722 \cdot 10^{+09}$
0.98	$4.7568 \cdot 10^{-05}$	$2.6275 \cdot 10^{-05}$	$1.8104 \cdot 10^{+09}$
1.00	$4.5599 \cdot 10^{-05}$	$2.7232 \cdot 10^{-05}$	$1.6745 \cdot 10^{+09}$

Device temperature $T = 100°\mathrm{C}$

$\mathcal{V}_{\mathrm{BE}}\,(\mathrm{V})$	$\lvert i_C\rvert\,(\mathrm{A})$	$\lvert i_B\rvert\,(\mathrm{A})$	$f_T\,(\mathrm{Hz})$
0.70	$1.7942 \cdot 10^{-05}$	$3.1922 \cdot 10^{-06}$	$5.6205 \cdot 10^{+09}$
0.72	$2.7792 \cdot 10^{-05}$	$4.5464 \cdot 10^{-06}$	$6.1129 \cdot 10^{+09}$
0.74	$3.8727 \cdot 10^{-05}$	$7.2524 \cdot 10^{-06}$	$5.3399 \cdot 10^{+09}$
0.76	$4.3039 \cdot 10^{-05}$	$1.2464 \cdot 10^{-05}$	$3.4532 \cdot 10^{+09}$
0.78	$3.9912 \cdot 10^{-05}$	$1.6559 \cdot 10^{-05}$	$2.4103 \cdot 10^{+09}$
0.80	$3.7841 \cdot 10^{-05}$	$1.8771 \cdot 10^{-05}$	$2.0159 \cdot 10^{+09}$
0.82	$3.6295 \cdot 10^{-05}$	$2.0316 \cdot 10^{-05}$	$1.7865 \cdot 10^{+09}$
0.84	$3.4742 \cdot 10^{-05}$	$2.1556 \cdot 10^{-05}$	$1.6117 \cdot 10^{+09}$
0.86	$3.3203 \cdot 10^{-05}$	$2.2614 \cdot 10^{-05}$	$1.4683 \cdot 10^{+09}$
0.88	$3.1741 \cdot 10^{-05}$	$2.3545 \cdot 10^{-05}$	$1.3481 \cdot 10^{+09}$
0.90	$3.0392 \cdot 10^{-05}$	$2.4380 \cdot 10^{-05}$	$1.2466 \cdot 10^{+09}$
0.92	$2.9166 \cdot 10^{-05}$	$2.5134 \cdot 10^{-05}$	$1.1604 \cdot 10^{+09}$
0.94	$2.8062 \cdot 10^{-05}$	$2.5826 \cdot 10^{-05}$	$1.0866 \cdot 10^{+09}$
0.96	$2.7097 \cdot 10^{-05}$	$2.6497 \cdot 10^{-05}$	$1.0226 \cdot 10^{+09}$
0.98	$2.6416 \cdot 10^{-05}$	$2.7340 \cdot 10^{-05}$	$9.6623 \cdot 10^{+08}$
1.00	$2.6804 \cdot 10^{-05}$	$2.9323 \cdot 10^{-05}$	$9.1407 \cdot 10^{+08}$

6.5 Y-parameters

In the last example we show the two-port Y-parameters as a function of frequency f. The transistor is biased around the top of the f_T: $\mathcal{V}_{\mathrm{B}} = 0.85\,\mathrm{V}$, $\mathcal{V}_{\mathrm{C}} = 2.0\,\mathrm{V}$ and both emitter and substrate are grounded. In the first data set (two tables) the distributed high frequency effects are switched on. In the second set they are switched off.

Device temperature $T = 25°\mathrm{C}$, EXPHI $= 1$

$f\,(\mathrm{Hz})$	$\mathrm{Re}\,Y_{11}\,(\mathrm{S})$	$\mathrm{Im}\,Y_{11}\,(\mathrm{S})$	$\mathrm{Re}\,Y_{21}\,(\mathrm{S})$	$\mathrm{Im}\,Y_{21}\,(\mathrm{S})$
$1.0 \cdot 10^{+06}$	$4.4048 \cdot 10^{-04}$	$6.5967 \cdot 10^{-06}$	$5.2977 \cdot 10^{-02}$	$-1.5626 \cdot 10^{-05}$
$2.0 \cdot 10^{+06}$	$4.4048 \cdot 10^{-04}$	$1.3193 \cdot 10^{-05}$	$5.2977 \cdot 10^{-02}$	$-3.1251 \cdot 10^{-05}$
$5.0 \cdot 10^{+06}$	$4.4051 \cdot 10^{-04}$	$3.2984 \cdot 10^{-05}$	$5.2977 \cdot 10^{-02}$	$-7.8128 \cdot 10^{-05}$
$1.0 \cdot 10^{+07}$	$4.4062 \cdot 10^{-04}$	$6.5967 \cdot 10^{-05}$	$5.2976 \cdot 10^{-02}$	$-1.5626 \cdot 10^{-04}$
$2.0 \cdot 10^{+07}$	$4.4107 \cdot 10^{-04}$	$1.3193 \cdot 10^{-04}$	$5.2975 \cdot 10^{-02}$	$-3.1251 \cdot 10^{-04}$
$5.0 \cdot 10^{+07}$	$4.4421 \cdot 10^{-04}$	$3.2979 \cdot 10^{-04}$	$5.2967 \cdot 10^{-02}$	$-7.8117 \cdot 10^{-04}$
$1.0 \cdot 10^{+08}$	$4.5542 \cdot 10^{-04}$	$6.5932 \cdot 10^{-04}$	$5.2939 \cdot 10^{-02}$	$-1.5617 \cdot 10^{-03}$
$2.0 \cdot 10^{+08}$	$5.0016 \cdot 10^{-04}$	$1.3165 \cdot 10^{-03}$	$5.2827 \cdot 10^{-02}$	$-3.1180 \cdot 10^{-03}$
$5.0 \cdot 10^{+08}$	$8.0909 \cdot 10^{-04}$	$3.2542 \cdot 10^{-03}$	$5.2053 \cdot 10^{-02}$	$-7.7020 \cdot 10^{-03}$
$1.0 \cdot 10^{+09}$	$1.8549 \cdot 10^{-03}$	$6.2581 \cdot 10^{-03}$	$4.9432 \cdot 10^{-02}$	$-1.4776 \cdot 10^{-02}$
$2.0 \cdot 10^{+09}$	$5.3061 \cdot 10^{-03}$	$1.0865 \cdot 10^{-02}$	$4.0788 \cdot 10^{-02}$	$-2.5405 \cdot 10^{-02}$
$5.0 \cdot 10^{+09}$	$1.5819 \cdot 10^{-02}$	$1.4624 \cdot 10^{-02}$	$1.4542 \cdot 10^{-02}$	$-3.2040 \cdot 10^{-02}$

Device temperature $T = 25°\mathrm{C}$, EXPHI $= 1$

f (Hz)	$\mathrm{Re}\, Y_{12}$ (S)	$\mathrm{Im}\, Y_{12}$ (S)	$\mathrm{Re}\, Y_{22}$ (S)	$\mathrm{Im}\, Y_{22}$ (S)
$1.0 \cdot 10^{+06}$	$-7.5618 \cdot 10^{-08}$	$-3.7249 \cdot 10^{-07}$	$1.4843 \cdot 10^{-05}$	$1.7837 \cdot 10^{-06}$
$2.0 \cdot 10^{+06}$	$-7.5710 \cdot 10^{-08}$	$-7.4497 \cdot 10^{-07}$	$1.4844 \cdot 10^{-05}$	$3.5675 \cdot 10^{-06}$
$5.0 \cdot 10^{+06}$	$-7.6354 \cdot 10^{-08}$	$-1.8624 \cdot 10^{-06}$	$1.4846 \cdot 10^{-05}$	$8.9186 \cdot 10^{-06}$
$1.0 \cdot 10^{+07}$	$-7.8655 \cdot 10^{-08}$	$-3.7248 \cdot 10^{-06}$	$1.4853 \cdot 10^{-05}$	$1.7837 \cdot 10^{-05}$
$2.0 \cdot 10^{+07}$	$-8.7860 \cdot 10^{-08}$	$-7.4497 \cdot 10^{-06}$	$1.4880 \cdot 10^{-05}$	$3.5674 \cdot 10^{-05}$
$5.0 \cdot 10^{+07}$	$-1.5228 \cdot 10^{-07}$	$-1.8623 \cdot 10^{-05}$	$1.5072 \cdot 10^{-05}$	$8.9184 \cdot 10^{-05}$
$1.0 \cdot 10^{+08}$	$-3.8227 \cdot 10^{-07}$	$-3.7242 \cdot 10^{-05}$	$1.5757 \cdot 10^{-05}$	$1.7836 \cdot 10^{-04}$
$2.0 \cdot 10^{+08}$	$-1.3006 \cdot 10^{-06}$	$-7.4448 \cdot 10^{-05}$	$1.8493 \cdot 10^{-05}$	$3.5662 \cdot 10^{-04}$
$5.0 \cdot 10^{+08}$	$-7.6569 \cdot 10^{-06}$	$-1.8549 \cdot 10^{-04}$	$3.7464 \cdot 10^{-05}$	$8.8993 \cdot 10^{-04}$
$1.0 \cdot 10^{+09}$	$-2.9387 \cdot 10^{-05}$	$-3.6667 \cdot 10^{-04}$	$1.0278 \cdot 10^{-04}$	$1.7689 \cdot 10^{-03}$
$2.0 \cdot 10^{+09}$	$-1.0395 \cdot 10^{-04}$	$-7.0484 \cdot 10^{-04}$	$3.3293 \cdot 10^{-04}$	$3.4647 \cdot 10^{-03}$
$5.0 \cdot 10^{+09}$	$-3.9478 \cdot 10^{-04}$	$-1.5393 \cdot 10^{-03}$	$1.3617 \cdot 10^{-03}$	$8.0768 \cdot 10^{-03}$

Device temperature $T = 25°\mathrm{C}$, EXPHI $= 0$

f (Hz)	$\mathrm{Re}\, Y_{11}$ (S)	$\mathrm{Im}\, Y_{11}$ (S)	$\mathrm{Re}\, Y_{21}$ (S)	$\mathrm{Im}\, Y_{21}$ (S)
$1.0 \cdot 10^{+06}$	$4.4048 \cdot 10^{-04}$	$6.5941 \cdot 10^{-06}$	$5.2977 \cdot 10^{-02}$	$-1.4779 \cdot 10^{-05}$
$2.0 \cdot 10^{+06}$	$4.4048 \cdot 10^{-04}$	$1.3188 \cdot 10^{-05}$	$5.2977 \cdot 10^{-02}$	$-2.9559 \cdot 10^{-05}$
$5.0 \cdot 10^{+06}$	$4.4051 \cdot 10^{-04}$	$3.2971 \cdot 10^{-05}$	$5.2977 \cdot 10^{-02}$	$-7.3897 \cdot 10^{-05}$
$1.0 \cdot 10^{+07}$	$4.4063 \cdot 10^{-04}$	$6.5941 \cdot 10^{-05}$	$5.2976 \cdot 10^{-02}$	$-1.4779 \cdot 10^{-04}$
$2.0 \cdot 10^{+07}$	$4.4108 \cdot 10^{-04}$	$1.3188 \cdot 10^{-04}$	$5.2975 \cdot 10^{-02}$	$-2.9558 \cdot 10^{-04}$
$5.0 \cdot 10^{+07}$	$4.4426 \cdot 10^{-04}$	$3.2966 \cdot 10^{-04}$	$5.2968 \cdot 10^{-02}$	$-7.3887 \cdot 10^{-04}$
$1.0 \cdot 10^{+08}$	$4.5561 \cdot 10^{-04}$	$6.5905 \cdot 10^{-04}$	$5.2942 \cdot 10^{-02}$	$-1.4771 \cdot 10^{-03}$
$2.0 \cdot 10^{+08}$	$5.0090 \cdot 10^{-04}$	$1.3159 \cdot 10^{-03}$	$5.2837 \cdot 10^{-02}$	$-2.9492 \cdot 10^{-03}$
$5.0 \cdot 10^{+08}$	$8.1369 \cdot 10^{-04}$	$3.2526 \cdot 10^{-03}$	$5.2112 \cdot 10^{-02}$	$-7.2866 \cdot 10^{-03}$
$1.0 \cdot 10^{+09}$	$1.8731 \cdot 10^{-03}$	$6.2525 \cdot 10^{-03}$	$4.9656 \cdot 10^{-02}$	$-1.3988 \cdot 10^{-02}$
$2.0 \cdot 10^{+09}$	$5.3743 \cdot 10^{-03}$	$1.0835 \cdot 10^{-02}$	$4.1541 \cdot 10^{-02}$	$-2.4106 \cdot 10^{-02}$
$5.0 \cdot 10^{+09}$	$1.6073 \cdot 10^{-02}$	$1.4339 \cdot 10^{-02}$	$1.6744 \cdot 10^{-02}$	$-3.0715 \cdot 10^{-02}$

Device temperature $T = 25°\mathrm{C}$, EXPHI $= 0$

f (Hz)	$\mathrm{Re}\, Y_{12}$ (S)	$\mathrm{Im}\, Y_{12}$ (S)	$\mathrm{Re}\, Y_{22}$ (S)	$\mathrm{Im}\, Y_{22}$ (S)
$1.0 \cdot 10^{+06}$	$-7.5618 \cdot 10^{-08}$	$-3.7248 \cdot 10^{-07}$	$1.4843 \cdot 10^{-05}$	$1.7832 \cdot 10^{-06}$
$2.0 \cdot 10^{+06}$	$-7.5710 \cdot 10^{-08}$	$-7.4497 \cdot 10^{-07}$	$1.4844 \cdot 10^{-05}$	$3.5665 \cdot 10^{-06}$
$5.0 \cdot 10^{+06}$	$-7.6354 \cdot 10^{-08}$	$-1.8624 \cdot 10^{-06}$	$1.4846 \cdot 10^{-05}$	$8.9162 \cdot 10^{-06}$
$1.0 \cdot 10^{+07}$	$-7.8656 \cdot 10^{-08}$	$-3.7248 \cdot 10^{-06}$	$1.4852 \cdot 10^{-05}$	$1.7832 \cdot 10^{-05}$
$2.0 \cdot 10^{+07}$	$-8.7861 \cdot 10^{-08}$	$-7.4496 \cdot 10^{-06}$	$1.4879 \cdot 10^{-05}$	$3.5665 \cdot 10^{-05}$
$5.0 \cdot 10^{+07}$	$-1.5229 \cdot 10^{-07}$	$-1.8623 \cdot 10^{-05}$	$1.5064 \cdot 10^{-05}$	$8.9160 \cdot 10^{-05}$
$1.0 \cdot 10^{+08}$	$-3.8229 \cdot 10^{-07}$	$-3.7242 \cdot 10^{-05}$	$1.5724 \cdot 10^{-05}$	$1.7831 \cdot 10^{-04}$
$2.0 \cdot 10^{+08}$	$-1.3006 \cdot 10^{-06}$	$-7.4447 \cdot 10^{-05}$	$1.8360 \cdot 10^{-05}$	$3.5653 \cdot 10^{-04}$
$5.0 \cdot 10^{+08}$	$-7.6569 \cdot 10^{-06}$	$-1.8548 \cdot 10^{-04}$	$3.6649 \cdot 10^{-05}$	$8.8981 \cdot 10^{-04}$
$1.0 \cdot 10^{+09}$	$-2.9382 \cdot 10^{-05}$	$-3.6662 \cdot 10^{-04}$	$9.9701 \cdot 10^{-05}$	$1.7693 \cdot 10^{-03}$
$2.0 \cdot 10^{+09}$	$-1.0383 \cdot 10^{-04}$	$-7.0445 \cdot 10^{-04}$	$3.2297 \cdot 10^{-04}$	$3.4701 \cdot 10^{-03}$
$5.0 \cdot 10^{+09}$	$-3.9076 \cdot 10^{-04}$	$-1.5358 \cdot 10^{-03}$	$1.3402 \cdot 10^{-03}$	$8.1198 \cdot 10^{-03}$

Acknowledgements

I would like to thank my current graduate students for their help with Verilog-A coding, QA test routine development, parameter extraction program coding, and document preparation of 504.12: Huaiyuan Zhang, Rongchen Ma, Pengyu Li, Yiao Li, Yili Wang, Zhen Li, Jiabi Zhang, and former "noise modeling" students who worked on correlated noise modeling of SiGe HBTs, part of which is put into 504.12: Kejun Xia, Ziyan Xu, Xiaojia Jia. Acknowledgments are also due to:

- Jin Tang, Keith Green, Hisen-Chang Wu (TI), for helping me get started, and providing backgrounds on wishlist items.
- Francesco Vitale, Andries Scholten (NXP), for extensive technical discussions and suggestions on avalanche and high frequency noise modeling implementation, and honest feedback to me on parameter extraction.
- Geoffrey Coram (ADI), Jushan Xie (Cadence), for helping with the KE/Qepi implementation and test case.
- Colin Shaw (Silvaco), for helping with developer transition from Silvaco to Auburn.
- David Harame (IBM), for long time support with hardware and data used in model validation.
- John Cressler (Georgia Tech), for long time collaboration.

Guofu Niu, Auburn University, 7/30/2015.

Acknowledgements are due to the GEIA/ Compact Model Council for countinuous support of Mextram.

Furthermore we would like to express gratitude to:

– Marjan Driessen, Jos Dohmen and Jos Peters (NXP Semiconductors) for detailed feedback on the Mextram documentation and the Verilog-A implementation,

– Geoffrey Coram (Analog Devices) for continued discussions on Verilog-A implementation matters,

– Paul Humphries (Analog Devices Inc.) for fruitful discussions,

– Colin McAndrew (Freescale), Rob Jones (IBM), Teresa Cruz Ravelo (NXP Semiconductors), Rick Poore (Agilent), Doug Weiser (Texas Instruments Inc.), Jos Dohmen (NXP) and Shariar Moinian (LSI) for advice on development of Mextram support for the CMC QA toolkit, and vice versa.

At Delft University, the following have contributed to the development of the Mextram model as a student and member of the Mextram development team:

- Vladimir Milovanovic [30]
- Daniel Vidal
- Francesco Vitale

January 2012, RvdT.

We would like to express gratitude to:

– Dr. H.C. de Graaff, for continued discussions on device physics and the foundations of the Mextram model.

– Dr. D.B.M. Klaassen, Dr. A.J. Scholten (NXP Semiconductors), Prof. J. Burghartz and Dr. L.C.N. de Vreede (Delft University of Technology) for their support to the Mextram model.

– Dr. S. Mijalković, Dr. H.C. Wu and K. Buisman (Delft Univ.) for their extensive work on implementation of Mextram in the Verilog-A language and to L. Lemaitre (Freescale) for advice on this work.

– to G. Coram (Analog Devices) for extensive support on the development of the Verilog-A implementation.

March 2008, RvdT.

For the development of the model we have had valuable discussions with Dr. Henk C. de Graaff.

For testing it we leaned heavily on measurements of Ramon Havens and on the benchmarking effort of the Compact Model Council (CMC). For the implementation we made use of the modelkit features of Pstar made by ED&T. We especially thank Jos Peters for creating the many executables we needed. For their feedback we thank the members of the implementation team, Michiel Stoutjesdijk, Kees van Velthooven, Rob Heeres, Jan Symons and Jan-Hein Egbers. A final acknowledgement is made to Dick Klaassen and Reinout Woltjer for their continuous support of this work.

October 2004, J.P.

References

[1] For the most recent model descriptions, source code, and documentation, see the web-site www.nxp.com/models.

[2] J. C. J. Paasschens, W. J. Kloosterman, and R. van der Toorn, "Model derivation of Mextram 504. The physics behind the model," Unclassified Report NL-UR 2002/806, Philips Nat.Lab., 2002. See Ref. [1].

[3] J. C. J. Paasschens, W. J. Kloosterman, and R. J. Havens, "Parameter extraction for the bipolar transistor model Mextram, level 504," Unclassified Report NL-UR 2001/801, Philips Nat.Lab., 2001. See Ref. [1].

[4] J. C. J. Paasschens and R. van der Toorn, "Introduction to and usage of the bipolar transistor model Mextram," Unclassified Report NL-UR 2002/823, Philips Nat.Lab., 2002. See Ref. [1].

[5] H. K. Gummel and H. C. Poon, "An integral charge control model of bipolar transistors," *Bell Sys. Techn. J.*, vol. May-June, pp. 827–852, 1970.

[6] J. L. Moll and I. M. Ross, "The dependence of transistor parameters on the distribution of base layer resistivity," *Proc. IRE*, vol. 44, pp. 72–78, Jan. 1956.

[7] H. K. Gummel, "A charge control relation for bipolar transistors," *Bell Sys. Techn. J.*, vol. January, pp. 115–120, 1970.

[8] The term 'integral charge control model' was introduced by Gummel and Poon [5]. Their 'integral' means the combination of Gummel's new charge control relation [7] and conventional charge control theory, such "that parameters for the ac response also shape the dc characteristics" [5]. Unfortunately, nowadays the term 'integral charge control relation' (ICCR) is used to refer to Gummel's new charge control relation only, and not to the model by Gummel and Poon.

[9] E. O. Kane, "Theory of tunneling," *Journal of Applied Physics*, vol. 32, pp. 83–91, January 1961.

[10] G. A. M. Hurkx, "On the modelling of tunneling currents in reverse-biased p-n junctions," *Solid-State Electronics*, vol. 32, no. 8, pp. 665–668, 1989.

[11] J. L. Moll, *Physics of Semiconductors*. New York: McGraw-Hill, 1964.

[12] A. J. Scholten, G. D. Smit, M. Durand, R. van Langevelde, and D. B. Klaassen, "The physical background of JUNCAP2," *IEEE Trans. Elec. Dev.*, vol. 53, pp. 2098–2107, September 2006.

[13] M. P. J. G. Versleijen, "Distributed high frequency effects in bipolar transistors," in *Proc. of the Bipolar Circuits and Technology Meeting*, pp. 85–88, 1991.

[14] G. M. Kull, L. W. Nagel, S. Lee, P. Lloyd, E. J. Prendergast, and H. Dirks, "A unified circuit model for bipolar transistors including quasi-saturation effects," *IEEE Trans. Elec. Dev.*, vol. ED-32, no. 6, pp. 1103–1113, 1985.

[15] H. C. de Graaff and W. J. Kloosterman, "Modeling of the collector epilayer of a bipolar transistor in the Mextram model," *IEEE Trans. Elec. Dev.*, vol. ED-42, pp. 274–282, Feb. 1995.

[16] J. C. J. Paasschens, W. J. Kloosterman, R. J. Havens, and H. C. de Graaff, "Improved modeling of ouput conductance and cut-off frequency of bipolar transistors," in *Proc. of the Bipolar Circuits and Technology Meeting*, pp. 62–65, 2000.

[17] J. C. J. Paasschens, W. J. Kloosterman, R. J. Havens, and H. C. de Graaff, "Improved compact modeling of ouput conductance and cutoff frequency of bipolar transistors," *IEEE J. of Solid-State Circuits*, vol. 36, pp. 1390–1398, 2001.

[18] W. J. Kloosterman and H. C. de Graaff, "Avalanche multiplication in a compact bipolar transistor model for circuit simulation," *IEEE Trans. Elec. Dev.*, vol. ED-36, pp. 1376–1380, 1989.

[19] H. Zhang and G. Niu, "An analytical model of avalanche multiplication factor for wide temperature range compact modeling of silicon-germanium heterojunction bipolar transistors," *ECS Transactions*, vol. 75, no. 8, pp. 141 – 148, 2016.

[20] R. van der Toorn, J. J. Dohmen, and O. Hubert, "Distribution of the collector resistance of planar bipolar transistors: Impact on small signal characteristics and compact modelling," in *Proc. Bipolar/BiCMOS Circuits and Technology Meeting*, no. 07CH37879, pp. 184–187, IEEE, 2007.

[21] J. C. J. Paasschens, S. Harmsma, and R. van der Toorn, "Dependence of thermal resistance on ambient and actual temperature," in *Proc. of the Bipolar Circuits and Technology Meeting*, pp. 96–99, 2004.

[22] J. C. J. Paasschens, "Compact modeling of the noise of a bipolar transistor under DC and AC current crowding conditions," *IEEE Trans. Elec. Dev.*, vol. 51, pp. 1483–1495, 2004.

[23] H. C. de Graaff, W. J. Kloosterman, J. A. M. Geelen, and M. C. A. M. Koolen, "Experience with the new compact Mextram model for bipolar transistors," in *Proc. of the Bipolar Circuits and Technology Meeting*, pp. 246–249, 1989.

[24] J. C. J. Paasschens and R. de Kort, "Modelling the excess noise due to avalanche multiplication in (heterojunction) bipolar transistors," in *Proc. of the Bipolar Circuits and Technology Meeting*, pp. 108–111, 2004.

[25] W. J. Kloosterman, J. A. M. Geelen, and D. B. M. Klaassen, "Efficient parameter extraction for the Mextram model," in *Proc. of the Bipolar Circuits and Technology Meeting*, pp. 70–73, 1995.

[26] W. J. Kloosterman, J. C. J. Paasschens, and D. B. M. Klaassen, "Improved extraction of base and emitter resistance from small signal high frequency admittance measurements," in *Proc. of the Bipolar Circuits and Technology Meeting*, pp. 93–96, 1999.

[27] J. C. J. Paasschens, "Usage of thermal networks of compact models. Some tips for non-specialists," Technical Note PR-TN 2004/00528, Philips Nat.Lab., 2004.

[28] V. Palankovski, R. Schultheis, and S. Selberherr, "Simulation of power heterojunction bipolar transistor on gallium arsenide," *IEEE Trans. Elec. Dev.*, vol. 48, pp. 1264–1269, 2001. Note: the paper uses $\alpha = 1.65$ for Si, but $\alpha = 1.3$ gives a better fit; also, κ_{300} for GaAs is closer to 40 than to the published value of 46 (Palankovski, personal communication).

[29] S. M. Sze, *Physics of Semiconductor Devices*. Wiley, New York, 2 ed., 1981.

[30] V. Milovanovic, R. van der Toorn, P. Humphries, D. P. Vidal, and A. Vafanejad, "Compact model of zener tunneling current in bipolar transistors featuring a smooth transistion to zero forward bias current," in *Proc. of the Bipolar Circuits and Technology Meeting*, IEEE, 2009.

